

**Adaptation and survival of *Burkholderia cepacia* and
Burkholderia contaminans in saline solutions containing
benzalkonium chloride: impact on microbiological
quality of pharmaceuticals**

Mariana Belez Silva Tavares

Thesis to obtain the Master of Science Degree in

Biotechnology

Supervisor: Prof. Dr. Isabel Maria de Sá-Correia Leite de Almeida

Examination Committee

Chairperson: Prof. Dr. Ana Cristina Anjinho Madeira Viegas

Supervisor: Prof. Dr. Isabel Maria de Sá-Correia Leite de Almeida

Member of the Committee: Dr. Ricardo Jaime Pereira Rosário dos Santos

October 2019

PREFACE

The work presented in this thesis was performed at the Institute for Bioengineering and Biosciences of Instituto superior Técnico (Lisbon, Portugal), during the period of September 2018 – September 2019, under the supervision of Prof. Dr. Isabel Maria de Sá Correia Leite de Almeida.

DECLARATION

I declare that this document is an original work of my own authorship and that it fulfils all the requirements of the Code of Conduct and Good Practices of the Universidade de Lisboa.

ACKNOWLEDGMENTS

Firstly, I would like to acknowledge my supervisor, Professor Isabel Sá Correia for her continuous guidance and availability, representing an important role in my academic and personal development. This work was performed in the Biological Sciences Research Group of the Institute for Bioengineering and Biosciences (iBB), Instituto Superior Técnico, Universidade de Lisboa. Funding received by iBB from the Portuguese Foundation for Science and Technology (FCT) (UID/BIO/04565/2019) is acknowledged.

I would also like to thank Dr. Vaughn Cooper's group, from University of Pittsburgh, for kindly providing the genome sequences of the *Burkholderia cepacia* isolates here analysed. A special word of appreciation is also directed to the former MSc students Alexandra Balola and Mariya Kozak, for the hard work developed to initiate this project and for kindly welcoming me in the laboratory. I also thank Dr. Sandra Pinto for all the help provided with the confocal microscope. A special thanks to my colleague and PhD student Amir Hassan, for all his help and patience to answer my multiple questions related with the bioinformatics work, for his friendship and daily motivational speeches and for staying at the lab to make sure I finished my work safely.

I would also like to thank my lab partner Inês Peixoto, for her kindness and support while sharing both frustrations and joys, for being my 7 a.m. companion during the long days at the lab and for making this journey more enjoyable. To my Biotechnology friends Ana Rita Valente, Andreia Pereira, Cristiana Domingues and Maria Joana Pinheiro, a very special thanks for all the moments we have spent together in the past two years, from the coffee breaks and dinners, to the long days spent at IST finishing group projects. Thank you for walking beside me on this path and for being the funniest and most supportive friends.

This has been a challenging year, in every sense of the word, and I wouldn't have been able to overcome the obstacles that stood in my way without the love and support from my most loved ones. Having said that, I send the most heartfelt thank you to my partner in life, Nelson Barreira, for never giving up on me, for giving me the strength and courage to fight my own personal battles and for never allowing me to forget my own value. You were the spark that shined through the darker times that marked this last year and words cannot suffice how proud and thankful I am for having a person like you in my life.

The following personal acknowledgments will be addressed in Portuguese:

Agradeço igualmente e do fundo do meu coração aos meus pais, Dália e Eduardo Tavares, por constituírem os meus maiores exemplos de força, dedicação e honestidade, por me transmitirem os valores corretos e por dedicarem a vossa vida em prol da nossa família. Só vocês sabem o quão difícil foi chegar até aqui e é impossível não recordar com emoção os momentos que marcaram a minha vida académica, mas principalmente este último ano, que sei que viveram tão ou mais intensamente do que eu. Obrigada por estarem do meu lado em todos os momentos e por apoiarem todas as minhas decisões.

Por fim, agradeço às minhas avós, Antónia Marouca e Conceição Tavares, outros dos meus maiores alicerces e fonte de inspiração, por tudo o que conseguiram alcançar, fruto do seu esforço e dedicação. Dedico esta tese à minha avó Antónia, pois sei que este era um dos teus grandes sonhos e espero ser para ti um motivo de orgulho. Obrigada por cuidares de mim, por todos os “mimos” e apoio incondicional.

ABSTRACT

The *Burkholderia cepacia* complex (Bcc) is a group of opportunistic pathogenic bacteria, equipped with an extraordinary phenotypic and genotypic plasticity, allowing their adaptation to diverse hostile conditions, particularly water-based environments, solutions with low nutrient concentrations and the presence of antimicrobial agents. Bcc bacteria are feared contaminants in pharmaceutical industries and the underlying cause of numerous nosocomial outbreaks, posing a serious threat to susceptible individuals, particularly Cystic Fibrosis (CF) patients. In the present study, the survival and adaptation of clonal isolates of *B. cepacia* and *B. contaminans* was investigated after long-term incubation in nutrient depleted saline solutions, and in the presence of two concentrations of benzalkonium chloride (BZK), a biocidal preservative commonly used in pharmaceutical settings. Bacterial strains were previously recovered from contaminated saline solutions for nasal application or from two CF patients under surveillance at a Lisbon hospital, and their clonal nature examined by molecular typing. Viability studies revealed that the bacterial populations persisted for at least 16 months under the three incubation conditions examined, suffering a viability reduction in the range of 90 - 99.9%. Long-term incubation resulted in a marked phenotypic heterogeneity, characterized by a progressive decrease of colony size (with development of small colony variants [SCVs]), loss of pigmentation, rough to smooth morphotype switch and a shift from bacilli to a coccoid-like cellular shape. The development of macroscopically visible cellular aggregates, rich in polysaccharide, was also linked to the presence of BZK. The existence of a metabolic pathway for BZK degradation was confirmed through comparative genomic analysis.

Keywords: *Burkholderia cepacia* complex, pharmaceutical products' contamination, nutrient starvation adaptation, benzalkonium chloride adaptation, small colony variants, comparative genomic analysis.

RESUMO

O complexo *Burkholderia cepacia* é um grupo de bactérias patogénicas oportunistas, com enorme plasticidade genética e capacidade de adaptação a condições hostis, nomeadamente ambientes aquáticos, soluções com baixo teor de nutrientes e na presença de agentes antimicrobianos. As contaminações causadas por estas bactérias são preocupantes, provocando numerosos surtos de infeção e comprometendo a saúde de indivíduos suscetíveis, particularmente doentes com fibrose cística (FC). Neste estudo, a sobrevivência e adaptação de isolados clonais de *B. cepacia* e *B. contaminans* foram avaliadas, mediante incubação a longo prazo em condições de carência de nutrientes e na presença de duas concentrações de cloreto de benzalcónio (BZC), um biocida tipicamente usado em produtos farmacêuticos. As estirpes analisadas foram isoladas de soluções salinas para aplicação nasal contaminadas, e de amostras de dois pacientes com FC, seguidos num hospital de Lisboa, tendo-se examinado a sua clonalidade através de tipagem molecular. Os ensaios de viabilidade evidenciam a sobrevivência das populações bacterianas nas três condições referidas durante pelo menos 16 meses, sofrendo uma redução de viabilidade entre 90 a 99.9%. A incubação a longo prazo resultou numa heterogeneidade fenotípica, com diminuição do tamanho das colónias (e desenvolvimento de pequenas variantes clonais), perda de pigmentação, transição entre morfologias rugosa e lisa e alteração do formato celular de bacilos para uma estrutura semelhante a cocos. A formação de agregados celulares ricos em polissacárido e visíveis macroscopicamente foi também associada à presença de BZC. A existência de uma via metabólica de degradação do BZC foi confirmada através de ferramentas de genómica comparativa.

Palavras-chave: Complexo *Burkholderia cepacia*, contaminação de produtos farmacêuticos, adaptação à carência de nutrientes, adaptação ao cloreto de benzalcónio, pequenas variantes clonais, análise genómica comparativa.

TABLE OF CONTENTS

1. THESIS MOTIVATION AND OUTLINE	1
2. INTRODUCTION	3
2.1. <i>Burkholderia cepacia</i> Complex (Bcc)	3
2.1.1. Diversity of species and taxonomy	3
2.1.2. Genomics	4
2.1.3. Environmental distribution and biotechnological applications	4
2.1.4. Bcc bacteria as human pathogens.....	5
2.2. Bcc Bacteria Survival in Water and Nutrient Depleted Conditions	6
2.2.1. Examples of Bcc survival in water environments.....	6
2.2.2. Mechanisms of adaptation to water	7
2.2.3. Adaptation to nutrient starvation and associated molecular mechanisms in Gram-negative bacteria	8
2.2.4. How stress affects cell size and the development of small colony variants (SCVs).....	9
2.3. Bacterial Persistence and Its Implications in Chronic Infections.....	10
2.3.1. Mechanisms of bacterial persistence.....	11
2.3.2. Biofilm formation and bacterial persistence	12
2.3.3. Exopolysaccharides (EPS) and their involvement in chronic infections	12
2.4. Bcc Bacteria as Contaminants of Pharmaceutical Products.....	14
2.4.1. Product recalls associated with the presence of Bcc bacteria.....	14
2.4.2. Bcc bacteria ability to survive and proliferate in pharmaceutical products	15
2.4.3. Reasons underlying Bcc contamination in pharmaceutical settings and preventive measures	15
2.5. Unique Ability of Bcc to Overcome Biocide Action, In Particular Benzalkonium Chloride	17
2.5.1. Bacterial resistance to biocides and associated implications	17
2.5.2. Contamination of solutions containing benzalkonium chloride	18
2.5.3. Bcc bacteria ability to catabolize and resist to BZK: the degradation pathway.....	19
2.6. Contamination Outbreaks in Healthcare Settings	20
3. MATERIALS AND METHODS	25
3.1. Bacterial Isolates	25
3.2. Random Amplified Polymorphic DNA (RAPD) Typing	26
3.3. Long-Term Incubation of the Bacterial Isolates in Saline Solutions and in the Presence of BZK	28

3.4. Viability and Morphology Studies	28
3.5. Susceptibility of <i>B. cepacia</i> Isolates to BZK - Minimum Inhibitory Concentration (MIC) Determination	29
3.6. Characterization of the Cellular Aggregates' Matrix Composition	30
3.7. Comparative Genomic Analysis	31
3.7.1. <i>De novo</i> assembly of <i>B. cepacia</i> isolates' genomes.....	31
3.7.2. <i>In silico</i> Multilocus Sequence Typing (MLST) analysis.....	31
3.7.3. Phylogenetic tree construction.....	32
3.7.4. BLAST® (Basic Local Alignment Search Tool)	32
3.7.5. Comparative analysis of genes from the BZK degradation pathway using the Artemis Comparison Tool (ACT).....	32
4. RESULTS	33
4.1. Molecular Typing of <i>B. cepacia</i> Isolates Examined in This Study and Obtained from Saline Solutions for Nasal Application.....	33
4.1.1. RAPD fingerprinting	33
4.1.2. MLST Analysis	34
4.2. Phylogenetic Analysis of the <i>B. cepacia</i> Isolates Obtained from Intrinsically Contaminated Saline Solutions	35
4.3. Long-Term Survival of <i>B. cepacia</i> and <i>B. contaminans</i> Cellular Populations Under Nutrient Starvation and Benzalkonium Induced Stress.....	36
4.3.1. Analysis of cellular viability during long-term incubation in saline solutions supplemented or not with BZK	36
4.3.2. Reduction of colony size and morphology alterations after 16 months of incubation in nutrient deprived conditions and under BZK induced stress.....	41
4.4. Susceptibility of the <i>B. cepacia</i> Isolates to BZK – MIC Assays	45
4.5. Monitorization of <i>B. cepacia</i> Bacterial Populations' Viability During the First 24h of Incubation in Saline Solutions Supplemented or Not With BZK	45
4.6. Cellular Aggregates/Biofilm-Like Structures Formed by Bcc Isolates in Response to Long-Term Incubation in Nutrient Limited Conditions and BZK Induced Stress	46
4.7. Characterization of the Cellular Aggregates Produced by <i>B. cepacia</i> and <i>B. contaminans</i> Bacterial Populations	49
4.7.1. Comparison of the polysaccharide/protein ratio of the cellular aggregates.....	49
4.7.2. Polysaccharide staining with Alcian blue	50

4.8. Genomic Analysis of the <i>B. cepacia</i> Saline Solutions' Isolates IST612 and IST701: Focus on Benzalkonium and Nutrient Starvation Tolerance Genes	51
4.8.1. Whole genome alignment – identification of genomic rearrangements.....	51
4.8.2. Identification of genes related with tolerance to nutrient starvation and BZK catabolism in the genomes of <i>B. cepacia</i> IST612 and IST701	52
4.8.3. Identification of BZK catabolism genes in <i>B. cepacia</i> IST612 and IST701	56
5. DISCUSSION	58
6. CONCLUSIONS AND FUTURE PERSPECTIVES	64
7. REFERENCES	65
ANNEXES.....	a
Annex I	a
Annex II	b
Annex III	c
Annex IV	d
Annex V	d

LIST OF TABLES

Table 1 – Updated list of the 24 species that comprise the <i>Burkholderia cepacia</i> complex.....	3
Table 2 - <i>Burkholderia cepacia</i> complex related outbreaks described in the literature published during the past five years. The Bcc outbreaks that have occurred in different settings and the diverse types of products identified as sources of Bcc contamination are summarized.	21
Table 3 - List of clonal isolates from <i>B. cepacia</i> and <i>B. contaminans</i> used in this study. The isolates selected to study the effects of long-term incubation in saline solutions supplemented with BZK are indicated in bold and underlined.....	26
Table 4 - Specifications of the PCR programme employed for RAPD analysis of the 22 <i>B. cepacia</i> isolates from saline solutions examined in this study.....	27
Table 5 – Summary of the results obtained after the <i>in silico</i> MLST analysis of the <i>B. cepacia</i> original isolates obtained from contaminated saline solutions inspected by INFARMED in 2003 and 2006.....	34
Table 6 – Maximum specific death rates (μ_d), calculated for the <i>B. cepacia</i> and <i>B. contaminans</i> bacterial populations during long-term incubation in saline solutions containing different BZK concentrations. This parameter was calculated based on the slope of the exponential part of the viability plot.	40
Table 7 – MIC values obtained for three original <i>B. cepacia</i> isolates in study (IST612, IST701 and IST4152), as an indicator of their intrinsic resistance towards BZK. All values are means of at least two replicates and three biologically independent experiments.....	45
Table 8 - List of the 178 genes reported in the literature to be involved in BZK resistance and survival under nutrient starvation. The genes are divided in three main categories (genes encoding transporters, genes encoding degradative enzymes and genes related to nutrient starvation tolerance). The locus tag is indicated for each gene, as well as the main function. The genes that were absent from the genomes of <i>B. cepacia</i> IST612 and IST701 are highlighted in grey.....	53
Table 9 - Putative coordinates (in base pairs) of the genes from the BZK degradation pathway within the draft genomes (after assembly) of <i>B. cepacia</i> IST612 and IST701, originally recovered from contaminated saline solutions in 2003 and 2006, respectively. The percentage of identity obtained after comparison against the <i>B. cenocepacia</i> AU1054 reference genome are also indicated. These results were obtain using the ACT Artemis.	56

LIST OF FIGURES

Figure 1 – Positive and negative impacts of the presence of Bcc bacteria in natural and man-made environments. Despite being known as human opportunistic pathogens responsible for multiple nosocomial outbreaks, Bcc bacteria also have a positive environmental impact, including their role in bioremediation, the production of antimicrobial compounds and their effects in plant growth promotion.	6
Figure 2 - Under stressful conditions, WT bacteria can undergo a shift to the SCV phenotype, exhibiting a slower growth rate but increased antibiotic resistance. They can revert to a WT-like phenotype or give rise to a new phenotype, distinct from both the progenitor and the SCV. Image from Johns <i>et al.</i> (2015).	9
Figure 3 – Biphasic killing curve, representing the killing kinetics of a heterogeneous bacterial population, composed of regular and persister cells. Image from Maisonneuve <i>et al.</i> (2014).....	11
Figure 4 - Representativeness (in percentage) of the bacterial species isolated from pharmaceutical products in the first semester of 2012. Image from Jimenez <i>et al.</i> (2015).	14
Figure 5 - Schematic description of the main intrinsic and acquired mechanisms for reduced susceptibility to biocides adopted by Gram-negative bacteria.	18
Figure 6 - Representation of the possible pathways responsible for BZK degradation in <i>B. cenocepacia</i> AU1054. Only the main reactional steps are schematized. One-step reactions are indicated by solid arrows, while reactions involving more than one step are indicated by dashed arrows. Image adapted from Ahn <i>et al.</i> (2016).....	20
Figure 7 - RAPD fingerprint profiles of the <i>B. cepacia</i> isolates obtained from contaminated saline solutions in 2003 (left panels) and 2006 (right panels), amplified using the RAPD primers 270 (A) , 208 (B) and 272 (C) . Molecular size markers (MM) were run on the first lane of each gel and their size (in base pairs) is indicated on the leftmost side of the image.	34
Figure 8 - Phylogenetic tree representing the evolutionary relationships between the <i>B. cepacia</i> isolates obtained from saline solutions, examined in this study. Isolation dates are indicated, in brackets, next to each isolate's ID. The numbers next to the tree nodes and above each branch represent node and branch age, respectively. This phylogenetic tree was constructed using the Figtree v1.4.3 software.	36
Figure 9 – Schematic representation of the <i>B. cepacia</i> and <i>B. contaminans</i> isolates originally obtained from contaminated saline solutions and from two CF patients, which were used to evaluate the effects of long-term incubation in conditions of nutrient starvation and BZK induced stress.	37
Figure 10 - Effect of long-term incubation in saline solutions (A) and saline solutions supplemented with 0.0053% (B) and 0.05% BZK (C) on the number of CFUs of five <i>B. cepacia</i> isolates, obtained from contaminated batches of saline solutions (IST612 and IST701) and from the sputum of a CF patient (IST4152, IST4168 and IST4222). Cellular viability was measured in terms of CFU's/mL, obtained through colony counts from three separate plates, correspondent to a range of three different serial dilutions. The datapoints correspondent to an incubation period of 10 months were obtained during a previous MSc project (indicated by a grey shade) (144).....	38
Figure 11 - Effect of long-term incubation in saline solutions (A) and saline solutions supplemented with 0.0053% (B) and 0.05% BZK (C) on the number of CFUs of four <i>B. contaminans</i> isolates, obtained from	

contaminated batches of saline solutions (IST601) and from the sputum of a CF patient (IST4148, IST4241 and IST4224). Cellular viability was measured in terms of CFU's/mL, obtained through colony counts from three separate plates, correspondent to a range of three different serial dilutions. The datapoints correspondent to an incubation period of 10 months were obtained during a previous MSc project (indicated by a grey shade) (144)..... 39

Figure 12 – Different colony morphotypes exhibited by the *B. cepacia* IST612 and *B. contaminans* IST601 cellular populations incubated in saline solutions without BZK and in saline solutions supplemented with 0.0053% and 0.05% BZK, after 16 months of incubation. Colony morphologies were compared with those obtained for the same bacterial isolates at initial inoculation (“day-zero”) in the same conditions. It is possible to observe differences in terms of colony size, morphology and pigmentation. 41

Figure 13 - Comparison of the mean diameters of a group of ~100 colonies, representative of each *B. cepacia* and *B. contaminans* cellular populations (■ non-SCV ■ SCV), incubated for 16 months in saline solutions without BZK **(A)**, saline solutions supplemented with 0.0053% **(B)** and 0.05% BZK **(C)**. Colonies with an average diameter inferior to 0.5 mm were termed SCVs and their respective percentages are indicated above the grey bars. 42

Figure 14 - Colony diameter distribution of the cellular populations corresponding to *B. contaminans* isolates IST601 **(A)**, IST4148 **(B)**, IST4224 **(C)**, and IST4241 **(D)** incubated for 16 months under three different stress conditions. The colony diameters of the original isolates, grown on LB medium, were also assessed and used as a control. 30-260 individual colonies were selected for measurement. Mean colony diameters ± SD are also plotted..... 43

Figure 15 - Colony diameter distribution of the cellular populations corresponding to *B. cepacia* isolates IST612 **(A)**, IST701 **(B)**, IST4152 **(C)**, IST4168 **(D)** and IST4222 **(E)** incubated for 16 months under three different stress conditions. The colony diameters of the original isolates, grown on LB medium, were also assessed and used as a control. 30-260 individual colonies were selected for measurement. Mean colony diameters ± SD are also plotted..... 44

Figure 16 – Evolution of cellular viability during the first 24h of incubation of the *B. cepacia* IST612 (circles) and IST701 (squares) bacterial populations in saline solutions (red) and saline solutions supplemented with 0.0053% (green) or 0.05% BZK (blue). Cell viability was assessed in terms of CFU's/mL, obtained through colony counts from three separate plates, correspondent to a range of three different serial dilutions..... 46

Figure 17 - General aspect of bacterial suspensions correspondent to *B. cepacia* IST612 **(A)** and *B. contaminans* IST601 **(B)** after 16 months of incubation in saline solutions and in saline solutions containing 0.0053% or 0.05% BZK. 47

Figure 18 - Microscopic observation of the structures formed by *B. cepacia* IST612 and *B. contaminans* IST601, after 16 months of exposure to saline solutions supplemented with increasing concentrations of BZK. **(A1; B1)** Control, with only saline solution (NaCl 0.9% (w/v)); **(A2; B2)** Cells exposed to 0.0053% (w/v) of BZK; **(A3; B3)** Cells exposed to 0.05% (w/v) of BZK. Cellular viability was assessed through co-staining of cells with SYTO 9 (green) and TO-PRO-3 iodide (red). Images were acquired using a

confocal microscope (the same settings were applied for each image) and are equally scaled to allow direct comparison. 47

Figure 19 - Detailed microscopic observation of the biofilm structures formed by *B. cepacia* IST612 (**A**) and *B. contaminans* IST601 (**B**), after 16 months of exposure to saline solutions supplemented with 0.05% BZK, where the coccus/coccobacilli-like shape of bacterial cells is observable (indicated by solid arrows). Images were acquired using a confocal microscope (the same settings were applied for each image) and are equally scaled to allow direct comparison..... 48

Figure 20 - Levels of polysaccharide (**A**) and protein (**B**) produced by the *B. cepacia* isolate IST612 and the *B. contaminans* isolate IST601, assessed by the phenol-sulphuric method and expressed in mg per mL of bacterial sample, at initial incubation ("Time = 0") and after 1 and 18 months of incubation in saline solutions and saline solutions supplemented with 0.0053% or 0.05% BZK,. The results are means of two independent experiments with three replicates each. At initial inoculation ("Time = 0") no polysaccharides were detected. 49

Figure 21 - Ratio of polysaccharides/proteins present within the aggregate structures produced by *B. cepacia* IST612 and the *B. contaminans* IST601, assessed by the phenol-sulphuric acid method and expressed in grams of total sugars per grams of protein (g.g protein⁻¹), after 1 and 18 months of incubation in saline solutions and saline solutions supplemented with 0.0053% or 0.05% BZK. The results are means of two independent experiments with three replicates each. The ratios of polysaccharide/protein at initial inoculation ("Time = 0") are not represented, due to the lack of polysaccharides registered at that time. 50

Figure 22 - Microscopic observation of the bacterial population corresponding to *B. cepacia* IST612 and *B. contaminans* IST601, after exposure to saline solutions supplemented with 0.05% BZK. Cell populations were visualized using fluorescence microscopy (**A, C**). Polysaccharides stained with Alcian blue were visualized using bright field microscopy (**B, D**). Cellular viability was assessed through co-staining of cells with SYTO 9 (green) and propidium iodide (red). Images **A/B** and **C/D** correspond to the exact same field. The same scaling was applied, to allow direct comparison. 51

Figure 23 – Multiple genome alignment of the *B. cepacia* isolates IST612 (**A**) and IST701 (**B**), performed with Mauve (The Darling Lab). Boxes sharing the same color correspond to local colinear blocks (LCB) and denote shared homologous regions, without sequence rearrangements. Blocks displayed below the central black line indicate regions that align in the reverse complement (inverse) orientation. Red circles – genomic translocation; Blue circles – genomic inversion..... 52

Figure 24 – Schematic diagram of the genomic organization of the 15 homologues of the *B. cenocepacia* AU1054 BZK catabolism genes, identified within the genomes of *B. cepacia* IST612 and IST701. *B. cenocepacia* AU1054 was used as a reference genome. Genes are represented by labelled arrows and their respective locus-tag and products are listed below the diagram. Blue arrows – reference genes; Green arrows – genes inverted with respect to the reference genome; Orange arrows – genes that are in the same orientation with respect to the reference genome. The real distances between the genes were modified to assist visual interpretation. Image not to scale. 57

LIST OF ABBREVIATIONS

ABC	ATP-binding cassette	MH	Muller-Hinton broth
ACT	Artemis comparison tool	MIC	Minimum inhibitory concentration
ANI	Average nucleotide identity	MIT	Metal Ion Transporter
ArAE	Aromatic Acid Exporter	MLST	Multilocus sequence typing
ATP	Adenosine triphosphate	MOP	Multidrug/Oligosaccharidyl-lipid/Polysaccharide
BA	Benzylamine	NCS	Nucleobase:Cation Symporter
Bcc	<i>Burkholderia cepacia</i> complex	OD	Optical density
BDMA	Benzyl dimethylamine	OMP	Outer membrane proteins
BLAST	Basic local alignment search tool	OOP	OmpA-OmpF Porin
BMA	Benzylmethylamine	OTC	Over-the-counter
BSA	Bovine serum albumin	PCR	Polymerase chain reaction
BZK	Benzalkonium chloride	PDA	Parenteral drug association
CDC	Centre of disease control	PIA	<i>Pseudomonas</i> isolation agar
CF	Cystic fibrosis	PMF	Proton motive force
CFTR	Cystic fibrosis transmembrane regulator	QAC	Quaternary ammonium compounds
CFU	Colony forming units	RAPD	Random amplified polymorphic DNA
CGD	Chronic granulomatous disease	RFLP	Restriction fragment length polymorphism
CHLN	Centro hospitalar Lisboa Norte	RNA	Ribonucleic acid
CHR	Chromate Ion Transporter	rRNA	Ribosomal ribonucleic acid
CPA	Cation:Proton Antiporter	RND	Resistance-nodulation-cell division
DAACS	Dicarboxylate/Amino Acid:Cation Symporter	ROS	Reactive oxygen species
ddH₂O	Double distilled water	rpm	Rotations per minute
DNA	Deoxyribonucleic acid	SCV	Small colony variants
EPS	Exopolysaccharide	SMRT	Single-molecule real-time
FDA	Food and drug administration	TA	Toxin-Antitoxin
GMP	Good manufacturing practices	TCA	Tricarboxylic acid
HSM	Hospital de Santa Maria	TCE	Trichloroethylene
IS	Insertion sequences	TSA	Tryptic soy agar
KUP	K ⁺ Uptake Permease	UBS	Unknown BART Superfamily
LB	Luria-Bertani medium	USP	United States pharmacopeia
LPS	Lipopolysaccharide	VBNC	Viable but non-culturable
MFS	Major facilitator superfamily	WT	Wild type

1. THESIS MOTIVATION AND OUTLINE

The *Burkholderia cepacia* complex (Bcc) is a group of Gram-negative non-fermenting β -proteobacteria, which are ubiquitously distributed in the environment, presenting an extraordinary metabolic diversity and an intrinsic resistance to multiple antibiotics and antiseptics, as well as the capacity to grow in nutritionally limited environments. These features are greatly attributed to their genotypic and phenotypic plasticity, which confers the ability for rapid mutation and adaptation in such challenging environments (1, 2). Bcc bacteria are described as one of the major contaminants of sterile and non-sterile pharmaceutical and personal care products, such as nasal sprays, ultrasound gel, mouthwash, pre-operative skin solutions and hand sanitizers, being the reason behind numerous product recalls. In addition, contamination with Bcc bacteria has caused many nosocomial outbreaks in the last two decades, posing a serious health threat to susceptible individuals, namely immunocompromised patients (HIV and cancer patients) and individuals suffering from chronic granulomatous disease (CGD) or cystic fibrosis (CF) (3), (4).

Many contamination episodes have been associated with the ability of Bcc bacteria to thrive in the presence of antimicrobials and disinfectants, particularly biocides used as preservatives in pharmaceutical products' formulations (5). Contamination of benzalkonium chloride (BZK) solutions with Bcc bacteria has been pointed out as the cause of frequent outbreaks, especially with *B. cepacia*, which has been described as the most prevalent contaminant species (6–9). Bcc bacteria have developed an array of strategies to cope with the presence of BZK, including the active extrusion from the bacterial cell through the action of efflux pumps or its inactivation by catabolic enzymes and further use as carbon source for bacterial growth (10–13). Remarkably, Bcc bacteria also possess the ability to survive and proliferate in water-based environments (water bodies, lakes, rivers, drinking water, pharmaceutical grade water) and under nutrient starvation (14). To accomplish that, Bcc bacteria must undergo several genetic changes, giving rise to diverse genotypes and phenotypes, which confer them the much-needed selective advantage in an ever-changing environment. For that reason, Bcc is still the number one group of bacterial species found in contaminated health products (5).

In an epidemiological survey performed by our laboratory between 1995 and 2002, which included patients under surveillance at the major Portuguese CF center at Hospital de Santa Maria (HSM), Lisbon, an unusually high representativeness of *B. cepacia* was detected in sputum cultures (in 36% of the patients) (15). From 2002 to 2005, the prevalence of *B. cepacia* continued to increase, affecting 85% of the CF patients receiving treatment at HSM (16). Parallel to these events, a market surveillance performed by INFARMED, the National Authority of Medicines and Health Products, in 2003 and 2006, detected Bcc contamination in several batches of non-sterile saline solutions for nasal application (16). Since those types of products are often administered to CF patients during inhalant therapy, a correlation between these contamination outbreaks and the prevalence of *B. cepacia* was hypothesized. Further analysis by gas chromatography and molecular methods, confirmed that the clinical clones obtained from CF patients and the strains detected in saline solutions were epidemiologically related (16). When this outbreak occurred, all of the clones identified by our laboratory were classified as *B. cepacia*. In 2015, a re-examination of the isolates was conducted and 20 of them were reclassified as *B.*

contaminans (17). Considering these latest results, two different Bcc species (*B. cepacia* and *B. contaminans*) were apparently involved in the outbreak, demonstrating that species which are considered less predominant in CF respiratory infections may also be associated with poor clinical outcomes (17).

B. cenocepacia and *B. multivorans* are described as the most representative Bcc species in CF patients, accounting for 85-97% of CF related infections (18). On the other hand, *B. cepacia* and *B. contaminans* are considered to have a low prevalence in CF infections worldwide. Nevertheless, these two particular species have a high incidence in the Portuguese CF patients, which might be related with the aforementioned contamination outbreak involving sterile saline solutions. Moreover, the frequency of *B. contaminans* associated infections has increased considerably in countries such as Spain or Argentina (19, 20) and has also been associated with contamination of pharmaceutical products and healthcare facilities, being the underlying cause of several nosocomial outbreaks (21–23).

The aim of this work was to study the phenotypic alterations that Bcc bacteria undergo during long-term incubation in stressful environmental conditions, including nutrient depletion and the presence of a specific biocidal preservative. This approach was intended to shed some light on some of the inherent mechanisms underlying bacterial persistence and adaptability, until the conditions become more favourable for growth. In the present study, two sets of clonal isolates of *B. cepacia* and *B. contaminans*, recovered from batches of saline solutions inspected by INFARMED in 2003 and 2006, as well as clinical isolates obtained from two CF patients under surveillance at HSM during that contamination outbreak were selected to evaluate the effects of prolonged storage under nutrient scarcity and BZK induced stress. The clonal nature of these *B. cepacia* and *B. contaminans* isolates was confirmed by molecular typing, using RAPD PCR and *in silico* MLST. These original isolates were used to induce artificial contamination of saline solutions supplemented with two distinct concentrations of BZK, leading to different deleterious effects (0.0053% (w/v) and 0.05% (w/v)), and incubated at 23°C to mimic the typical storage conditions applied for this type of pharmaceutical products. This long-term incubation experiment is a follow-up of the work initiated by a former MSc student, Mariya Kozak, who has studied the adaptation of the same bacterial populations during the first 10 months of incubation.

Long-term incubation in such conditions resulted in a global adaptive response, characterized by the development of sub-populations with different phenotypic characteristics. The evolution of those traits was accompanied during the course of the experiment in regular intervals of time. Cellular viability, colony diameter, morphology and pigmentation changes were evaluated. Intrinsic resistance of the original isolates towards BZK was also assessed. Other adaptation strategies were studied, including the formation of cellular aggregates, which were characterized in terms of polysaccharide and protein contents. Additionally, the comparative genomic analysis performed for two *B. cepacia* saline solutions' isolates confirmed the presence of genes from the BZK degradation pathway, already described in another Bcc strain (10), indicating that this preservative can be used as carbon and energy source by these bacteria. Differences between isolates obtained in 2003 and 2006 from contaminated saline solutions for nasal application were also detected.

2. INTRODUCTION

Disclaimer: The text of this Introduction chapter is based on a revision paper to be published (“*Burkholderia cepacia* complex bacteria: a feared contamination risk in water-based pharmaceutical products”, American Society for Microbiology (ASM), acceptable after the ongoing revision). The text was written by me, under the guidance of my thesis advisor with contributions of two other MSc students, who carried out the first literature search on the topic during their MSc thesis work.

2.1. *Burkholderia cepacia* Complex (Bcc)

2.1.1. Diversity of species and taxonomy

The *Burkholderia cepacia* complex (Bcc) is composed of at least 24 closely related Gram-negative non-fermenting β -proteobacteria (**Table 1**), which are ubiquitously distributed in the environment, presenting the ability to colonize diverse niches, whether natural or man-made (24–28). Some Bcc species occur in the soil and fresh water, while others proliferate within a host (fungi, plants, humans or other animals) (1). The first species of this complex, at the time designated *Pseudomonas cepacia*, was described in the 1950s by Walter Burkholder as the cause of “sour skin”, a bacterial disease that causes onion bulb rot (29). Later, in 1992, the separation of seven species of the *Pseudomonas* homology group II into the new genus *Burkholderia* was proposed, based on supportive evidence from 16S rRNA sequences, DNA–DNA homology values, lipid and fatty acid composition, as well as phenotypic characteristics (30). In 1997, an integrated genotypic and phenotypic analysis was conducted, resulting in the division of the species into five distinct genomovars, with similar phenotypic characteristics but differences in terms of genotype (31).

Since then, there have been major developments in this field, driven by the rising interest in studying this particular group of bacteria, which allowed proper taxonomic and systematic classification. The analysis of the *recA* gene sequence variations, the multilocus sequence typing (MLST) and, more recently, the introduction of whole genome sequencing have shed some light on species and strains identification, as well as on intra-species relationships between members of the *Burkholderia* genus. It was acknowledged that different members of the Bcc share high similarity values in terms of 16S rRNA (>97.7%) and *recA* (94-95%) gene sequences. Moreover, moderate DNA-DNA hybridization levels (between 30-60%) (32) and an average nucleotide identity (ANI) along the whole genome varying between 85.04 and 89.92% (33) were also reported.

Table 1 – Updated list of the 24 species that comprise the *Burkholderia cepacia* complex (24–28).

<i>B. alpina</i>	<i>B. cepacia</i>	<i>B. metallica</i>	<i>B. seminalis</i>
<i>B. ambifaria</i>	<i>B. contaminans</i>	<i>B. multivorans</i>	<i>B. stabilis</i>
<i>B. anthina</i>	<i>B. diffusa</i>	<i>B. pseudomultivorans</i>	<i>B. stagnalis</i>
<i>B. arboris</i>	<i>B. dolosa</i>	<i>B. paludis</i>	<i>B. territorii</i>
<i>B. catarinensis</i>	<i>B. lata</i>	<i>B. puraquae</i>	<i>B. ubonensis</i>
<i>B. cenocepacia</i>	<i>B. latens</i>	<i>B. pyrrocinia</i>	<i>B. vietnamiensis</i>

2.1.2. Genomics

Bcc bacteria possess some of the largest genomes among Gram-negative bacteria, with sizes ranging from 6 to 9 Mb and a GC content of around 67% (34, 35). Their genomes are usually composed of three (although the number can vary from two to four, according to the strain) multiple large replicons (chromosomes) with more than 500 Kb, and one or more plasmids (36). The first genome sequence to be publicly available corresponds to one of the best studied Bcc strains, *B. cenocepacia* J2315. The total size of this strain's genome is 8.06 Mb, comprising three circular chromosomes (replicons) and one small plasmid (92 Kb). Besides that, several insertion sequences and genomic islands were also identified as part of the genome (34),(37). The presence of numerous insertion sequences (IS elements) has been reported to promote genomic rearrangements and increase the expression of genes that are located near them, therefore contributing to the genomic plasticity of these bacteria (2). It is thought that 10% of the 7000 genes encoded on average by Bcc species result from horizontal gene transfer phenomena, residing in the genome as genomic islands, integrated phages or plasmids (38).

2.1.3. Environmental distribution and biotechnological applications

Burkholderia cepacia complex bacteria are commonly found in natural environments, occupying diverse niches, such as soil, water, plant rhizosphere and agricultural products (34, 38–41). The distribution of Bcc species is not homogeneous among these habitats. For instance, *B. cepacia*, *B. cenocepacia*, *B. vietnamiensis* and *B. ambifaria* are the most representative Bcc species inhabiting the rhizosphere of plants (34, 36, 38, 40, 41). *B. cepacia*, *B. multivorans*, *B. cenocepacia*, *B. vietnamiensis*, *B. anthina* and *B. seminalis* are among the most common bacterial species found in water-based environments worldwide (41–44).

Due to their metabolic diversity and the ability to establish mutualistic and symbiotic interactions with plants, the exploitation of *Burkholderia* species for biological control, plant growth promotion and bioremediation has been attempted, but their pathogenic potential raises concern (**Figure 1**) (40). Since Bcc species are closely related, from the genetic point of view, exchange of genetic material between different strains/species might occur, creating the possibility for apparently innocuous strains to acquire pathogenic characteristics (41). This hypothesis has not yet been verified in natural settings but has been demonstrated *in vitro* (41). Field tests have shown that Bcc bacteria are able to colonize the rhizosphere of several economically relevant crops, including rice (where *B. vietnamiensis* has been found in high numbers), pea roots (colonized by *B. ambifaria*) and wheat (with *B. cepacia* and *B. cenocepacia* colonizing its rhizosphere) (38). Some of these species are capable of N₂ fixation, therefore contributing to plant-growth, an extremely useful trait in agricultural contexts, namely under N-limiting conditions (36). Another important capacity is the production of biopesticides which can protect crops against other bacteria, protozoa, nematodes and fungal diseases such as root rot or seed damaging infections (39, 40). Due to their marked metabolic versatility, namely the ability to use complex and diverse carbon sources, some *Burkholderia* isolates have the potential to degrade a number of xenobiotic compounds and other organic pollutants, including constituents of crude oils (polycyclic aromatic hydrocarbons), herbicides and other pesticides, phthalates and solvents like trichloroethylene

(TCE). One example of the potential of this bacterial group for bioremediation is the *B. vietnamiensis* strain G4, which can degrade toluene and chlorinated solvents (34),(36).

Unlike other opportunistic pathogens, Bcc bacteria are not prone to commensal carriage, meaning that infection is either acquired in hospital settings or directly from the environment (34). In 2002, a soil isolate was proven to be genetically identical to a *B. cenocepacia* clone responsible for extensive infection in CF patients, proving that strains which are pathogenic to humans do not necessarily differ from those found in the environment (45). Understanding if the natural environment could constitute a source of direct acquisition of Bcc infection in humans is therefore of utmost importance.

2.1.4. Bcc bacteria as human pathogens

Despite their applications in bioremediation, the large-scale use of Bcc bacteria deserves attention from the scientific community, especially in what concerns their release in the environment. This is important since the multiple bacterial species that constitute the Bcc complex are the underlying cause of serious respiratory infections among immunocompromised individuals and patients suffering from cystic fibrosis (CF) or chronic granulomatous disease (CGD) (46, 47). Mechanically ventilated patients, infants and the elderly are also highly susceptible to Bcc colonization, with very unpredictable outcomes, ranging from asymptomatic carriage to a rapid and sometimes unexpected decline in the patient's condition, leading to increased risk of death (4). Bcc strains rarely cause infection in healthy (immunocompetent) individuals, since they are cleared by normal airway mucociliary activity (36). Patient-to-patient transmissibility is thought to occur through spreading of aerosol particles, direct physical interaction with infected people or upon contact with contaminated surfaces (34).

Bcc bacteria colonize the lungs of CF patients, establishing a chronic infection that often leads to rapid deterioration of lung function, which can culminate in the "cepacia syndrome", characterized by necrotizing pneumonia and septicaemia (34). CF patients have a mutation in the cystic fibrosis transmembrane conductance regulator (CFTR) gene, resulting in the accumulation of mucus, abnormal submucosal gland function, exacerbated inflammatory response and reduced antimicrobial peptide efficacy (48). Within the characteristic environment of the CF lung, colonizing bacteria more than often face stressing selection pressures thought to be the driving force for the emergence of phenotypic and genotypic variation within the same clonal population (46), often conferring evolutionary and adaptive advantage in a constantly changing environment (46).

In comparison with *Pseudomonas aeruginosa*, infections caused by Bcc bacteria affect a smaller percentage of CF patients. However, they represent a major concern since the clinical outcome is very unpredictable, even in patients infected with the same clonal strain (4, 34). Although the Bcc comprises 24 bacterial species, the two most prevalent and feared among the CF community are *B. cenocepacia* and *B. multivorans* (4, 38, 49) However, the less represented species, in particular, *B. dolosa*, *B. stabilis*, *B. contaminans* and *B. cepacia* may also be associated with poor clinical outcomes (50, 51).

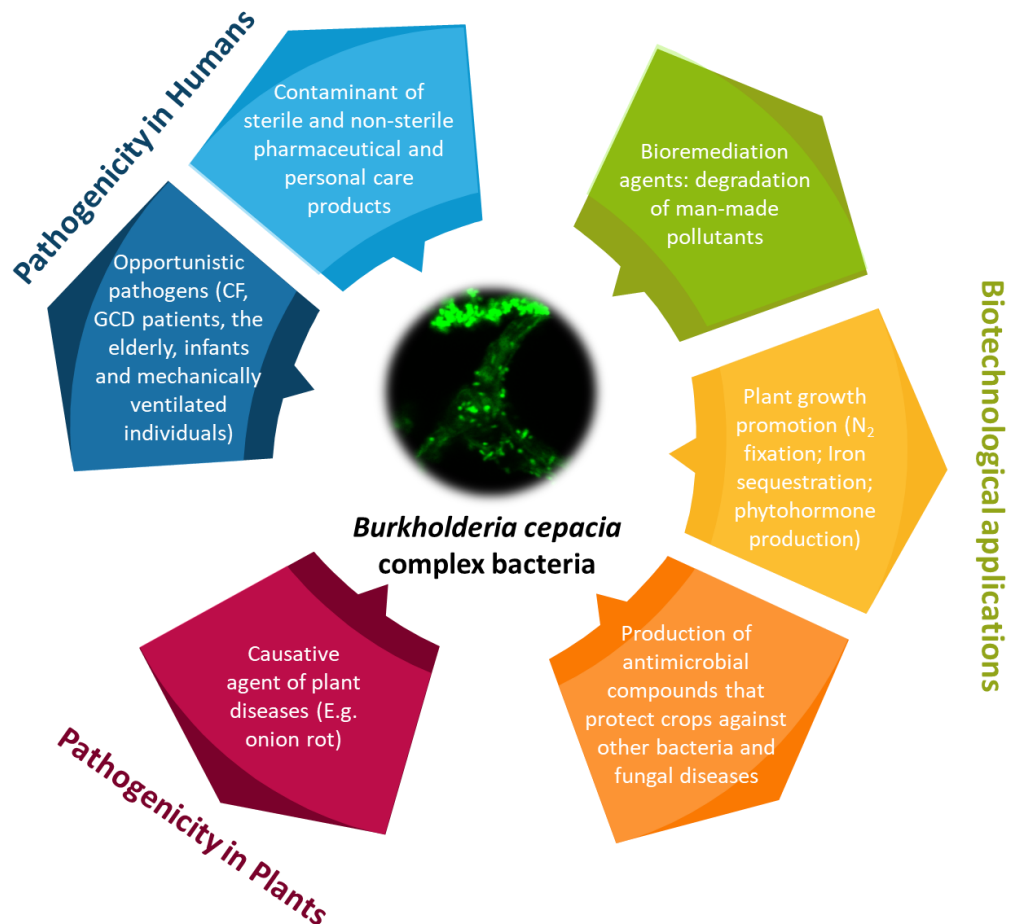


Figure 1 – Positive and negative impacts of the presence of Bcc bacteria in natural and man-made environments. Despite being known as human opportunistic pathogens responsible for multiple nosocomial outbreaks, Bcc bacteria also have a positive environmental impact, including their role in bioremediation, the production of antimicrobial compounds and their effects in plant growth promotion.

2.2. Bcc Bacteria Survival in Water and Nutrient Depleted Conditions

Besides being widely distributed in the soil, Bcc bacteria can also survive and proliferate in water-based environments, such as water bodies, lakes, rivers, drinking water and liquids containing low amounts of nutrients. This characteristic is mainly attributed to the genetic and nutritional diversity of these species, which might be responsible for the ability of certain Bcc bacteria to metabolize the organic matter present in oligotrophic aquatic environments (14).

2.2.1. Examples of Bcc survival in water environments

In a study carried out in the province of Bologna (Italy), eighty five water samples from public and private buildings were examined and *B. cepacia* was found to be present in 3.5% of the samples, growing in water at a temperature of approximately 24°C (42). Additionally, it was demonstrated that the organic matter from the biofilm that is normally formed around the inner walls of the waterpipes was probably metabolized by the bacterial cells (42). In 2003, twenty eight water samples, collected from the European rivers Schelde and Leie were also analysed and ten of them were positive for the presence of Bcc bacteria, namely *B. cepacia*, *B. multivorans*, *B. cenocepacia*, *B. vietnamiensis* and *B. anthina* (43). More

recently, the presence of Bcc bacteria in water bodies of the West Lake in China was also confirmed, representing 39.6% of the bacterial species detected in those water samples (44). *B. cenocepacia* was the most prevalent Bcc species, although *B. multivorans*, *B. cenocepacia*, *B. stabilis*, *B. vietnamiensis* and *B. seminalis* were also detected (44).

Bcc bacteria also exhibit the capacity to survive in water-based environments for long periods of time, under different and sometimes stressful conditions. Early studies performed on three different *B. cepacia* strains incubated in distilled water revealed that optimum growth rates were achieved at 37°C. Nevertheless, those strains could also tolerate temperature variations in the range of 18°C to 42°C, without compromising cellular viability. Moreover, two strains were able to survive for 48h at 50°C and for 21 days at 10°C (52). Another study has identified six *B. cenocepacia* strains that were able to survive in water at 18°C and 23°C for at least 40 days (14).

2.2.2. Mechanisms of adaptation to water

There are several factors that can influence bacterial survival in water, namely their physiological state, intrinsic tolerance to nutrient scarcity, interaction with other bacteria and also variations in temperature (14). However, in the case of Bcc bacteria, the reasons behind their ability to persist in water-based environments for long periods of time have still not been broadly assessed and, currently, there are no published studies concerning the mechanisms involved in Bcc survival in water.

Within the *Burkholderia* genus, *B. pseudomallei*, an endemic pathogen of tropical and subtropical regions and the causing agent of melioidosis disease in humans and animals [53], despite not being a member of the Bcc complex, is the best studied *Burkholderia* species in terms of survival in water environments. A microarray analysis performed on *B. pseudomallei* cells incubated in distilled water revealed several alterations in gene expression patterns, particularly the upregulation of a gene encoding a putative phosphatidylglycerol phosphatase, possibly involved in cell membrane biosynthesis (53). Furthermore, the lack of an intact core of the lipopolysaccharide (LPS) led to a pronounced viability loss after 200 days of incubation in water, suggesting that the ability to maintain an intact outer membrane architecture might be relevant for prolonged survival in water environments (53). Another strain of *B. pseudomallei* was reported to have survived in distilled water at 25°C for 16 years, presumably by inducing a switch of cellular morphology from typical Gram-negative rods to cocci or coccobacilli and by entering a viable but non-culturable (VBNC) state (54).

Water constitutes a hostile environment, presenting several challenges to bacterial growth, including the lack of nutrients and low osmolarity (53). The fact that Bcc bacteria are able to persist in such conditions is indicative of their remarkable metabolic capacity and deserves special attention, as they can pose serious threats to public safety and health.

2.2.3. Adaptation to nutrient starvation and associated molecular mechanisms in Gram-negative bacteria

In order to survive during prolonged periods of starvation, many bacteria have developed strategies to cope and persist in the environment, until the conditions become favourable for growth. The starvation-survival response of some Gram-negative bacteria such as *Escherichia coli*, *Salmonella typhimurium*, *P. aeruginosa* and *Vibrio* spp. has been well characterized. However, more studies are required to better understand the mechanisms underlying Bcc bacteria adaptation to nutrient starvation. A number of Gram-negative bacteria are thought to undergo a reversible process in which their metabolic activity drops to very low levels and no replication occurs. In these conditions, cells might be viable and maintain their integrity and proton motive force (PMF) but cannot be cultured. This state is referred to as the viable but non-culturable state (VBNC) and is thought to allow bacterial persistence in adverse conditions, such as prolonged starvation or high osmolarity. The mechanisms by which different bacterial species enter this process are not completely understood, but it may be subject to genetic regulation (55–57).

Since environmental perturbations often occur, it is critical that cells are able to recognize those changes, integrate such information and adjust the metabolism accordingly. A recent study on the mechanisms behind *P. aeruginosa* capability of long-term survival under nutrient starvation demonstrated that this species was able to remain viable in water during 8 weeks by switching to a state of low metabolic activity and by inducing a shift in cell morphology from a rod to a coccoid shape (55). The phospholipid composition of the outer membrane changed, leading to a reduction in permeability and increased tolerance to disruption induced by antimicrobial peptides (55). In terms of gene expression, there was an overall tendency for downregulation of genes involved in DNA replication and cellular metabolism. Genes involved in fatty acid oxidation, phospholipid metabolism, amino acid uptake and catabolism were upregulated, suggesting that these compounds might be used as alternative sources of energy under nutrient limitation (57).

Some of the alterations reported for *P. aeruginosa* PAO1 had already been described for *P. putida* KT2442, including cell size decrease and the switch towards a round/coccoid cellular shape. Additionally, protein synthesis decreased and the number of chromosomes was reduced from three to one during long-term starvation. Bacterial cells also displayed increased adhesive properties, forming clumps in liquid culture (58).

Under severe substrate limitation, cells might use alternative sources of energy and biosynthetic substrates, which can require the degradation of cellular components like ribosomes and membrane phospholipids. Besides providing nutrients, degradation of internal sources also removes the burden of maintaining cellular machinery that has become dispensable. Consequently, a decrease in cell size and volume occurs, increasing the surface area-to-volume ratio, leading, in theory, to a more efficient transport of substrates (57).

2.2.4. How stress affects cell size and the development of small colony variants (SCVs)

Bacterial cultures are not genetically homogeneous, presenting a high degree of genomic plasticity. This intrinsic heterogeneity allows for the adaptation of bacterial populations to diverse environmental conditions, often leading to the appearance of subpopulations with different phenotypical characteristics. One example of such adaptation capacity is the development of slow-growing subpopulations of bacteria, termed small colony variants (SCVs), which are characterized for being approximately one-tenth the size of colonies associated with wild-type bacteria and for growing at a rate nine times slower in comparison with their progenitor cells (59, 60). SCVs have been described for a variety of bacterial genera and species, including *Staphylococcus aureus*, *P. aeruginosa*, *B. cepacia*, *Salmonella* and *Vibrio* (60). The most common phenotypic characteristics associated with SCVs include atypical colony morphology, slow growth rate, lack of pigmentation, reduced haemolytic and coagulase activity, low virulence potential and increased resistance to antibiotics (60). Depending on the environmental stimuli, some SCVs undergo permanent genetic changes, whereas others revert to the wild-type phenotype or give rise to a new phenotype, distinct from both the progenitor and the SCV (**Figure 2**) (59).

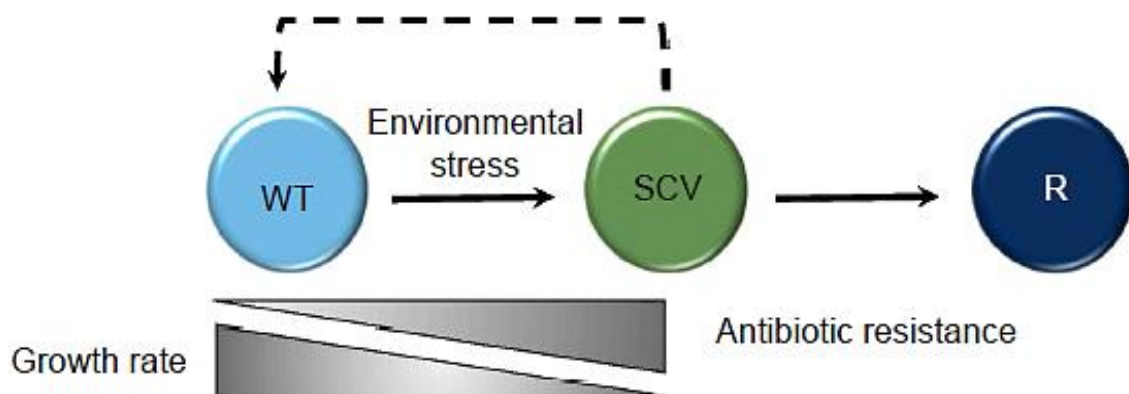


Figure 2 - Under stressful conditions, WT bacteria can undergo a shift to the SCV phenotype, exhibiting a slower growth rate but increased antibiotic resistance. They can revert to a WT-like phenotype or give rise to a new phenotype, distinct from both the progenitor and the SCV. Image from Johns *et al.* (2015).

One common characteristic of SCVs is a deficiency in electron transport, normally associated with mutations that affect the function of menadione, hemin and thiamine, which are required for biosynthesis of the electron transport chain components. Deficient electron transport leads to a decrease in the electrochemical gradient, leading to lower ATP production. Since ATP is required in large quantities for cell wall biosynthesis and production of carotenoid pigments, it may explain the decreased colony size and the colourless aspect of many SCVs (59, 60). Additionally, SCVs usually lack the small regulatory RNA molecule (RNAIII), which, in normal situations, positively regulates the production of toxins and proteases, while negatively regulating adhesins. Therefore, SCVs tend to be less toxicogenic but more prone to adhesion to biotic and abiotic surfaces (59).

SCVs constitute a serious problem in clinical settings, often being associated with recurrent and chronic infection. The extended incubation time required for their manifestation together with altered phenotypic

and biochemical properties means that SCVs might not be detected using conventional diagnostic tests. Most of the times, antibiotic treatment is interrupted before SCVs are cleared from an infection state, leading to their persistence and re-emergence (59). In fact, there are several examples corroborating the hypothesis that SCVs may favour the establishment and recurrence of infection. For instance, *P. aeruginosa* SCVs showed auto aggregative behaviour, increased biofilm formation and the capacity to adhere to a respiratory cell line (61). In the specific case of CF patients, *P. aeruginosa* SCVs led to poorer lung function and an overall worse prognosis (62). In *S. aureus*, SCVs have shown the ability to persist within the vascular endothelium, where they were able to evade the host's immune system by escaping from intracellular phagosomes (63). Another study has correlated the presence of *B. multivorans* and *B. cepacia* SCVs in the lungs of three CF patients prior to lung transplantation with the development of fatal systemic infections (64).

Recently, the genetic basis of phenotypic conversion towards the formation of SCVs was investigated in a *P. aeruginosa* chronic lung infection model. A combination of single-molecule real-time (SMRT) and Illumina sequencing revealed a large genomic inversion and a 250 bp deletion within the 16S rRNA genes, which reflected the reduced genome size of the SCVs when compared to the parent strain (65). RNA sequencing (RNA-Seq) analysis revealed that genes involved in energy metabolism, amino acid and protein biosynthesis, DNA replication and recombination, as well as cell wall/LPS/capsule biosynthesis were downregulated, which might explain the slow growth rate observed for SCVs (65). Contrastingly, genes encoding proteins that respond to oxidative stress and those encoding virulence factors were upregulated, resulting in increased virulence, which might explain the link between the appearance of SCVs in the context of lung infection and a worse clinical prognosis (65). Despite suggesting a global rewiring of genomic expression, the mechanisms underlying the aforementioned transcriptional changes are not clear and deserve further studies (65).

2.3. Bacterial Persistence and Its Implications in Chronic Infections

Antibiotic treatment failure constitutes an emergent and alarming public health concern, which is broadly attributed to the development of bacterial resistance. Although this phenomenon is responsible for the great majority of chronic infections, special attention is starting to be paid to other mechanisms, such as the formation of persister cells. Persister cell development is thought to be a universal trait and their prevalence in bacterial populations ranges from 0.001% to 1% (66). Persisters constitute a fraction within a bacterial population, composed by transiently antibiotic tolerant individuals, characterized by a slow growth rate or total growth arrest, as well as a reduced metabolic activity (67–69). Unlike antibiotic resistance, which is due to acquired genetic modifications that confer the ability to modify, degrade or export the antibiotic, persistence is a non-genetic and non-inheritable trait (66, 67). The dormant state that characterizes persister cells is responsible for their ability to survive antibiotic treatment without being genetically modified. This is achieved, for instance, through a lower antibiotic uptake combined with a decreased drug target activity (67, 68). The phenotypic heterogeneity conferred by the development of persister cells can be viewed as a factor contributing to increase the chances of successful adaptation to environmental changes (67). Isogenic bacterial populations composed by a

small fraction of persister cells are typically characterized by a biphasic killing curve (**Figure 3**). Following antibiotic treatment, the majority of the population, consisting mainly of susceptible cells, is quickly killed, following an exponential killing kinetics (68). As a consequence, the population is enriched in persister cells that survived antibiotic treatment, lowering the rate of bacterial killing (the killing curve reaches a plateau) (66). After removal of the antibiotic, the persister cells will regrow (with a more or less pronounced lag time), giving rise to a population that is as sensitive to antibiotic action as the original one and that contains a similar percentage of persisters (66).

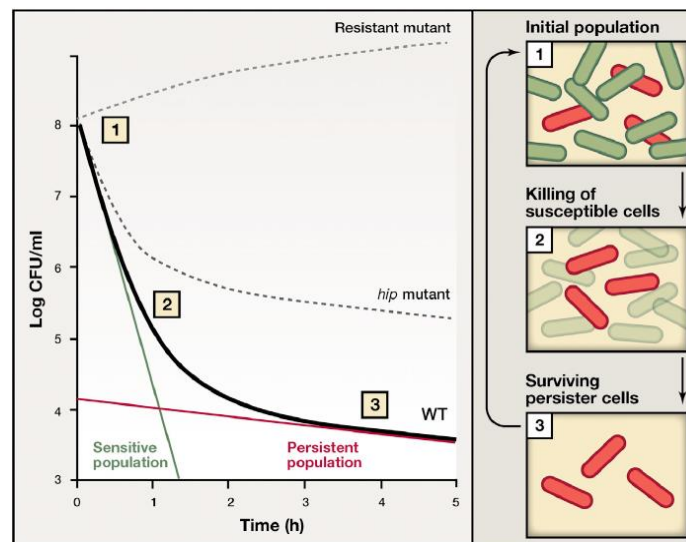


Figure 3 – Biphasic killing curve, representing the killing kinetics of a heterogeneous bacterial population, composed of regular and persister cells. Image from Maisonneuve *et al.* (2014).

2.3.1. Mechanisms of bacterial persistence

Different environmental stresses are thought to act as triggers for persister cell formation, including nutrient limitation, DNA damage, extreme pH variations and diauxic shift (67). Additionally, the formation of microenvironments that further aggravate any of these stress factors can also contribute to bacterial persistence. For example, during biofilm formation, a particularly nutrient depleted environment is created, especially towards the center of the biofilm, which could contribute to the formation of persister cells in that particular region (67, 68).

Toxin-antitoxin (TA) systems have been described as one of the major factors responsible for the formation of persister cells. These systems are typically composed of two genes, one that encodes a stable toxin protein and another that encodes an antitoxin (protein or small non-coding RNA) (68, 70). On one hand, the toxin activity might inhibit one of several metabolic processes, resulting in reduced bacterial growth. On the other hand, the antitoxin is able to bind directly to the toxin, neutralizing its effects. However, in stressful conditions, the antitoxin might be degraded, allowing the toxin to exert its effects on bacterial growth (67, 70). In Bcc species, TA systems have already been described and associated with the development of persisters. One study identified 16 pairs of genes as putative TA modules in the genome of *B. cenocepacia* J2315. From these 16 putative TA systems, 12 were also present in other *B. cenocepacia* strains (AU1054, HI2424, MC0-3 and PC184), as well as other Bcc

species, such as *B. ambifaria*, *B. multivorans*, *B. vietnamiensis*, *B. dolosa* and *B. cepacia*, demonstrating a certain level of conservation within the *Burkholderia* genus (71). The same study revealed that the overexpression of toxins that inhibited cell growth resulted in an increase of the number of persister cells (71). Moreover, 10 toxin genes were found to have a higher expression in cells residing within biofilms, in comparison to planktonic cells, suggesting that biofilm formation might also be correlated with bacterial persistence (71). Treatment of cells with tobramycin resulted in the upregulation of nine toxin-encoding genes, while treatment with ciprofloxacin did not lead to any upregulation. Overall, the results indicate that the role of TA systems in *B. cenocepacia* J1315 depends on the type of antibiotic and growth lifestyle (sessile or planktonic) (71).

2.3.2. Biofilm formation and bacterial persistence

Biofilm formation has been broadly associated with the development of chronic infections. In fact, in Bcc bacteria, it has been linked to an increased ability to cause persistent infections, especially in CF patients (72–74). It might induce the development of resistant bacteria by restricting the diffusion of antimicrobial agents, thanks to the composition of the biofilm matrix, which is rich in polymeric substances (72). However, some antibiotics can still freely penetrate biofilm structures (72, 75). Another mechanism of biofilm related persistence that has been proposed states that instead of forming a barrier against the diffusion of antibiotics, biofilms protect cells against components of the immune system (75).

In order to gain insights on the importance of biofilm formation for the success of Bcc infections, the formation of persister cells within biofilms has been object of study. The presence of persister cells residing within a *B. cenocepacia* J2315 biofilm has been reported, even after treatment with tobramycin, ciprofloxacin and fluoroquinolones (76). Persister cells were also found among planktonic cells, but in a considerably lower percentage (76). In the same study, the effects of reactive oxygen species (ROS) on the survival of persister cells were also evaluated. Transcriptomic analysis revealed that the surviving persister cells displayed a downregulation of genes involved in the major metabolic pathways, including the tricarboxylic acid (TCA) cycle and the electron transport chain. However, other proteins related to the oxidative stress response were upregulated, namely those involved in alternative metabolic pathways, like the glyoxylate shunt (76). These results suggest that persister cells inhabiting biofilms are able to redirect their metabolism in order to survive and protect themselves against environmental stress (76).

2.3.3. Exopolysaccharides (EPS) and their involvement in chronic infections

Extracellular polysaccharides, also termed exopolysaccharides (EPS) are sugar based polymers with high molecular weight, that have also been described as important factors contributing for bacterial virulence, adaptation to several stress conditions, and ultimately to bacterial persistence (77, 78).

Differences in EPS expression can lead to the formation of different colony morphotypes, which are, in turn, associated with persistent infections and the switch from acute to chronic disease (79). Conversion from mucoid to nonmucoid phenotypes has been observed in a variety of Bcc strains. A comprehensive

study involving 560 isolates from 100 patients revealed the occurrence of 15 phenotypic switches: 13 mucoid to nonmucoid transitions occurred in *B. multivorans*, *B. cenocepacia* and *B. vietnamiensis*, and 2 nonmucoid to mucoid transitions occurred in *B. cenocepacia* and *B. vietnamiensis* (80). Moreover, the nonmucoid phenotype was associated with increased disease severity, while the mucoid one, characterized by a high EPS production, was associated with persistence and decreased virulence factor production. In that sense, the nonmucoid isolates are thought to be more invasive and capable of inducing damage to the host. It was postulated that the lack of EPS production in nonmucoid isolates removes a metabolic burden, conferring those isolates a competitive advantage within the lung (80). The intensity of the mucoid phenotype in Bcc bacteria has also been inversely correlated with the rate of decline in pulmonary function, since one study indicated that CF patients exclusively infected with nonmucoid bacteria experienced a significant decline in lung function in comparison to those infected with only mucoid bacteria (81). The reasons underlying the transition from nonmucoid to mucoid phenotype remain broadly unknown, however, it was observed that the presence of antibiotics such as ceftazidime and ciprofloxacin could trigger this phenotype switch (81).

EPS have also been described as adjuvants for biofilm production, since three EPS-defective *B. cepacia* IST408 isolates were described to produce much less biofilms in comparison to the wild-type strain, demonstrating that EPS contributed for the formation of thick and mature biofilms (73). When comparing different Bcc species (*B. cepacia*, *B. multivorans*, *B. cenocepacia* and *B. stabilis*) isolated from 21 CF patients during a period of 7 years, several differences were identified in terms of EPS yield and biofilm size, suggesting that strain-related factors (e.g. differences in growth kinetics) may account for such discrepancies (73). From the persistently infected patients examined in this study, 75% had at least one highly EPS and/or biofilm producing strain. However, the other 25% make it impossible to establish a correlation between EPS and biofilm production and the development of chronic infections (73).

EPS are also thought to have a protective role against environmental stress, namely desiccation, presence of antibiotics, binding of toxic metal ions and predation by competing pathogens (77–79). The hygroscopic properties of EPS, together with the ability to form a hydrated anionic matrix that encapsulates bacterial cells might contribute for reducing water loss, allowing survival in dry conditions (82). One study revealed that when two Bcc soil isolates of *B. multivorans* and *B. xenovorans* were dried in the absence of the EPS cepacian, a drastic reduction of cellular viability occurred in the first 24 hours of exposure and both strains were completely eliminated after 3 days. On the contrary, cells dried in the presence of cepacian could remain viable for up to 7 days, demonstrating the importance of EPS production (79). The same study also indicated that EPS plays an important role in protecting cells against iron stress, while the presence of carbonyl, carboxyl and hydroxyl groups within the EPS matrix might allow the formation of complexes with cations, namely metal ions (77, 78, 82). In terms of protection against antimicrobial activity, cepacian has been shown to form complexes with positively charged antimicrobial peptides, due to the negative charge conferred by its acetyl substituents. These complexes are thought to lower the antimicrobial peptides' biological activity (83).

2.4. Bcc Bacteria as Contaminants of Pharmaceutical Products

2.4.1. Product recalls associated with the presence of Bcc bacteria

Burkholderia cepacia (whether the species was definitively identified as *B. cepacia*, the type species, or just meaning a member of the *Burkholderia cepacia* complex) is reported as one of the most common contaminants of pharmaceutical products, being transmitted through raw materials, water used in pharmaceutical manufacturing and also on machine surfaces (84). According to the United States Food and Drug Administration (FDA) recall data, from 1998 to 2006, *B. cepacia* was identified as the cause of 22% of non-sterile products recalls (3). This tendency has grown over the last years, with this species being associated with 34% of the non-sterile product recalls from 2004 to 2011 (3). From January 2012 to July 2012, *B. cepacia* was considered the most frequent microbial contaminant found in non-sterile products, corresponding to 39% of the bacterial species isolated from contaminated product samples (Figure 4) (84).

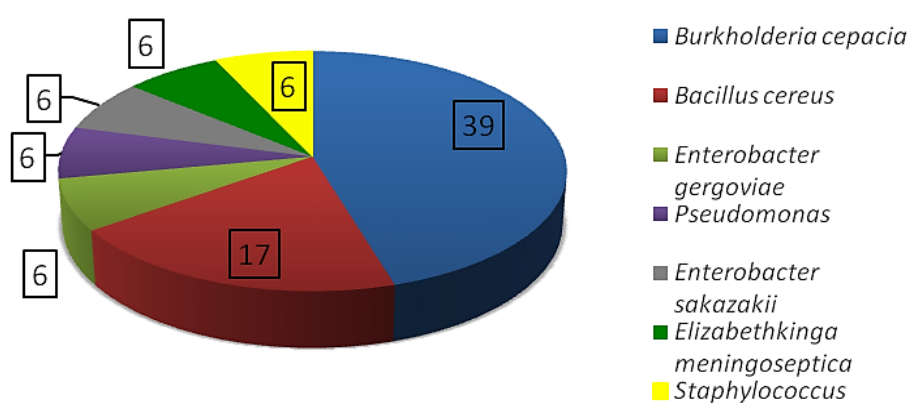


Figure 4 - Representativeness (in percentage) of the bacterial species isolated from pharmaceutical products in the first semester of 2012. Image from Jimenez *et al.* (2015).

In an epidemiological survey performed by our group between 1995 and 2002, which included patients under surveillance at the major Portuguese CF center at a central Lisbon Hospital, an unusually high prevalence of *B. cepacia* was detected in sputum cultures (15). Later on, a market surveillance performed by INFARMED, the National Authority of Medicines and Health Products, in 2003 and 2006, detected Bcc bacteria contamination in several batches of non-sterile saline solutions for nasal application. Since saline solutions are often administered to CF patients, a correlation between these contamination events and the prevalence of *B. cepacia* was hypothesized. Further analysis confirmed that the clinical clones obtained from CF patients and the strains identified in saline solutions were epidemiologically related (16).

Bcc bacteria have been found as contaminants of diverse types of pharmaceutical and personal care products, including nasal sprays (15), multiple lotions and oils (3), water-based products (122), mouthwash (139), (115), cleansing washcloths and baby wipes, pre-operative skin solutions, hand sanitizers (120) and gas relief liquid drops (3), (84). In recent years, FDA has launched several alerts concerning the presence of Bcc bacteria in a wide variety of products (85). In October 2016, FDA in collaboration with the Centre of Disease Control (CDC), detected the presence of *B. cepacia* in the water

system used for the manufacture of oral liquid docusate sodium. This resulted in a national alert and the product was voluntarily recalled from the market by its producing pharmaceutical company (86). In 2017, FDA detected a potential contamination of decongestant relief syrups for the treatment of cough, cold and allergies with *B. cepacia*, advising a voluntary recall of the products from the market (87). More recently, in 2018, FDA detected several microbial contaminants in homeopathic drug products, including *B. multivorans*. The regulatory agency recommended the recall of all water-based products from that company (88).

2.4.2. Bcc bacteria ability to survive and proliferate in pharmaceutical products

The presence of Bcc species in pharmaceutical products is associated with the intrinsic genetic, metabolic and phenotypic features that characterize these bacteria (89, 90). Since Bcc bacteria can use a great variety of organic compounds as carbon and energy sources, several of them xenobiotic compounds of very difficult catabolism (38, 91), these bacteria can grow and proliferate in pharmaceutical products, catabolizing active ingredients and excipients (5). One example is the oxidation of aromatic structures and breakdown of halogenated compounds through the action of monooxygenases and dioxygenases, allowing growth on nitroaromatic and aromatic compounds (92, 93). Since nitroaromatic compounds make up a vast array of pharmaceutical drugs, Bcc bacteria can lead to the degradation of the active ingredients and excipients, compromising the stability and purity of the drugs, as well as their potency and effectiveness (5, 94). This poses a serious health threat to the consumers of such products, who typically suffer from pathological conditions. Products contaminated with Bcc strains constitute a vehicle for the transmission of these opportunistic pathogens to susceptible patients, favouring the development of life-threatening chronic infections.

2.4.3. Reasons underlying Bcc contamination in pharmaceutical settings and preventive measures

The persistence of *B. cepacia* in pharmaceutical products is greatly attributed to the lack of good manufacturing practices (GMP). Pharmaceutical companies are responsible for the quality control of their products as well as for monitoring the processing steps and the components that are used (95). However, the inexistence of adequate cleaning procedures, the use of unsuitable grade water associated with poor water control and design systems, insufficient microbiological controls and application of the same disinfectants for long periods of time constitute some of the main causes of bacterial contamination in pharmaceutical settings (84).

According to the Parenteral Drug Association (PDA) Technical Report No. 67 – “Exclusion of Objectionable Microorganisms from Nonsterile Pharmaceutical and Over-the-Counter (OTC) Drug Products, Medical Devices and Cosmetics”, an objectionable organism is defined as a microorganism which is able to proliferate in a certain pharmaceutical product, causing adverse effects on its chemical, physical, functional and therapeutic properties (96). This definition also comprises microorganisms with a pathogenic character that, when present in high numbers, can cause infection upon administration (3, 96, 97). The high prevalence of product recalls and the numerous nosocomial outbreaks verified

throughout the years, owing to Bcc contamination of both sterile and non-sterile products (3, 5, 84, 90) are among the main reasons behind their inclusion in the objectionable microorganisms category. Moreover, their role as human opportunistic pathogens (in both CF and non-CF patients) (4, 34) and their unique ability to overcome antibiotics and antimicrobial preservatives' action also contribute for that designation (9, 10, 89, 98).

The United States Pharmacopeia (USP) provides several guidelines and methodologies to detect the presence of specific indicator organisms in non-sterile products, namely the USP chapters <61> Microbial Enumeration Tests (99) and <62> Tests for Specified Microorganisms (100). However, despite the fact that Bcc bacteria are widely recognized as objectionable organisms, the USP does not provide any specific test to determine their presence in non-sterile drug products (84, 89). Due to the lack of information and adequate detection methods, Bcc contamination is often disregarded, since these microorganisms are not considered a priority for pharmaceutical manufacturers, who are often unaware of their impact and the consequences that might result from releasing Bcc contaminated products in the market (89).

Nowadays, the high number of product recalls due to Bcc contamination remains a topic of major concern for FDA and has prompted the emission, on May 2017, of a new regulatory guide for manufacturers of non-sterile, water-based drug products, stating the importance of establishing measures to prevent contamination with such objectionable organisms, including correct process design and quality assurance of incoming materials, as well as monitorization of storage conditions and cleaning procedures (101). In the specific case of Bcc bacteria, antimicrobial preservatives are not effective as a way of preventing contamination, since several strains are able to proliferate in preserved solutions (89). In that sense, manufacturers cannot rely on the addition of antimicrobial preservatives for contamination control and must, instead, apply stringent in-process control and guarantee sterile conditions during the manufacturing process (89, 95, 102). Water is the most commonly used raw material in pharmaceutical settings and is considered a frequent source of Bcc contamination. In fact, several Bcc outbreaks that occurred throughout the years have identified pharmaceutical grade water as the root cause of product contamination (102). Therefore, in industrial settings, every piece of equipment used for processing (tanks, pumps, filling lines) should be properly cleaned, disinfected and dried, especially the product contact surfaces (102).

Both the FDA and USP have provided technical guides concerning the water used for pharmaceutical manufacturing. Potable water might only be used for bulk drug manufacturing and not to prepare USP compliant dosage form products or laboratory reagents. Non-potable water systems, such as cooling water for air conditioning or fire sprinklers, should be correctly identified and cross-connections with potable water must be avoided (103). Regular collection of water samples from piping systems should be a common practice, since these constitute one major source of contamination. Maintaining the water circulation systems at constantly high temperatures (typically 80°C) is also advised to prevent significant microbial growth (103). Additionally, during formulation of aqueous oral and topic dosage form products, a reduced water activity (a_w) is important to prevent microbial contamination and to guarantee the product's self-preservation capacity (104). Pharmaceutical products with a_w below 0.75 are significantly

less prone to contamination, while nasal inhalants, hair shampoos and antacids, which have high water activities ($a_w = 0.99$) are very susceptible to contamination by Gram-negative bacteria, namely Bcc (104).

2.5. Unique Ability of Bcc to Overcome Biocide Action, In Particular Benzalkonium Chloride

2.5.1. Bacterial resistance to biocides and associated implications

The term biocide is generally employed to describe a chemical agent, usually with a broad spectrum, that inactivates microorganisms. A wide variety of biocides are found as components of antiseptics and disinfectants, which have been used for hundreds of years for antiseptics, disinfection and preservation (105). Biocides can be classified into 22 categories, based on their respective functional groups. In terms of the target of action, these chemical agents are divided into four classes: those that exert their action on proteins, membrane, nucleic acids and cell wall (106). The mode of action of biocides is not as extensively studied as that of antibiotics but, in general, biocides have a broader spectrum of activity and tend to act upon multiple targets, whereas antibiotics usually have specific intracellular targets (105). In recent years, there has been a rising concern about the application of biocides in common use products, due to the emergence of resistant/more tolerant bacteria after exposure to suboptimal or sublethal concentrations of biocides. It is even possible that some biocides might induce cross-resistance to antibiotics due to common resistance mechanisms (106).

The mechanisms of resistance to biocides can be intrinsic or acquired through mutation events or horizontal gene transfer. Gram-negative bacteria generally have a higher inherent resistance to biocides when compared to Gram-positive bacteria. The structure of the outer membrane of Gram-negative bacteria might be the reason behind such resistance, since it acts as a barrier against the entry of many antibacterial agents. The presence of an intact highly charged lipopolysaccharide (LPS) layer is an intrinsic characteristic that helps prevent the diffusion of hydrophobic antimicrobials (105, 106). Activation of efflux pump systems is one of the major mechanisms of intrinsic biocide resistance adopted by Gram-negative bacteria. The most relevant family of efflux pumps regarding antimicrobial resistance comprises the resistance-nodulation-cell division (RND) transporters. These are usually chromosomally encoded and composed by a periplasmic membrane fusion protein and an outer membrane factor, causing efflux across both the inner and outer membranes, without accumulation in the periplasm (107). Genomic expression analysis of two sequential *B. cenocepacia* isolates recovered from a cystic fibrosis patient revealed an increased transcription of various genes encoding efflux pumps, namely those encoding RND transporters, drug efflux pumps of the Major Facilitator Superfamily (MFS), as well as ATP-binding cassette (ABC) transporters (108). Simultaneously, a reduced outer membrane permeability was observed, which could be related with the downregulation of genes encoding porines that may function as channels for the entry of antibiotics (108). Phenotypic adaptations, such as biofilm formation, can also be considered intrinsic resistance mechanisms. Within the biofilm, the access of the biocide to the cells is reduced and a microenvironment modulation is likely to occur, resulting in regions of low nutrient availability, which might affect the bacterial growth rates and overall susceptibility to antimicrobials (105).

In terms of acquired resistance, it can occur through mutations in genes responsible for the formation of the cell wall, membrane lipids, porins or OMPs. Horizontal gene transfer may contribute to the acquisition of mobile genetic elements like plasmids or genes that encode proteins responsible for the modification/degradation of the biocide (including α -phosphotransferases, α -adenyltransferases and n -acetyltransferases), which might also be achieved via alteration of pre-existing genes (106). Target alteration is another mechanism by which microorganisms gain resistance. For instance, in *E. coli*, a missense mutation in the FabI protein is sufficient to alter the target site for triclosan, conferring resistance to that compound (106). The main mechanisms that confer Gram-negative bacteria resistance to biocides are summarized in **Figure 5**.

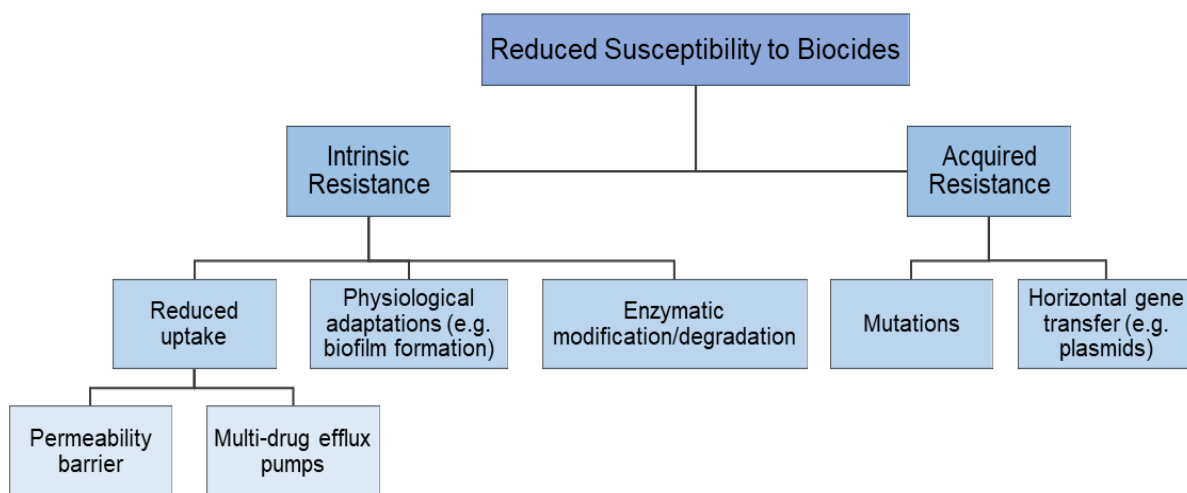


Figure 5 - Schematic description of the main intrinsic and acquired mechanisms for reduced susceptibility to biocides adopted by Gram-negative bacteria.

2.5.2. Contamination of solutions containing benzalkonium chloride

Benzalkonium chloride (BZK) is a biocide that belongs to a group of cationic membrane-acting agents, termed quaternary ammonium compounds (QACs), which are characterized by a positively charged nitrogen covalently bonded to three alkyl group substituents and a benzyl substituent (11, 109). BZK is a mixture of alkylbenzyltrimethylammonium chlorides, with chain lengths of C12, C14 and C16. It is used as an antimicrobial preservative for pharmaceutical products, being the biocide of choice for the majority of multidose aqueous nasal and ophthalmic products. It acts as a bactericidal and fungicidal to minimize microorganism growth in multidose containers (110).

From all antiseptics, contaminated BZK solutions have been described as the major cause of nosocomial outbreaks, which occur mainly because of improper product utilization, namely through the use of contaminated water in manufacturing processes, over-diluted antiseptic solutions, the use of outdated products, storage for prolonged periods of time after opening or improper storage conditions, such as the use of gauze or cotton for that purpose (6, 8). The use of preservatives beyond the expiration date is risky, because changes in the chemical concentration or composition are likely to occur, leading to a decreased bactericidal/bacteriostatic potency (8). In fact, there are several reports stating that Bcc

bacteria are able to survive in solutions preserved with BZK (6, 98). The ability of Bcc bacteria to survive and thrive for long periods of time in BZK solutions raises an alarming concern in terms of public health, since they can be transmitted to patients through the use of contaminated products and cause subsequent problems. Contaminated solutions may appear clear and therefore difficult to distinguish from truly sterile solutions (7). The typical concentrations of BZK used in a variety of commercial products range from 0.02% (200 µg/mL) to 5% (50,000 µg/mL), which might not be sufficient to eradicate resistant strains (9).

BZK's effects occur mainly at the level of membrane permeability, starting with its adsorption and penetration onto the bacterial cell surface. Then, the chemical binds and reacts with the cytoplasmic membrane containing acidic phospholipids, causing its destabilization/disorganization. Following that, leakage of cellular constituents (namely low molecular weight material) takes place, followed by degradation of proteins and nucleic acids, as well as cell wall lysis induced by autolytic enzymes. The hole process culminates in cell death, due to the loss of structural organization and integrity of the cytoplasmic membrane (105, 109, 111). Cationic compounds are particularly effective at adhering and penetrating the cell surface and integrating into the cytoplasmic membrane, thanks to their strong positive charge and hydrophobic region, allowing interaction with the outermost surface of bacterial cells, which is typically negatively charged (111).

2.5.3. Bcc bacteria ability to catabolize and resist to BZK: the degradation pathway

Early studies have identified a strain of *B. cepacia* that remained viable for 14 years under nutrient limitation in a saline solution supplemented with 0.05% BZK (7). More recently, the BZK susceptibility of 36 different Bcc strains that had been incubated in distilled water for 40 days was assessed through minimum inhibitory concentration (MIC) assays (9). The results indicated that although the majority of the Bcc strains became more vulnerable to BZK's effects, six *B. cenocepacia* strains still retained a high level of resistance to the biocide (9). The same study has also reported that clinical strains of *B. contaminans*, *B. multivorans*, *B. vietnamiensis* and *B. ambifaria* were better recovered after 14 days in the presence of BZK rather than in the first 24 hours (9). These observations suggest that BZK might be catabolized inside the cell, being degraded to inactive products, which can be used as carbon sources for bacterial growth (9). More recently, the antimicrobial effects of BZK at sublethal concentrations (10-50 µg/mL) were compared on six *B. cenocepacia* strains. All strains remained viable and with low susceptibility to the antiseptics upon incubation at 23°C for 28 days (8).

An extensive study on the resistance of Bcc bacteria to BZK was performed, exploring the possible role of efflux pumps, the potential of Bcc bacteria to degrade BZK and the proteomic changes induced in response to that biocide. All of the 20 Bcc strains tested were able to partially degrade (4.7 - 42.6% degradation) BZK in a period of 7 days (10). Proteomic analysis revealed that treatment with BZK resulted in a rapid and dynamic alteration in the expression pattern of several proteins at a genome-wide level. Genes encoding proteins of the major facilitator superfamily (Bcen_0548 and Bcen_4138) and of the RND family (Bcen_3015 and Bcen_4471), which are involved in multidrug efflux pumping, were upregulated (10). The pathway for BZK biodegradation was suggested to start with its N-

dealkylation (fission of the central C-N bond), yielding benzyldimethylamine (BDMA) and benzylmethylamine (BMA), which might be performed by an amine oxidase (Bcen_5179) or a Rieske-type oxygenase (Bcen_4588) (**Figure 6**). Subsequent demethylation and deamination reactions lead to the formation of benzylamine (BA) and benzaldehyde (10, 112). Dehydrogenation of benzaldehyde can result in the formation of benzoate, which in turn can give rise to the toxic intermediate catechol (**Figure 6**). All of the enzymes responsible for benzoate degradation were upregulated, including a catechol 1,2-dioxygenase (Bcen_1307), suggesting the generation of acetyl-CoA and succinyl-CoA. The aldehyde resultant from the initial N-dealkylation of BZK can also be oxidized to a fatty acid, conjugated with CoA and further processed by β -oxidation (**Figure 6**). The enzymes responsible for this process were also upregulated (10).

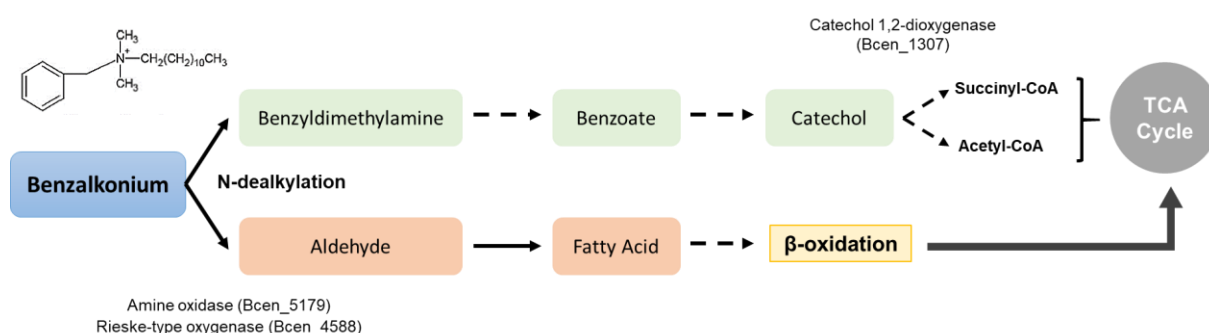


Figure 6 - Representation of the possible pathways responsible for BZK degradation in *B. cenocepacia* AU1054. Only the main reactional steps are schematized. One-step reactions are indicated by solid arrows, while reactions involving more than one step are indicated by dashed arrows. Image adapted from Ahn *et al.* (2016).

The data acquired in the study referred above suggest an innate ability of *B. cenocepacia* to resist BZK's action, which may involve extrusion of the chemical by chromosomally encoded efflux pumps and inherent production of metabolic enzymes capable of degrading the biocide. These two mechanisms seem to work synergistically to accelerate the development of resistance (10). From the toxicological point of view, the cleavage of the C-N bond in the early steps of the degradation pathway might be favourable for Bcc bacteria, reducing BZK's toxic effects. Finally, the ability of Bcc bacteria to generate acetyl-CoA, which can be used in the central carbon metabolism, allows the utilization of alternative energy and carbon sources, besides being an effective way of degrading BZK without accumulation of intermediates or toxic metabolites (10).

2.6. Contamination Outbreaks in Healthcare Settings

Throughout the years, a growing body of evidence has confirmed the impact of Bcc bacteria outbreaks, with multiple case-studies being reported in order to identify the sources of these bacteria and their implications in clinical settings. The majority of the cases in which Bcc bacteria have been detected in clinical samples have an environmental origin, typically from contaminated pharmaceutical/personal care products. Contamination of medical products can be classified as extrinsic, when it is induced during use of the product, or intrinsic, meaning that the product was already contaminated before use. The easy cross-transmission of Bcc bacteria is particularly worrying, since it facilitates the rapid

spreading of infections between different wards within the same facility, or even between hospitals situated in different regions of a country (113).

Bcc outbreaks have occurred in different settings including neonatal, pediatric and adult intensive care units, affecting both CF and non-CF patients. The types of products identified as sources of Bcc contamination are diverse, including anaesthetic eye drops (114), mouthwash solution (115), fentanyl infusion (21), ultrasound gel (22), antiemetic drugs (116), chlorhexidine solutions (117–119), liquid soap (120), caffeine citrate (121), distilled water (122), dextrose solutions (123), catheters (124), liquid docusate (125, 126), filters and water oxygen humidifiers (127), washing gloves (128), ventilators (129) and saline flush syringes (130) (**Table 2**).

Table 2 - *Burkholderia cepacia* complex related outbreaks described in the literature published during the past five years. The Bcc outbreaks that have occurred in different settings and the diverse types of products identified as sources of Bcc contamination are summarized.

Species	Product	Location	Year(s)	Information about the patients	Number of patients affected	Ref.
<i>B. cepacia</i>	Anaesthetic eye drops	Madurai, India (Aravind Eye Hospital)	December 2011 – February 2012	Patients who undergone cataract surgery and developed acute postoperative endophthalmitis	13	(114)
<i>B. cepacia</i>	Intrinsically contaminated alcohol-free mouthwash solution	General medical intensive care unit, Vozandes Hospital, Quito, Ecuador	March 2011 – May 2012	Ventilated, 3 developed ventilator associated pneumonia, non-CF patients	13	(115)
<i>B. contaminans</i>	Continuous fentanyl infusion prepared by institutional compounding pharmacy	Duke University Hospital, Durham, North Carolina	August 31 – September 6 2012	1 child, 6 adults Anaemia, cirrhosis, hepatic failure, trauma, HIV, infectious endocarditis, peritonitis	7	(21)
<i>B. cepacia</i>	Ultrasonic couplant	Hospital in Zhongshan, China	May 2013	Post C-section patients	4	(131)
<i>B. cepacia</i>	Antiemetic drug granisetron	Mumbai, India (day care unit of private hospital)	End of 2009	Cancer patients with tunnelled catheters	13	(116)
Bcc bacteria	0.5% chlorhexidine solution	Seoul, Republic of Korea (Boramae medical centre)	October 10 – December 16 2013	N/R	40	(117)

<i>B. stabilis</i>, <i>B. contaminans</i>, and <i>B. ambifaria</i>	Intrinsically contaminated ultrasound gel	Neonatal and adult intensive care units, Argentina	April – July 2013	7 preterm neonates with respiratory distress, 3 ICU patients who undergone recent cardiovascular surgery, 1 General Ward patient	11	(22)
<i>B. stabilis</i>	N/R	500-bed tertiary hospital in Beijing, China, ophthalmology and otolaryngology	March 19 – September 20 2013	Chronic bacterial or fungal sinusitis	53	(132)
<i>B. cepacia</i>	N/R	Haemodialysis centre, La Linea de la Concepción, Cadiz.	November 2013 – February 2014	N/R	7	(133)
<i>B. cepacia</i>, <i>B. contaminans</i>	Non-sterile saline solutions for nasal application	Major Portuguese CF center in Lisbon	2003-2005	CF patients		(16, 17)
<i>B. cepacia</i>	N/R	USA	February 1 – May 13 2016	Pediatric, Non-CF	18	(134)
Bcc bacteria	Liquid soap	Near East University Hospital, Nicosia, Cyprus	November 2013	Sickle cell anaemia	1	(120)
<i>B. cepacia</i>	Caffeine citrate	Neonatal intensive care unit, India	September – October 2015	Preterm infants	7	(121)
<i>B. cepacia</i>	Intravenous solutions of 5 % dextrose, normal saline (opened bottles) and continuous positive airway pressure humidifier water	Neonatal intensive care units of 2 hospitals, India	January – March 2014	Neonates, 10 preterm, 11 showed signs of sepsis	12	(123)
Bcc bacteria	Distilled water	Pediatric intensive care unit, Father Muller Medical College, India	N/R	Pediatric patients, 1 with subaortic ventricular septal defect, 1 with rhabdomyosarcoma, on chemotherapy, 1 with pneumonia and pneumothorax	3	(122)
Bcc bacteria	Central venous catheter, pneumonia	US Veterans Health Administration medical centers	1 January 1999 – 31 December 2015	Non-CF, advanced age, chronically ill, severe disease	248	(124)

Bcc bacteria	Liquid docusate	629-bed, tertiary-care, pediatric hospital in Houston, Texas	February 8 – July 4, 2016	Pediatric, Non-CF	24	(125)
Bcc bacteria	N/R	Urology clinics, Jordan	N/R	3 uncomplicated infections + 1 recurrent infection	4	(135)
<i>B. cepacia</i>	Flow filter, haemodialysis water, water oxygen humidifier	Haemodialysis unit, Regional Hospital Coronel Oviedo, Paraguay	November 2013 – February 2014	N/R	N/R	(127)
<i>B. cenocepacia</i>	Gel packaged in sachets for use within the sterile ultrasound probe cover	4 hospitals across Australia	March 26, 2017 – April 7, 2017	Patients with significant pre-existing morbidities	11	(136)
<i>B. stabilis</i>	Commercially available washing gloves	9 institutions in Switzerland	May 2015 – August 2016	Bloodstream and non-bloodstream infections	46	(128)
<i>B. cepacia</i>	Ventilators	General 1,600-bed hospital, Beijing, China	June 1-14 2015	Ventilator-associated pneumonia	4	(129)
Bcc bacteria	Rubber stopper of sealed multidose amikacin injection vials	Paediatric ICU (PICU) and the paediatric ward of a tertiary care hospital, India	June 2012 – January 2013	Children, with peripheral IV catheters	76	(137)
<i>B. cepacia</i>	Ultrasound probe gel	Referral hospital in Riyadh, Saudi Arabia	January 8 – June 15 2016	Non-CF patients	15	(138)
<i>B. cepacia</i>	Oral Liquid Docusate Sodium	Pediatric intensive care unit, The Johns Hopkins Hospital, Baltimore, Maryland, USA	May 19, 2017 – July 30, 2017	Infants with multiple chronic medical conditions	8	(126)
Bcc bacteria	Octenidine mouthwash solution	Cardiothoracic intensive care unit in Germany	August – September 2018	Critically ill, post-cardiac surgery patients	3	(139)
Bcc bacteria	Saline Flush Syringes	59 nursing facilities in 5 states of USA	September 2016 – January 2017	N/R	162	(130)
<i>B. lata</i>	Chlorhexidine Mouthwash	2 tertiary hospitals in Australia	May – June 2016	Intensive care patients	8	(140)

Bcc bacteria	Prefilled syringe containing liquid docusate	16 facilities in USA	February 2016	Infants, children, adults and older adults (80 mechanically ventilated and 41 with feeding tubes)	108 (63 confirmed and 45 suspect cases)	(141)
<i>B. cepacia</i>	Intrinsically contaminated commercial 0.5% chlorhexidine solution	600-bed university-affiliated teaching hospital in Korea	November 2014 – January 2015	Infants, mostly preterm, with respiratory distress syndrome	21	(118)
<i>B. cepacia</i>	4% chlorhexidine aqueous bodywash	Peritoneal Dialysis Unit, Middlemore Hospital, Auckland, New Zealand	N/R	Dialysis patients with peritoneal catheters	9	(119)
<i>B. cepacia</i>	N/R	Tertiary hospital, Turkey	2013-2018	N/R	46	(142)
<i>B. cepacia</i>	N/R	Neurotrauma critical care unit of a level 1 trauma care centre in India	August - November 2014	Mostly patients with head and spinal trauma	48 (15 of which with central line-associated bloodstream infections)	(143)
<i>B. contaminans</i>	N/R	Regional CF Centre of Policlinico Umberto I Hospital, Sapienza University of Rome, Italy	May-June 2008	CF patients	2	(23)

3. MATERIALS AND METHODS

3.1. Bacterial Isolates

In the present study, clonal variants of two Bcc strains (*B. cepacia* and *B. contaminans*), obtained from contaminated saline solutions for nasal application and from respiratory secretions of CF patients were selected (**Table 3**). The clinical isolates were obtained from sputum samples of two chronically infected CF patients (here designated patients AL and V), under surveillance at the major Portuguese CF Center in Hospital de Santa Maria (HSM), Centro Hospitalar Lisboa Norte (CHLN) EPE, from 2003 to 2006. Patient AL had been infected with a *B. cepacia* strain correspondent to the *recA* restriction fragment length polymorphism (RFLP) profile D and ribopattern 19 (16), while patient V harboured a *B. contaminans* strain correspondent to a *recA* RFLP profile E and ribopattern 17 (16, 17). Studies involving these isolates were approved by the CHLN ethics committee and the anonymity of the patients was safeguarded. Informed consent was also obtained from all participants and/or their legal guardians. All the methods were performed according to the relevant guidelines and regulations.

The isolates from saline solutions examined in the present study (22 from *B. cepacia* and one from *B. contaminans*) were obtained from batches of non-sterile saline solutions verified to exceed the microbiological quality limits established by the European Pharmacopoeia VII. Bacterial contamination was detected as part of a routine market surveillance performed by the Portuguese Medicines and Health Products Authority (INFARMED) by the end of 2003 and in March 2006 (16). Bacterial cultures of each isolate are currently stored at -80°C in glycerol at a proportion of 1:1 (v/v).

Assessment of clonal nature and phylogenetic analysis were performed for the 22 *B. cepacia* saline solutions' isolates. Phenotypic studies were also performed for five *B. cepacia* and four *B. contaminans* isolates from our laboratory collection. Among the *B. cepacia* isolates, three were recovered from patient AL (IST4152, IST4168 and IST4222) and two were obtained from contaminated saline solutions detected in 2003 and 2006 (IST612 and IST701, respectively). Within the *B. contaminans* isolates, three were recovered from patient V (IST4148, IST4241 and IST4224) and one was isolated from contaminated saline solutions detected in 2003 (IST601). These isolates had already been selected, in a previous work from our laboratory, to study the effects of long-term incubation in saline solutions supplemented with BZK, during a 10-months incubation period (144). In the present work, the behaviour of the same isolates incubated in the previous conditions was further analysed, totalling an 18-months incubation period.

Table 3 - List of clonal isolates from *B. cepacia* and *B. contaminans* used in this study. The isolates selected to study the effects of long-term incubation in saline solutions supplemented with BZK are indicated in bold and underlined.

Isolate Source	Species	Isolate ID	Isolation Date	<i>recA</i> RFLP profile	Ribopattern	Reference
Patient AL	<i>B. cepacia</i>	<u>IST4152</u>	October 2003	D	19	
		<u>IST4168</u>	May 2004	D	19	
		<u>IST4222</u>	December 2005	D	19	
Patient V	<i>B. contaminans</i>	<u>IST4148</u>	September 2003	E	17	
		<u>IST4241</u>	June 2004	E	17	
		<u>IST4224</u>	December 2005	E	17	
Saline Solutions	<i>B. contaminans</i>	<u>IST601</u>	2003	-	-	Cunha <i>et al.</i> (2007) (16, 17)
	<i>B. cepacia</i>	<u>IST612</u>	2003	-	-	
		IST621	2003	-	-	
		IST623	2003	-	-	
		IST624	2003	-	-	
		IST625	2003	-	-	
		IST626	2003	-	-	
		IST627	2003	-	-	
		IST628	2003	-	-	
		IST629	2003	-	-	
		<u>IST701</u>	March 2006	-	-	
		IST702	March 2006	-	-	
		IST704	March 2006	-	-	
		IST705	March 2006	-	-	
		IST706	March 2006	-	-	
		IST707	March 2006	-	-	
		IST708	March 2006	-	-	
		IST710	March 2006	-	-	
		IST711	March 2006	-	-	
		IST712	March 2006	-	-	
		IST713	March 2006	-	-	
		IST714	March 2006	-	-	
IST715	March 2006	-	-			

3.2. Random Amplified Polymorphic DNA (RAPD) Typing

To confirm the clonal nature of the 22 *B. cepacia* isolates obtained from saline solutions, RAPD analysis was conducted. This technique constitutes a PCR-based approach that is used to randomly amplify segments of genomic DNA, with the aim of identifying stable and discriminatory polymorphisms with high throughput and in a reproducible manner. The use of RAPD has already been reported in the literature for differentiating collections of *B. cepacia* and *P. aeruginosa* isolates (145, 146). Three 10-

base RAPD primers were selected for the analysis, based on their previously reported ability to produce fingerprinting profiles from *B. cepacia* (145). Primer 270 (5' TGCGCGCGGG 3') was used for a primary typing of the isolates and primers 208 (5' ACGGCCGACC 3') and 272 (5' AGCGGGCCAA 3') were used to confirm the strain types obtained in the first assessment with primer 270 (145).

Total genomic DNA was extracted from the 22 *B. cepacia* isolates, which had previously been grown overnight in liquid LB medium, at 37°C and with orbital agitation at 250 rpm. The extraction was performed using the Puregene® DNA Purification Kit (Gentra Systems, Qiagen, Germany), following the manufacturer's specifications for DNA purification from Gram-negative bacterial cultures. The genomic DNA concentration and purity was assessed using a ND-1000 spectrophotometer (NanoDrop, Thermo Fisher Scientific). The ratios of sample absorbance at 260/280 nm and at 260/230 nm were considered for purity assessment.

RAPD PCR reaction mixtures were prepared, each containing 50 ng of bacterial DNA (50 ng/µL), 1 µL of the respective primer (270, 208 or 272), 2.5U of Speedy Supreme NZYTaQ 2X Green Master Mix (NZYTech) and nuclease free water, up to a final volume of 25 µL. The reaction mixtures were then amplified in a GTC965 Thermal Cycler (Clever Scientific Ltd.). The temperatures, number of cycles and respective durations are specified in **Table 4**.

Table 4 - Specifications of the PCR programme employed for RAPD analysis of the 22 *B. cepacia* isolates from saline solutions examined in this study.

Temperature (°C)	Duration (mins)	Number of Cycles
94	5	4
36	5	
72	5	
94	1	30
36	1	
72	2	
72	10	1

The PCR products were then separated by electrophoresis in 1.5% agarose gels (NZYTech), previously stained with Gel Red (NZYTech), at 90V for approximately 2h30min. The total sample volume (25 µL) was used to load the gels. Molecular size markers (1 Kb Plus DNA Ladder, Invitrogen) were included in all gels, together with 10X loading buffer (Takara Bio Inc.). Finally, the gels were observed and photographed using the GelDoc™ XR software from Bio-Rad.

3.3. Long-Term Incubation of the Bacterial Isolates in Saline Solutions and in the Presence of BZK

To follow the bacterial populations' behaviour during extended incubation in stress conditions induced by the lack of nutrients and the presence of BZK, isolates from *B. cepacia* (IST612, IST701, IST4152, IST4168 and IST4222) and *B. contaminans* (IST601, IST4148, IST4241 and IST4224) were selected (refer to **Table 3** for detailed information about the isolates) and used to induce artificial contamination of saline solutions, in an experiment independent from this work (144). In the present study, not only the effects of long-term incubation were evaluated (from 12 to 18 months of incubation), but some phenotypic traits were also assessed during the early stages of incubation (up to one month) in order to compare the bacterial populations' stress responses in a chronologic manner.

When needed, bacterial cultures of each isolate, stored frozen at -80°C in 1:1 (vol/vol) glycerol, were streaked onto *Pseudomonas* Isolation Agar (PIA; Difco) plates and incubated at 37°C for 48h. An overnight culture of each isolate was prepared in liquid Luria-Bertani broth (LB; Difco) and incubated at 37°C with agitation at 250 rpm. Culture concentration was then adjusted to an Optical Density (OD) at 640 nm of 0.05, in a final volume of 50 mL of LB medium and incubated under the same temperature and agitation conditions, until reaching mid-exponential phase. After the incubation period, cultures were centrifuged for 10 minutes, at 7000 rpm and 20°C, followed by two subsequent washing steps with NaCl 0.9% (w/v). Finally, cells were resuspended in 50 mL of NaCl 0.9% (w/v). The OD_{640nm} of washed cells was assessed, adjusted to 0.2 (estimated to correspond to approximately 10⁷ CFU/mL) and used to inoculate glass flasks, in a final volume of 125 mL of saline solution (NaCl 0.9% (w/vol)). This condition was intended to mimic a nutrient depleted environment. To study bacterial adaptation to the presence of antimicrobials, the same procedure was applied, and the isolates were inoculated into glass flasks containing BZK solutions at two different concentrations: 0.0053% (w/v) (sub-minimum inhibitory concentration) and 0.05% (w/v) (above the MIC value) (9).

To prepare the BZK solutions, the respective amounts of the biocide were weighed and suspended in NaCl 0.9% (w/vol). Before being added to the glass flasks, the solutions were filtered using 0.2 µm pore size filters (Whatman). To simulate the typical storage conditions employed in the pharmaceutical industry for this type of products, the flasks were incubated at 23°C, in the dark, without agitation, during the entire course of the experiment.

3.4. Viability and Morphology Studies

Cellular viability was assessed using traditional cultivation methods and through microscopic observation (confocal and fluorescence microscopy).

To examine cellular viability using cultivation methods, 100 µL samples of each isolate were harvested from the glass flasks containing only NaCl 0.9%, and the same saline solution supplemented with 0.0053% or 0.05% BZK. The samples recovered from saline solutions without BZK were serially diluted and 50 µL were plated on Tryptic Soy Agar medium (TSA; BD Bacto™ Tryptic Soy Broth [Soybean-

Casein Digest Medium], Difco). Serial dilution of the samples recovered from saline solutions supplemented with BZK was also performed, followed by filtration with a previously sterilized filtration system and filters with a 0.2 µm pore size (Whatman™, GE Healthcare Life Sciences), under aseptic conditions. This step was required in order to remove the biocide and therefore prevent a possible inhibitory effect in terms of bacterial growth. The filter disks were placed on TSA plates, which were left to incubate for 72h at 30°C. After the incubation period, the number of colony forming units (CFUs) recovered within the range of serial dilutions plated on TSA solid media was determined.

In the morphology analysis, the global aspect of the colonies obtained after 72h of incubation in solid media was observed with a KL 2500 LCD cold light source (ZEISS) coupled to a microscope camera (ZEISS Axicam 503 color), using the ZEN 2.3 (ZEISS) software. For each agar plate, several pictures were taken using the same devices. Around 100 representative colonies of each bacterial isolate were then selected for diameter measurement, which was performed using the ZEN 2 lite (ZEISS) software.

For the confocal microscopy assessment of cellular viability, bacterial samples were visualized using the TCS SP5 Confocal Microscope (Leica). Sample preparation started with the addition of 200 µL of each bacterial suspension onto an 8 wells µ-Slide (Ibidi), which were allowed to settle for ~10 min. Then, 0.3 µL of SYTO™ 9 green-fluorescent probe (Life Technologies, ThermoFisher Scientific) were added to each well, followed by 1 µL of TO-PRO™-3 Iodide red-fluorescent probe (Life Technologies, ThermoFisher Scientific). Sample preparations were then incubated at room temperature, in the dark, for 20 minutes. Observations were performed using the water immersion objective, with 63x magnification, on top of which a drop of MilliQ water was placed. Images were collected using the Leica Application Suite, Advanced Fluorescence software.

When fluorescence microscopy was used, the LIVE/DEAD® BacLight™ Bacterial Viability Kit (Invitrogen) was applied. For that purpose, 1 mL samples were recovered from each flask (correspondent to 0%, 0.0053% and 0.05% BZK) and centrifuged at 10000 rpm, 4°C for 5 minutes. The supernatant was discarded, and the cells were resuspended in 30 µL of 0.9% NaCl (w/v). To that suspension, 1 µL of each probe (SYTO 9 and propidium iodide) was added, followed by thorough mixing and 15 minutes of incubation at room temperature, in the dark. After the incubation period, 5 µL of each stained bacterial suspension were placed on a microscope slide and covered with a coverslip. Microscopic observations were performed using the ZEISS Axioplan fluorescence microscope with an HBO 50 burner, a HAL 100 halogen illuminator and a filter with 450-490 nm excitation and 520 nm emission. Images were captured using a microscope Axicam 503 colour camera (Zeiss) and the ZEN 2.3 software (Zeiss).

3.5. Susceptibility of *B. cepacia* Isolates to BZK - Minimum Inhibitory Concentration (MIC) Determination

The effects exerted by different BZK concentrations on the growth of *B. cepacia* isolates were assessed by performing a modified broth minimum inhibitory concentration (MIC) assay, using 96-wells microplates (Greiner Bio-One, Germany). A 40 mg/mL BZK stock solution was prepared in double

distilled water (ddH₂O), sterilized by filtration with 0.2 µm pore size filters (Whatman) and diluted in sterile ddH₂O to obtain working solutions with concentrations of 16, 32, 64, 128, 192, 256, 384 and 512 µg/mL. Bacterial isolates were previously cultured overnight, at 37°C with shaking at 250 rpm. Then, the culture concentrations were adjusted to an OD_{640nm} of 0.05, in fresh liquid LB medium, and incubated in the same conditions for an additional ~3h period, until reaching mid-exponential phase. The bacterial cultures were then centrifuged for 10 min, at 7000 rpm, 17°C. The supernatants were discarded, and the pellets were resuspended in Mueller-Hinton broth (MH, Fluka Analytical). Cellular concentrations were adjusted to an OD_{640nm} of 0.011, which corresponds to ~ 1x10⁵ CFU/mL. A volume of 190 µL of each cell culture was added (in duplicate) to the 96-well microplates, together with 10 µL of each BZK solution. Duplicate control wells, containing either 200 µL of cell culture (positive control) or 200 µL of MH broth (negative control, not inoculated) were also used. The 96-well microplates were incubated in the dark, at 23°C, for 72h. After the 3-days incubation period, OD_{640nm} was measured using a microplate spectrophotometer (SPECTROstar^{NANO} - BMG LABTECH; software version 2.10), after homogenizing the content of the wells. The lowest BZK concentration leading to bacterial growth inhibition was defined as the MIC value.

3.6. Characterization of the Cellular Aggregates' Matrix Composition

The sugar content of the aggregate/biofilm-like structures formed during long-term incubation of *B. cepacia* and *B. contaminans* isolates in the presence of BZK was assessed using the phenol-sulfuric acid method (147). For that purpose, 1 mL samples were collected from each flask and centrifuged for 5 minutes at 10000 rpm, 4°C. The supernatant was removed and frozen at -20°C, while the pellet was resuspended in 1.1 mL of H₂O. From the resulting suspension, 100 µL were used for OD measurement at 640 nm, and the remaining 1 mL was transferred into glass tubes and mixed with 1.5 mL of phenol 0.05% (w/v) and 8 mL of H₂SO₄ 96%. After cooling, the OD_{490nm} was measured. The relative sugar content was determined using a previously created glucose standard curve (**Annex V**) (46).

For protein quantification, the Biuret method was applied (148). Samples of 1 mL were collected from the flasks and centrifuged for 10 minutes at 4°C, 15000 rpm. The supernatant was discarded, and the pellet resuspended in 1 mL of dH₂O. The resultant cell suspension was mixed with 1 mL of dH₂O and 1 mL of NaOH (1mM). The resulting solution was heated at 100°C for 5 min and let to cool at room temperature. Then, 1 mL of 0.025% CuSO₄.5H₂O (w/v) was added and the samples were left to incubate at room temperature for 5 minutes. After centrifugation at 5600g, 20°C, for 5 min, OD_{550nm} was measured. To estimate the protein content, a standard curve of bovine serum albumin (BSA) in the range of 1-10 mg/mL was prepared (**Annex V**).

Polysaccharide staining with the polyvalent basic dye Alcian Blue was performed, followed by microscopic observation of the stained aggregate structures. For that purpose, bacterial samples of 1 mL were collected from each flask and treated with the LIVE/DEAD™ BacLight™ Bacterial Viability Kit (Invitrogen), as described in **section 3.4**. Following the incubation period, 120 µL of a 0.02% Alcian Blue 8GX (Sigma-Aldrich) solution in 0.06% glacial acetic acid were added to each bacterial sample.

Afterwards, 5 μ L of each stained bacterial suspension were placed on a microscope slide and covered with a coverslip. Observation of stained polysaccharides was achieved using bright field microscopy, while observation of the aggregates was performed using fluorescence. Images were captured using the ZEISS Axioplan microscope, a microscope Axicam 503 colour camera (Zeiss) and the ZEN 2.3 software (Zeiss).

3.7. Comparative Genomic Analysis

3.7.1. *De novo* assembly of *B. cepacia* isolates' genomes

A comparative genomic analysis pipeline was proposed, starting with *de novo* assembly of the genome sequences belonging to 22 *B. cepacia* isolates recovered from saline solutions, available in our laboratory collection (listed in **Table 3**), which were derived from Illumina sequencing and kindly provided by Dr. Vaughn Cooper's group, from University of Pittsburgh.

An initial quality control of the genome sequences was performed using FastQC (Babraham Bioinformatics). Several parameters were considered in this analysis, including sequence length, CG content, per base sequence quality, sequence duplication levels, adapter content and overrepresented sequences. Afterwards, sequence clean-up for Illumina adapter removal was conducted, using Trimmomatic (149), followed by a new quality control, to validate this last step. The assembly was performed using two different softwares: SPAdes (CAB – Center for Algorithmic Biotechnology) (150) and VelvetOptimiser (Victorian Bioinformatics Consortium) (151, 152). Quality control of the assembly process was performed for the outputs of both assemblers using QUAST (Algorithmic Biology Lab – St. Petersburg Academic University of the Russian Academy of Sciences) (153). Further improvement of the assembly was achieved with Pilon (BROAD Institute) (154). After the assembly process was completed, a scaffolding step was applied using SSPACE (BaseClear), followed by its improvement by Pilon. Quality control by QUAST was included after each assembly and scaffolding improvement step. Towards the end of the process, the best assembly results were compared by QUAST against a reference genome sequence, in this case correspondent to IST612 sequenced by PacBio technology. Finally, the software Mauve (The Darling Lab) was used to order the contigs of the draft genomes, using the options Tools > Move Contigs.

3.7.2. *In silico* Multilocus Sequence Typing (MLST) analysis

After the assembly process, the clonal identity of the 22 *B. cepacia* isolates under study was re-examined through an *in silico* MLST analysis, using the best assembly outputs (whether from SPAdes or VelvetOptimiser). The sequence data corresponding to each bacterial isolate was compared against other known sequences deposited in the *Burkholderia cepacia* complex MLST database (<http://pubmlst.org/bcc>). The combination of alleles attributed to each of the seven housekeeping gene loci (*atpD*, *gltB*, *gyrB*, *lepA*, *phaC*, *recA*, and *trpB*) defined the allelic profile, using the same database. This analysis revealed that isolate IST708 belonged to a different *Burkholderia* species, *Burkholderia fungorum*, prompting its exclusion from further analysis.

3.7.3. Phylogenetic tree construction

After the assembly process, the resultant genome sequences were aligned by multiple sequence alignment using Mauve (The Darling Lab) and ClustalW (<https://www.genome.jp/tools-bin/clustalw>), and a phylogenetic tree of the *B. cepacia* saline solutions isolates (described in **Table 3**) was constructed, using the Figtree phylogenetic tree builder.

3.7.4. BLAST[®] (Basic Local Alignment Search Tool)

The genome sequences of the two *B. cepacia* saline solutions isolates selected for the phenotypic studies (IST612 and IST701), were compared (by BLAST[®]) against the sequences of genes reported in the literature as being involved in tolerance to nutrient starvation and in BZK resistance and catabolism (10, 55). A total of 178 genes to be screened against the *B. cepacia* isolates' genomes were selected from the literature: 15 that encode enzymes reported to be involved in BZK degradation, 117 which encode transporters related to BZK resistance and 46 genes involved in the survival under nutrient scarcity. These genes belong to two different bacterial strains, namely *B. cenocepacia* AU1054 and *P. aeruginosa* PAO1, and their respective sequences were retrieved from the *Burkholderia* genome database (155) and the *Pseudomonas* genome database (156), respectively. A complete list of the genes selected for this analysis is presented in **Table 8**.

3.7.5. Comparative analysis of genes from the BZK degradation pathway using the Artemis Comparison Tool (ACT)

To characterize the genes involved in BZK catabolism within the genome of the *B. cepacia* isolates examined in the phenotypic studies (IST612 and IST701), and to identify genetic features that could be responsible for the different behaviour exhibited by those isolates, the sequences of the 15 genes involved in BZK biodegradation, described in the literature (10), were compared against the genome sequences of the two selected *B. cepacia* isolates, using the Artemis Comparison Tool (ACT) (157). Through interactive visualization of the genome sequences, the software allowed the identification of the putative coordinates of each gene within the draft genomes of the *B. cepacia* isolates in study, as well as the detection of genomic rearrangements (inversions). Information pertaining to the putative gene location (in bp), score and identity percentages, genome inversions and gene order (synteny) was extracted for analysis.

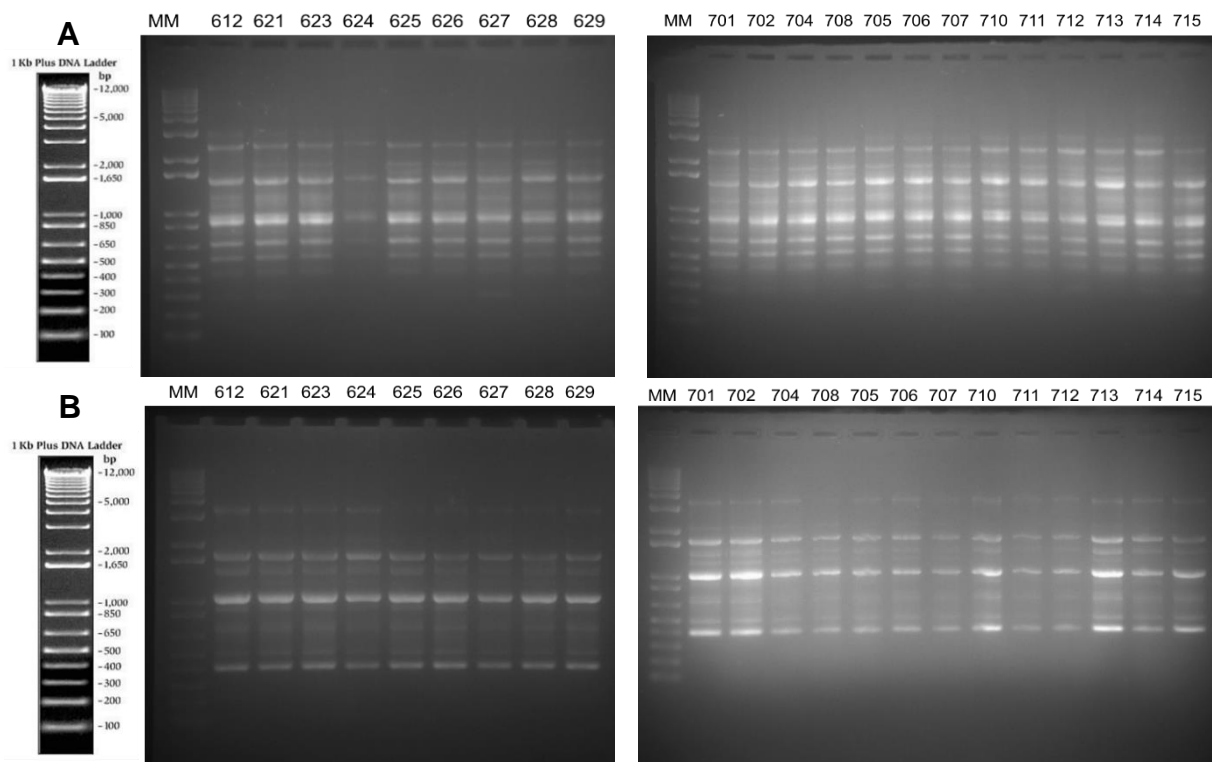
4. RESULTS

4.1. Molecular Typing of *B. cepacia* Isolates Examined in This Study and Obtained from Saline Solutions for Nasal Application

4.1.1. RAPD fingerprinting

The genomes of the 22 isolates of *B. cepacia* identified as contaminants of saline solutions for nasal application, detected by INFARMED in 2003 and 2006, had been previously sequenced, and the corresponding genome sequences were also available in our laboratory.

To confirm the clonal nature of those 22 *B. cepacia* isolates, a RAPD fingerprinting analysis was performed. The isolates recovered in 2003 presented a very similar RAPD fingerprint, for each of the three primers used, differing by no more than three bands, which is the criteria established for considering a group of bacterial isolates as belonging to the same epidemiologically related cluster (145). The isolates recovered from contaminated saline solutions in 2006 also share a similar RAPD profile, confirming that they are clonal variants of the same *B. cepacia* strain. Additionally, when comparing the fingerprints of the isolates obtained in 2003 with those of the isolates obtained in 2006, no significant differences were observed (**Figure 7**). The results point to a conservation and overall stability of the fingerprints between isolates obtained at different timepoints and seem to indicate a common source of contamination, i.e. the *B. cepacia* strain that contaminated the saline solutions in 2003 is probably the same that caused contamination of the saline solutions inspected by INFARMED three years later.



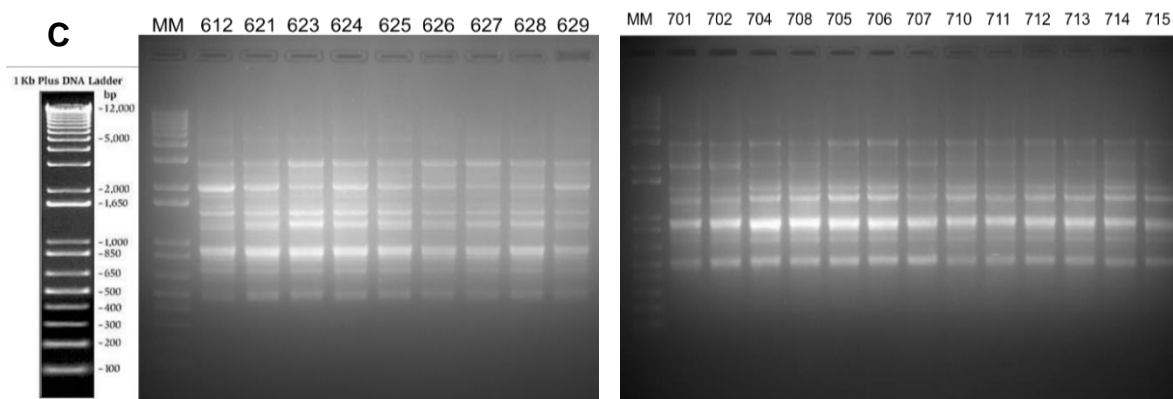


Figure 7 - RAPD fingerprint profiles of the *B. cepacia* isolates obtained from contaminated saline solutions in 2003 (left panels) and 2006 (right panels), amplified using the RAPD primers 270 (A), 208 (B) and 272 (C). Molecular size markers (MM) were run on the first lane of each gel and their size (in base pairs) is indicated on the leftmost side of the image.

4.1.2. MLST Analysis

To further validate the clonal nature and characterize the allelic profile of the 22 *B. cepacia* isolates obtained from contaminated saline solutions, based on the available genomic sequences, an *in silico* multilocus sequence typing (MLST) analysis was performed using bioinformatic tools. The nucleotide sequences of seven housekeeping genes (*atpD*, *gltB*, *gyrB*, *lepA*, *phaC*, *recA*, and *trpB*) were compared for each bacterial isolate, in order to identify possible variations (158). The different housekeeping gene sequences existent within each bacterial species were assigned with a different allele and, for each isolate, the combination of alleles attributed to each of the seven loci defined its allelic profile (159). MLST analysis has proven very useful for epidemiology studies, being able to correctly identify Bcc at the genus level, also presenting very good results in terms of species identification (160). The results of the MLST analysis are summarized in **Table 5**.

Table 5 – Summary of the results obtained after the *in silico* MLST analysis of the *B. cepacia* original isolates obtained from contaminated saline solutions inspected by INFARMED in 2003 and 2006.

Isolation Year	Isolate ID		Allelic Profile	<i>atpD</i>	<i>gltB</i>	<i>gyrB</i>	<i>recA</i>	<i>lepA</i>	<i>phaC</i>	<i>trpB</i>
2003	IST612	Bcc	9	91	93	96	103	42	1	21
	IST621	Bcc	9	91	93	96	103	42	1	21
	IST623	Bcc	9	91	93	96	103	42	1	21
	IST624	Bcc	9	91	93	96	103	42	1	21
	IST625	Bcc	9	91	93	96	103	42	1	21
	IST626	Bcc	9	91	93	96	103	42	1	21
	IST627	Bcc	9	91	93	96	103	42	1	21
	IST628	Bcc	9	91	93	96	103	42	1	21
	IST629	Bcc	9	91	93	96	103	42	1	21
2006	IST701	Bcc	-	91	93	96 (?)	103	42	1	21
	IST702	Bcc	9	91	93	96	103	42	1	21
	IST704	Bcc	9	91	93	96	103	42	1	21
	IST705	Bcc	9	91	93	96	103	42	1	21
	IST706	Bcc	9	91	93	96	103	42	1	21
	IST707	Bcc	9	91	93	96	103	42	1	21
	IST708	Bcc	485	249	275	406	256	305	216	274
	IST710	Bcc	9	91	93	96	103	42	1	21
	IST711	Bcc	9	91	93	96	103	42	1	21
	IST712	Bcc	9	91	93	96	103	42	1	21
	IST713	Bcc	9	91	93	96	103	42	1	21
	IST714	Bcc	9	91	93	96	103	42	1	21
IST715	Bcc	9	91	93	96	103	42	1	21	

The results obtained in this analysis further confirm that the isolates recovered in 2003 (IST612 to IST629) are all clonal variants of the same *B. cepacia* strain, since no differences were detected in the allelic profile of each housekeeping gene. Among the isolates recovered in 2006 (IST701 to IST715), IST708 is definitely not a clonal variant, registering significant differences in the allelic profile of each housekeeping gene analysed (highlighted in red) (**Table 5**). However, by RAPD fingerprinting, IST708 was indistinguishable from the remaining *B. cepacia* isolates. The allelic profile of this isolate was searched in the *Burkholderia cepacia* complex Multi Locus Sequence Typing website, from the PubMLST database (161), and was identified as *Burkholderia fungorum*; therefore, this isolate was discarded from further analysis. This species has a typical environmental origin, being identified in soil and plant-associated samples, where it is thought to establish a symbiotic relationship with some fungi (162, 163). Less frequently it has also been found in animal and human clinical samples (162).

IST701 displayed a warning sign for the *gyrB* gene (highlighted in yellow), which is indicative that this particular allele might have a mutation. Nevertheless, this isolate is most probably a clonal variant of the same *B. cepacia* strain, since the allelic profiles of the other housekeeping genes are matching those of the remaining isolates. The results of the MLST analysis indicate that, except for IST708, the isolates recovered from saline solutions during the market surveillance performed by INFARMED in 2003 belong to the same *B. cepacia* strain as the isolates obtained in 2006.

4.2. Phylogenetic Analysis of the *B. cepacia* Isolates Obtained from Intrinsically Contaminated Saline Solutions

After confirming the clonal identity of the *B. cepacia* isolates obtained from contaminated saline solutions (described in **Table 3**), by RAPD and *in silico* MLST, the genome sequences resultant from the assembly process were used to construct a phylogenetic tree of the evolutionary relationships between those isolates, using an available genome sequence from isolate IST612 as a reference, since it was obtained by PacBio sequencing technology. This analysis was intended to assess the possible differences existent between the *B. cepacia* isolates detected in 2003 and 2006, during market surveillances performed by INFARMED.

It was possible to distinguish two main clades, one that includes 13 genetically indistinguishable isolates, closely related to the reference genome (clade B), and another clade (A) composed by isolates which are distant from the *B. cepacia* IST612 reference genome (**Figure 8**). Isolates belonging to clade A were highly heterogeneous, giving rise to two sub-groups, composed by isolates that are essentially different (except the pairs of isolates IST624/IST713 and IST629/IST711). Given the results, it was not possible to distinguish the group of isolates obtained from contaminated saline solutions in 2003 from those obtained in 2006. According to the phylogenetic analysis and considering the confidential character of the information pertaining to the manufacturers of these saline solutions, one can only speculate about the reasons behind the registered differences. The two clades might correspond to different saline solutions, produced by two distinct manufacturers. The two sub-groups of clade A might correspond to different brands of saline solutions, produced by distinct manufacturers.

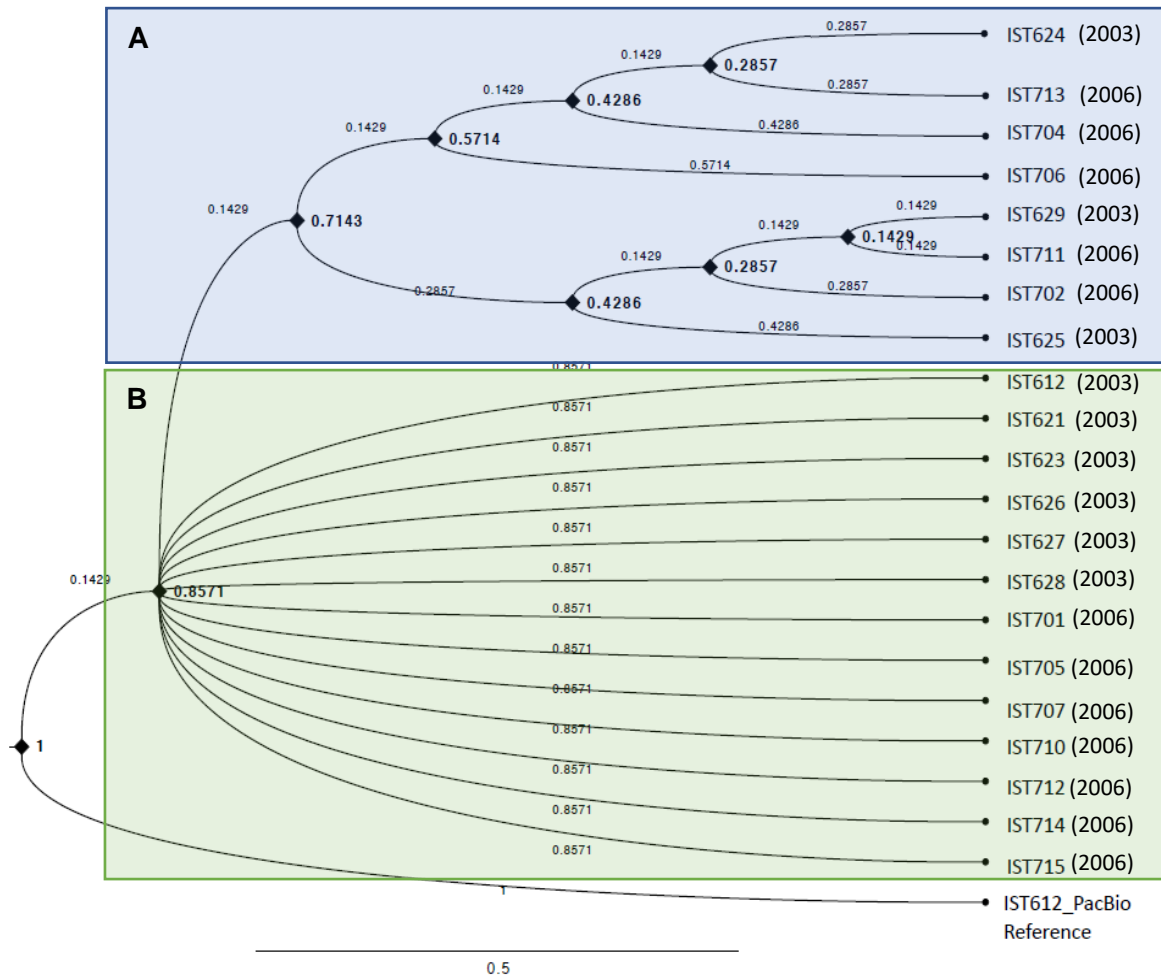


Figure 8 - Phylogenetic tree representing the evolutionary relationships between the *B. cepacia* isolates obtained from saline solutions, examined in this study. Isolation dates are indicated, in brackets, next to each isolate's ID. The numbers next to the tree nodes and above each branch represent node and branch age, respectively. This phylogenetic tree was constructed using the Figtree v1.4.3 software.

4.3. Long-Term Survival of *B. cepacia* and *B. contaminans* Cellular Populations Under Nutrient Starvation and Benzalkonium Induced Stress

4.3.1. Analysis of cellular viability during long-term incubation in saline solutions supplemented or not with BZK

To study the effects of prolonged exposure to stressful environmental conditions, five *B. cepacia* isolates (IST612, IST701, IST4152, IST4168 and IST4222) and four *B. contaminans* isolates (IST601, IST4148, IST4241 and IST4224) (**Figure 9**) from our laboratory collection were inoculated into glass flasks containing saline solutions (NaCl 0.9%), which were kept at 23°C, in order to simulate long-term incubation in a nutrient deprived environment. Additionally, the same isolates were subjected to the presence of two distinct concentrations of BZK (0.0053% (w/v) and 0.05% (w/v)), to recreate a condition of biocide stress, which is commonly verified during storage of aqueous pharmaceutical products. The Bcc isolates used were previously demonstrated to be clonal variants of the same *B. cepacia* and *B. contaminans* strain (164) and were originally obtained from intrinsically contaminated saline solutions detected during routine market surveillances performed by INFARMED, and from CF patients receiving

treatment at HSM (**Figure 9**) (16, 17). This long-term incubation experiment was initiated by a former MSc student, who analysed these bacterial populations during the first 10 months of incubation (144). In the present work, the behaviour of the same bacterial populations was further studied. Moreover, the same bacterial strains were reinoculated in the same conditions, to examine the evolution of cellular viability in the earlier stages of incubation, especially during the first 24h of incubation.

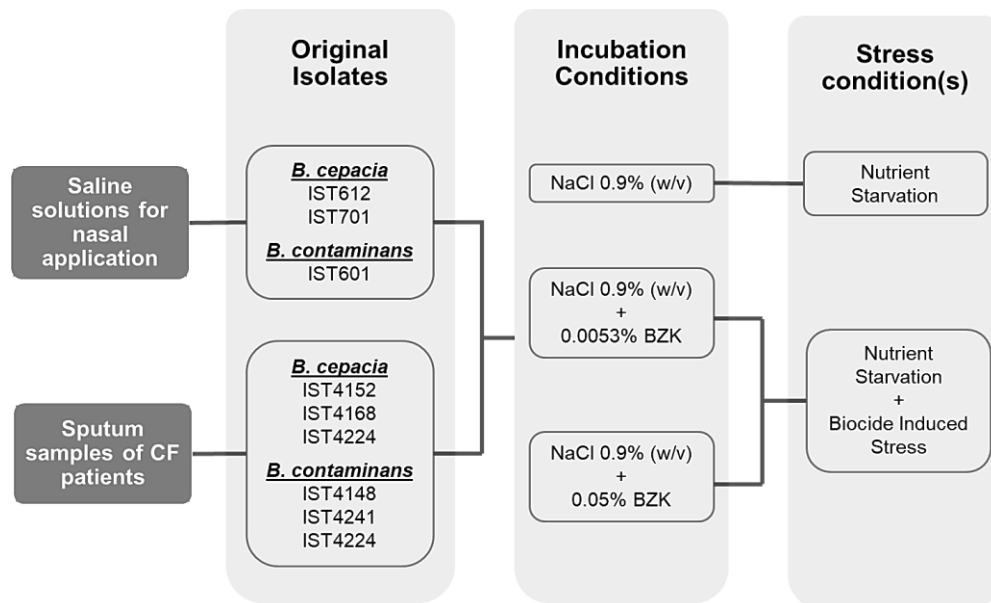


Figure 9 – Schematic representation of the *B. cepacia* and *B. contaminans* isolates originally obtained from contaminated saline solutions and from two CF patients, which were used to evaluate the effects of long-term incubation in conditions of nutrient starvation and BZK induced stress.

The effects of extended incubation in saline solutions and saline solutions supplemented with BZK in the cellular viability of the Bcc isolates were examined in terms of the number of CFUs/mL. Despite the apparent decrease in cellular viability registered for all of the isolates throughout the incubation period, both *B. cepacia* and *B. contaminans* cell populations remained viable during the period of 16 months in which the experiment was conducted, in the stress conditions tested (nutrient scarcity and BZK induced stress) (**Figure 10**; **Figure 11**). The decrease of cellular viability was more pronounced in the presence of BZK, reaching lower CFU counts when compared to isolates incubated in the absence of the biocide (difference of approximately one order of magnitude). This tendency was dose-dependent, being higher for 0.05% BZK in comparison to 0.0053% (**Table 6**).

In the absence of BZK, both *B. cepacia* and *B. contaminans* cell populations shared an initial phase, where relatively stable CFU counts were registered. However, after 10 and 8 months (in the case of saline solutions and clinical isolates, respectively), there was a clear and rapid decline in the bacterial population viability (**Figure 10A**; **Figure 11A**). In the case of isolates incubated in saline solutions supplemented with 0.0053% BZK, that initial phase was not detected and the expected decrease of cellular viability was observed (**Figure 10B**; **Figure 11B**). Concerning the isolates incubated in saline solutions supplemented with 0.05% BZK, there was an initial and abrupt decrease in the CFU counts during the first month, which was followed by a stabilization of the bacterial population, presumably due to the development of a persistent bacterial population (**Figure 10C**; **Figure 11C**).

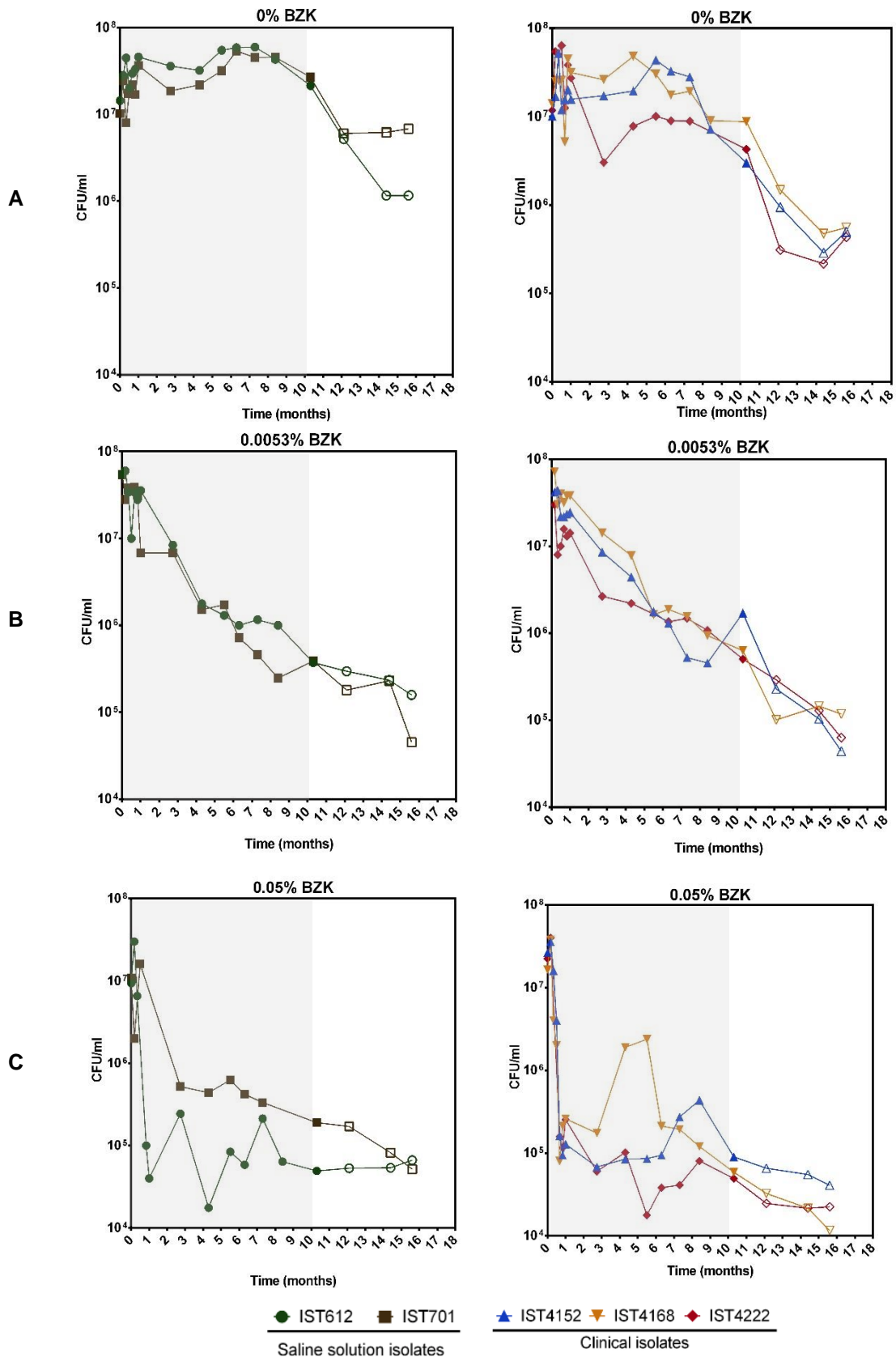


Figure 10 - Effect of long-term incubation in saline solutions (**A**) and saline solutions supplemented with 0.0053% (**B**) and 0.05% BZK (**C**) on the number of CFUs of five *B. cepacia* isolates, obtained from contaminated batches of saline solutions (IST612 and IST701) and from the sputum of a CF patient (IST4152, IST4168 and IST4222). Cellular viability was measured in terms of CFU's/mL, obtained through colony counts from three separate plates, correspondent to a range of three different serial dilutions. The datapoints correspondent to an incubation period of 10 months were obtained during a previous MSc project (indicated by a grey shade) (144).

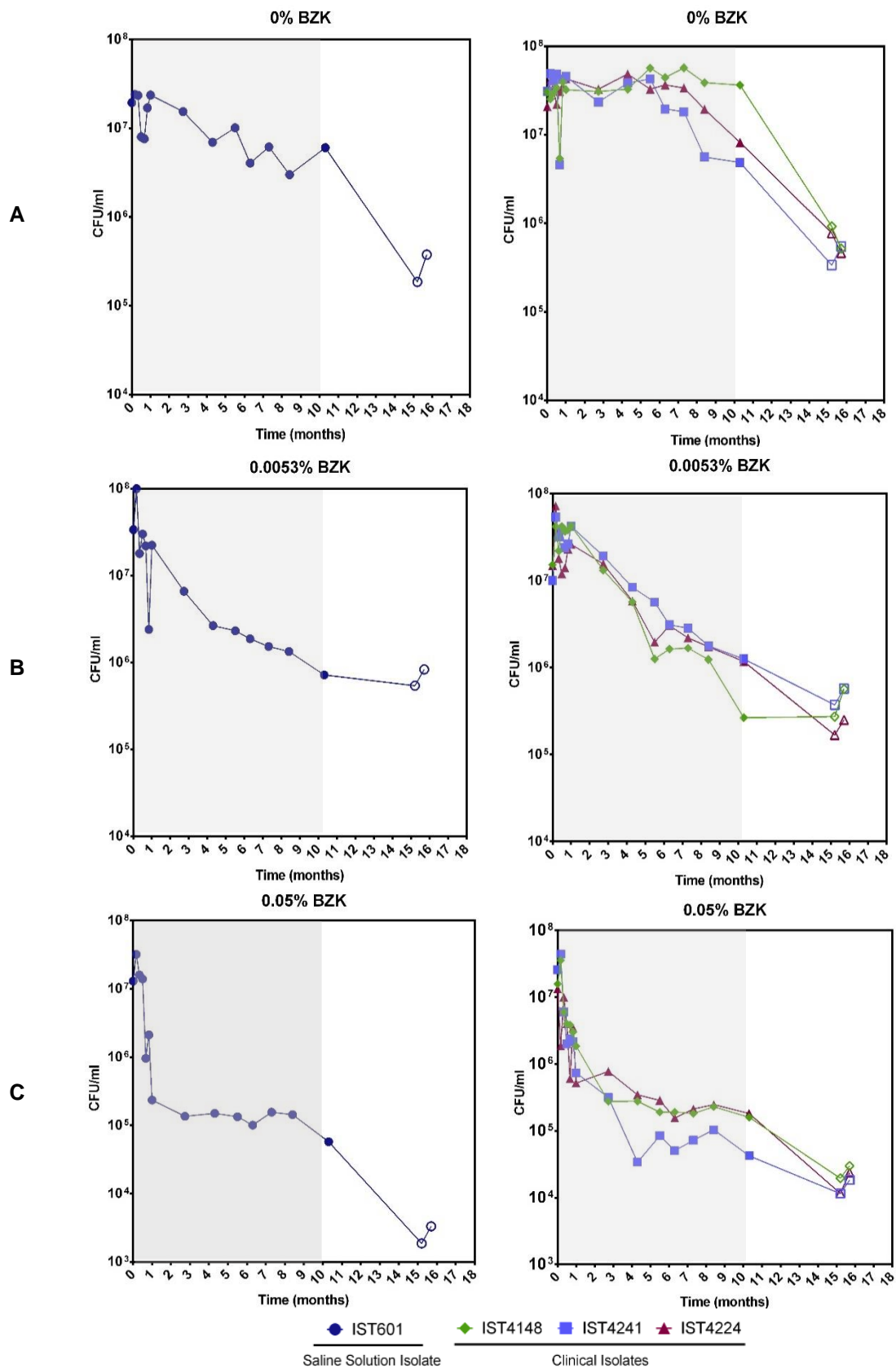


Figure 11 - Effect of long-term incubation in saline solutions (**A**) and saline solutions supplemented with 0.0053% (**B**) and 0.05% BZK (**C**) on the number of CFUs of four *B. contaminans* isolates, obtained from contaminated batches of saline solutions (IST601) and from the sputum of a CF patient (IST4148, IST4241 and IST4224). Cellular viability was measured in terms of CFU's/mL, obtained through colony counts from three separate plates, correspondent to a range of three different serial dilutions. The datapoints correspondent to an incubation period of 10 months were obtained during a previous MSc project (indicated by a grey shade) (144).

Table 6 – Maximum specific death rates (μ_d), calculated for the *B. cepacia* and *B. contaminans* bacterial populations during long-term incubation in saline solutions containing different BZK concentrations. This parameter was calculated based on the slope of the exponential part of the viability plot.

		Maximum Specific Death Rate (μ_d)			
		Without BZK	0.0053% BZK	0.05% BZK	
Period Considered for μ_d Calculation (month range)		8 - 16	0 - 16	0 - 1	2 - 16
<i>B. cepacia</i>	IST612	-0.60	-0.38	-5.50	-0.1
	IST701	-0.55	-0.45	-1.54	-0.18
	IST4152	-0.57	-0.44	-5.27	-0.04
	IST4168	-0.71	-0.42	-4.14	-0.21
	IST4222	-0.73	-0.40	-4.48	-0.08
<i>B. contaminans</i>	IST601	-0.71	-0.24	-4.00	-0.29
	IST4148	-0.79	-0.26	-2.14	-0.17
	IST4241	-0.50	-0.22	-3.54	-0.22
	IST4224	-0.51	-0.30	-3.24	-0.27

Since cellular viability was assessed in terms of CFUs/mL, the decline registered for all the studied conditions is not necessarily related with loss of cellular viability and might be due to intrinsic limitations of cultivation methods. For instance, formation of cellular aggregates under stress might lead to an underestimation of cellular viability, since one aggregate (which might have many live cells), in principle only originates one colony, upon plating on solid media.

During the first month of incubation in the presence of 0.05% BZK, higher specific death rates were registered (**Table 6**). However, after adaptation to the biocide (from the second month until the end of the experiment), which might include its biodegradation by catabolic enzymes and further use as carbon and energy source, the specific death rate decreased significantly, reaching lower values in comparison with the same bacterial populations incubated in the absence of BZK (**Table 6**). Nevertheless, it is important to notice that the higher specific death rates verified for saline solutions without BZK were only obtained after a long period where the population's viability remained relatively stable.

Considering the bacterial populations analysed, *B. cepacia* isolates from saline solutions (IST612 and IST701) appear to be more resistant to nutrient starvation, in comparison to the clonal clinical isolates of that same species (IST4152, IST4168 and IST4222). The *B. contaminans* isolates generally displayed lower specific death rates, considering all of the incubation conditions. For the highest BZK concentration (0.05%), the two *B. cepacia* isolates from saline solutions, IST701 (isolated in 2006) and IST612 (isolated in 2003), which were phylogenetically indistinguishable and whose clonal nature was confirmed by RAPD and *in silico* MLST, seem to differ in their capacity to tolerate BZK's effects. In fact, IST701 seems to be more tolerant than IST612, considering long-term incubation.

4.3.2. Reduction of colony size and morphology alterations after 16 months of incubation in nutrient deprived conditions and under BZK induced stress

To gain a better perception about the impact of long-term incubation in saline solutions (NaCl 0.9%), mimicking a nutrient depleted environment, and in saline solutions supplemented with 0.0053% or 0.05% BZK, a global phenotypic characterization was performed by evaluating the colony diameter and overall morphologies displayed by *B. cepacia* and *B. contaminans* cellular populations grown on TSA plates, after 16 months of adaptation under the aforementioned conditions. Overall, different incubation conditions resulted in the development of heterogeneous bacterial populations, characterized by major phenotypic differences, including a diversification of colony morphotypes and a clear decrease in terms of colony diameter (**Figure 12; Annex I 1; Annex II 1**).

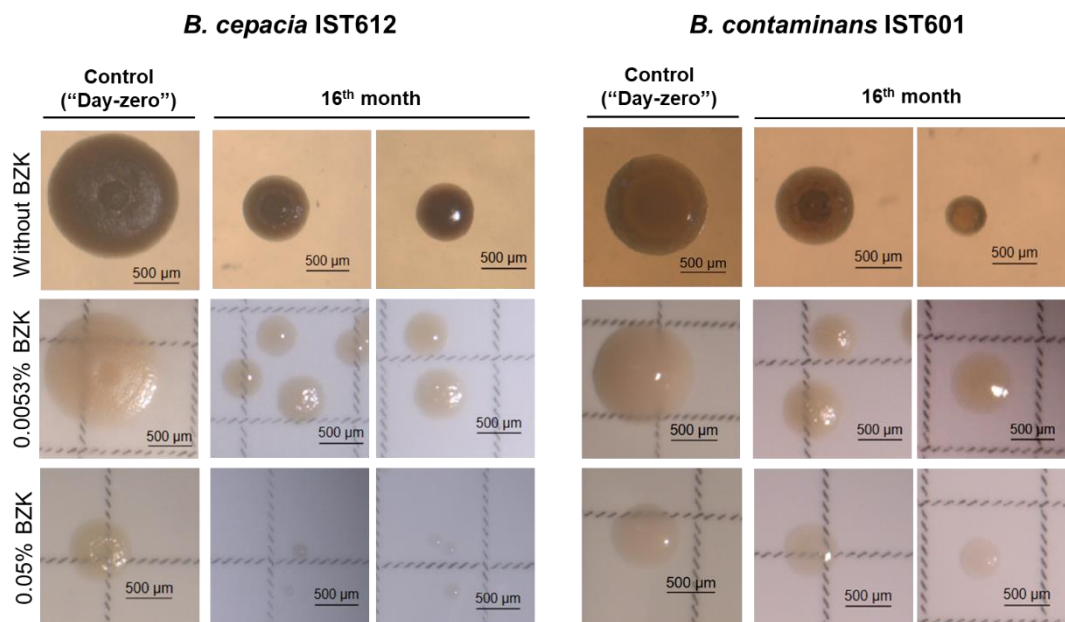


Figure 12 – Different colony morphotypes exhibited by the *B. cepacia* IST612 and *B. contaminans* IST601 cellular populations incubated in saline solutions without BZK and in saline solutions supplemented with 0.0053% and 0.05% BZK, after 16 months of incubation. Colony morphologies were compared with those obtained for the same bacterial isolates at initial inoculation (“day-zero”) in the same conditions. It is possible to observe differences in terms of colony size, morphology and pigmentation.

After 16 months of incubation in saline solutions without BZK, both *B. cepacia* and *B. contaminans* cellular populations displayed an essentially rough morphology. Punctually, it was also possible to observe colonies with a smooth morphology, for all of the *B. cepacia* isolates except IST4152, and for the three clinical *B. contaminans* isolates (IST4148, IST4241 and IST4224) (**Annex I 1; Annex II 1**). All of the colonies grown on TSA solid media were pigmented, and no significant changes were detected between the two Bcc species examined. In saline solutions supplemented with 0.0053% BZK, both rough and smooth colonies were observed. In terms of pigmentation, for *B. cepacia*, the majority of the colonies were yellow, although some colourless ones also appeared, particularly in the case of IST4222. *B. contaminans* cellular populations displayed rough colonies with yellow pigmentation, as well as smooth, less pigmented and mucous colonies. Incubation with high concentrations of BZK (0.05%) resulted in the loss of the rough morphology, which was replaced by a smooth phenotype in all the cases. The resulting colonies were also less pigmented/colourless (**Figure 12; Annex I 1; Annex II 1**).

Parallel to the alterations suffered in terms of colony morphology, the decrease of colony size was verified to be enhanced by increasing BZK concentrations, especially upon incubation with 0.05% BZK (**Figure 13; Figure 14; Figure 15**). In fact, long-term incubation in a nutrient depleted environment and the additional stress imposed by BZK resulted in the development of a heterogeneous bacterial population, from which two types of colonies could be distinguished, in terms of size: normal sized ones and smaller sized colonies (with diameters inferior to 0.5 mm), here termed small colony variants (SCVs). It is, however, important to notice that these smaller colonies cannot be considered as true SCVs, which are, by definition, one-tenth the size of colonies associated with wild-type bacteria (60). Despite being considerably smaller than the colonies generated by the parental strain, the size difference is not sufficient to fulfil the criteria stated above.

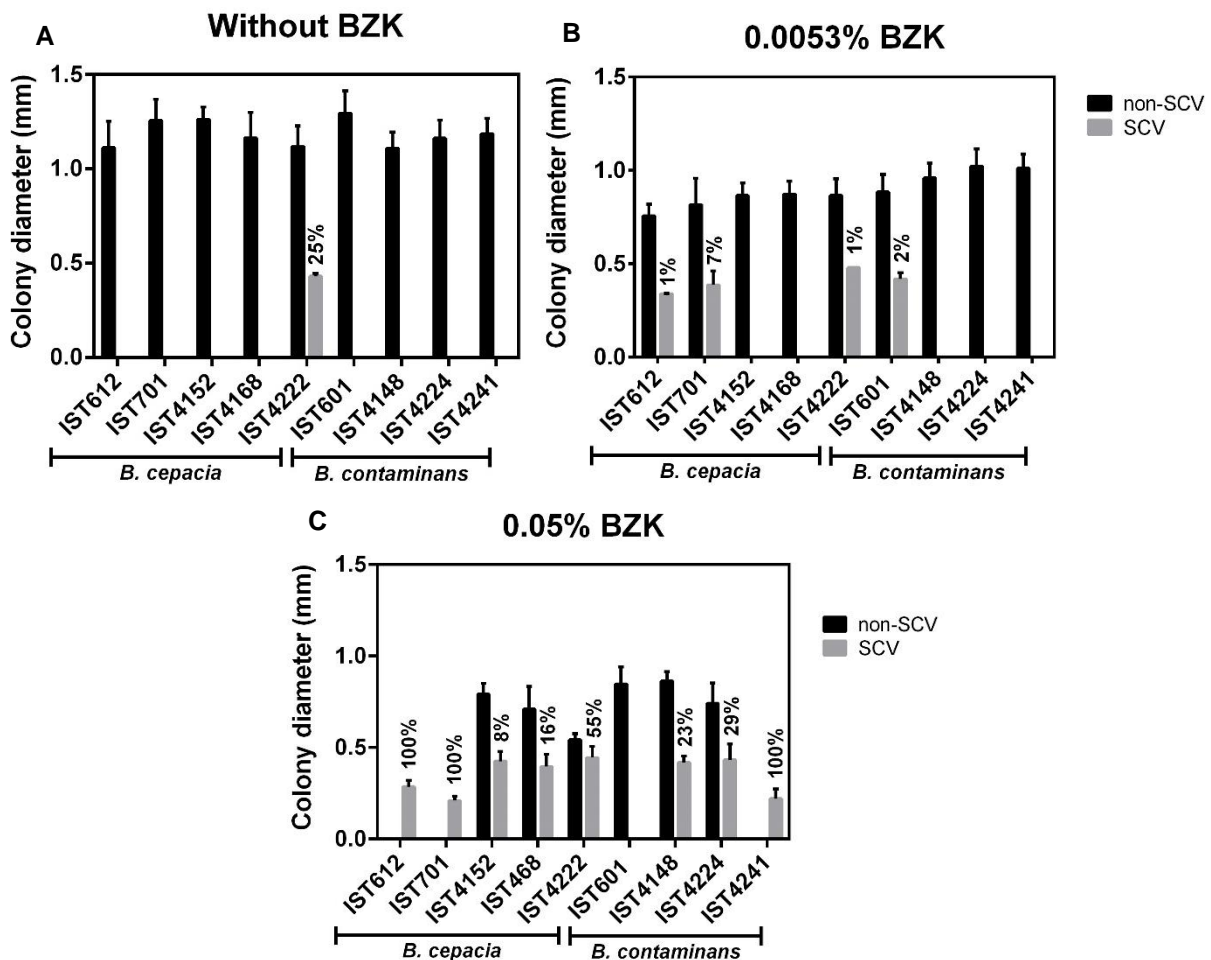


Figure 13 - Comparison of the mean diameters of a group of ~100 colonies, representative of each *B. cepacia* and *B. contaminans* cellular populations (■ non-SCV ■ SCV), incubated for 16 months in saline solutions without BZK (**A**), saline solutions supplemented with 0.0053% (**B**) and 0.05% BZK (**C**). Colonies with an average diameter inferior to 0.5 mm were termed SCVs and their respective percentages are indicated above the grey bars.

All of the isolates incubated in saline solutions without BZK exhibited normal sized colonies and only *B. cepacia* IST4222 gave rise to SCVs (25%), with an average colony diameter of 0.43 mm (\pm 0.02). The mean colony diameter of *B. cepacia* non-SCVs incubated in the aforementioned condition ranged from 1.11 mm (\pm 0.14) to 1.26 mm (\pm 0.11) (**Figure 13; Annex III 1**). *B. contaminans* cellular populations

displayed mean colony diameters in the range of 1.10 mm (± 0.09) to 1.29 mm (± 0.12). After 16 months of incubation in saline solutions supplemented with 0.0053% BZK, the mean colony diameter of *B. cepacia* non-SCVs ranged from 0.76 mm (± 0.06) to 0.87 mm (± 0.09), while the mean colony diameter of SCVs varied between 0.34 mm and 0.48 mm. For *B. contaminans*, non-SCVs showed a diameter variation in the range of 0.89 mm (± 0.09) to 1.02 mm (± 0.09) (**Figure 13; Annex III 1**). IST601 also exhibited SCVs (2%), with an average diameter of 0.42 mm (± 0.03) (**Figure 13; Annex III 1**). When subjected to incubation in saline solutions with 0.05% BZK, all of the *B. cepacia* isolates started to exhibit SCVs and, in fact, IST612 and IST701 did not originate any normal sized colonies. The average colony diameter of non-SCVs varied between 0.54 mm (± 0.04) and 0.79 mm (± 0.06) and, in the case of SCVs, the variation was situated between 0.21 mm (± 0.02) and 0.44 mm (± 0.06) (**Figure 13; Annex III 1**). In the case of *B. contaminans*, with exception of IST601, all isolates exhibited SCVs, with mean colony diameters ranging from 0.22 mm (± 0.05) to 0.43 mm (± 0.09). Non-SCVs attained diameters between 0.74 mm (± 0.11) and 0.86 mm (± 0.05). For the highest BZK concentration, in some cases, the size reduction was so pronounced that colony visualization was only possible with the aid of a stereo microscope.

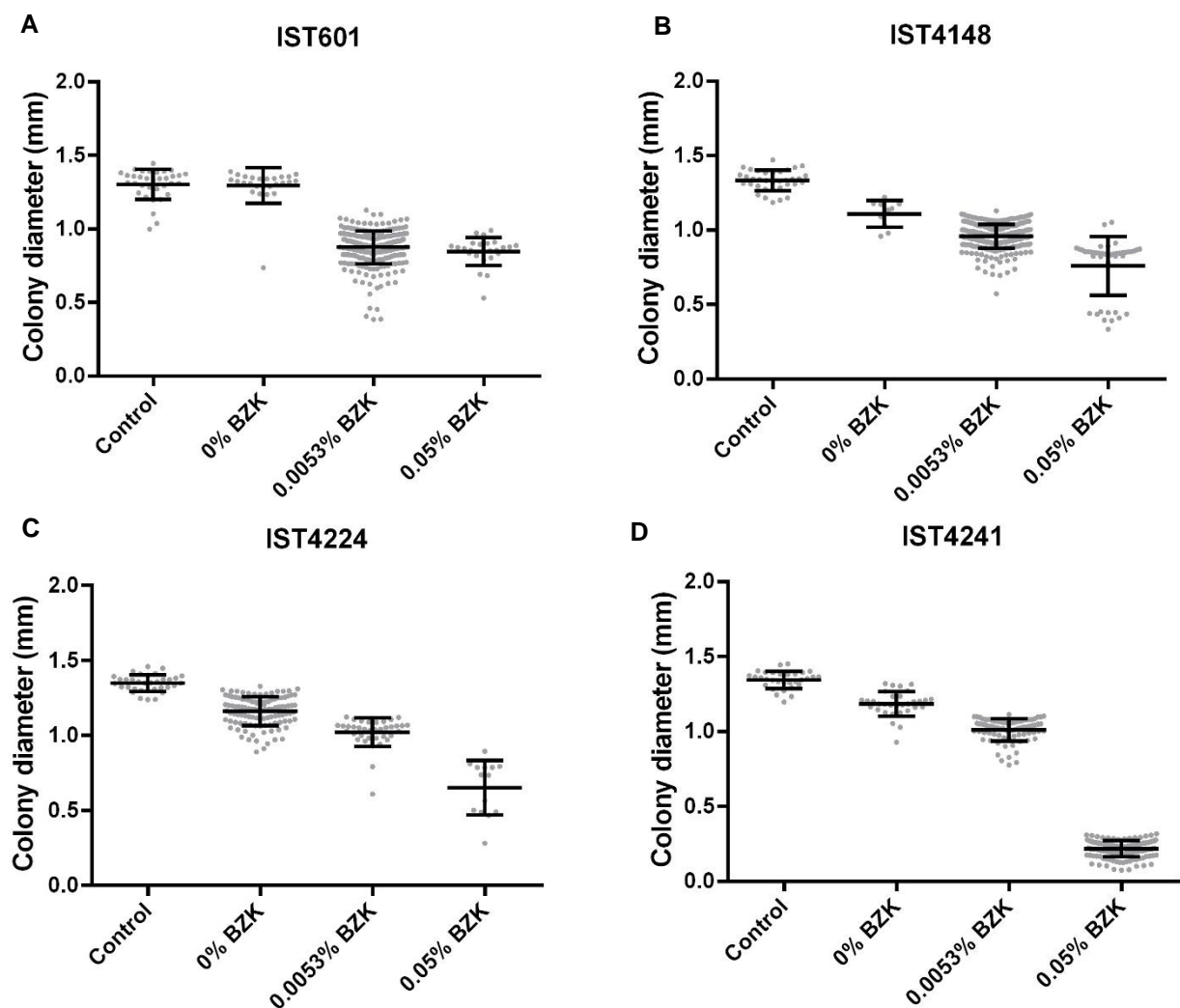


Figure 14 - Colony diameter distribution of the cellular populations corresponding to *B. contaminans* isolates IST601 (A), IST4148 (B), IST4224 (C), and IST4241 (D) incubated for 16 months under three different stress conditions. The colony diameters of the original isolates, grown on LB medium, were also assessed and used as a control. 30-260 individual colonies were selected for measurement. Mean colony diameters \pm SD are also plotted.

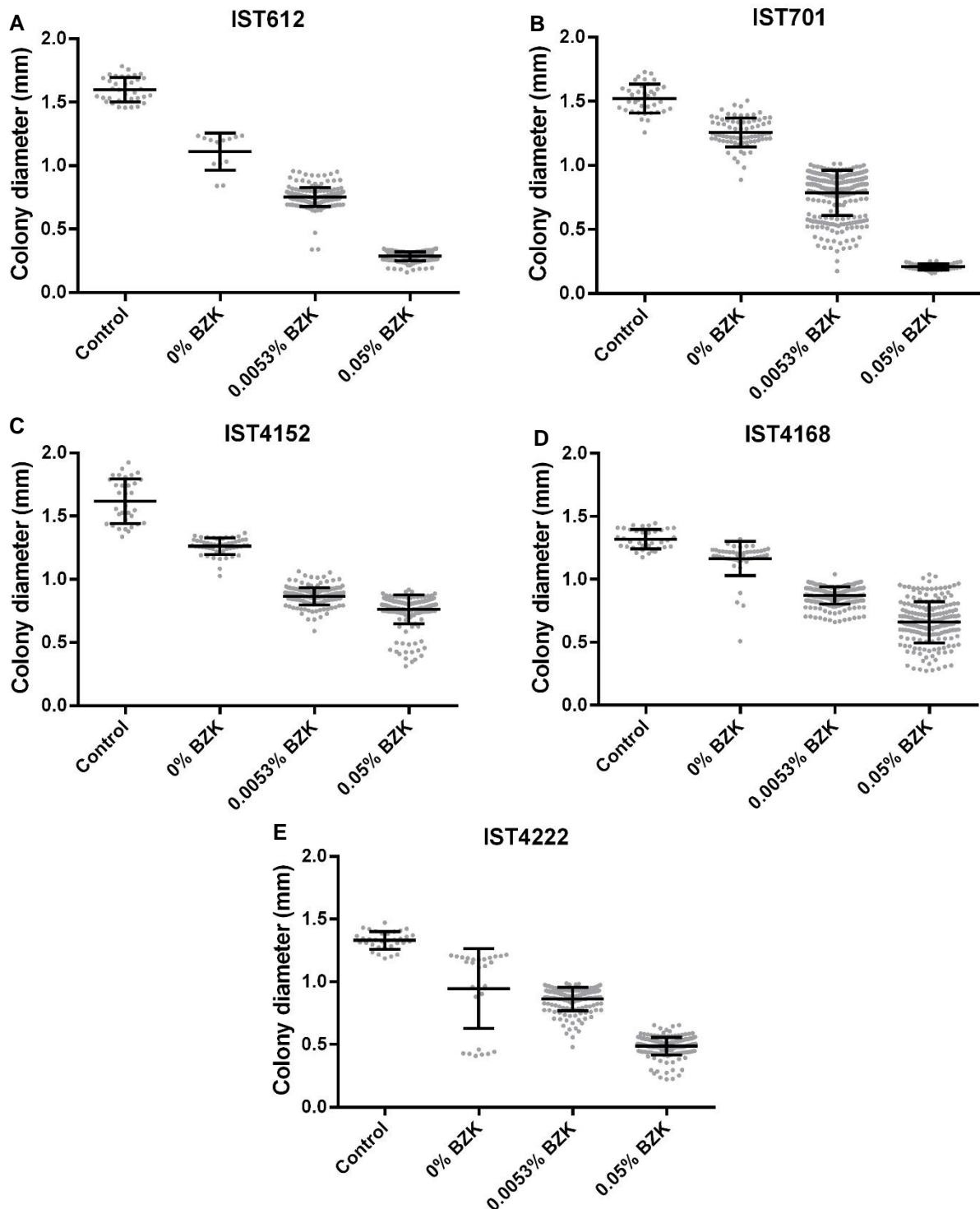


Figure 15 - Colony diameter distribution of the cellular populations corresponding to *B. cepacia* isolates IST612 (A), IST701 (B), IST4152 (C), IST4168 (D) and IST4222 (E) incubated for 16 months under three different stress conditions. The colony diameters of the original isolates, grown on LB medium, were also assessed and used as a control. 30-260 individual colonies were selected for measurement. Mean colony diameters \pm SD are also plotted.

The decrease in colony size, accompanied by the development of SCVs, appears to be a dose-dependent response to higher BZK concentrations. This tendency was common for both *B. cepacia* and *B. contaminans* cellular populations. However, the cell populations of *B. contaminans* incubated in the presence of BZK were composed by slightly bigger colonies, when compared to the *B. cepacia* populations. In terms of morphology, the smooth colonies displayed by *B. contaminans* were smoother

than those exhibited by *B. cepacia* and had a mucoid aspect. Mean diameters and respective standard deviation values (in mm) obtained for the *B. cepacia* and *B. contaminans* cellular populations after 16 months of incubation in the three stress conditions studied are provided for consultation in **Annex III 1**.

4.4. Susceptibility of the *B. cepacia* Isolates to BZK – MIC Assays

To evaluate the level of intrinsic resistance to BZK displayed by the *B. cepacia* isolates, minimum inhibitory concentration (MIC) assays were conducted. Original isolates IST612 and IST701, recovered from contaminated saline solutions in 2003 and 2006, respectively, and the first isolate recovered from patient AL, IST4152, were selected. Different concentrations of BZK, ranging from 16 to 512 µg/mL were applied and the experiment was conducted in 96-well plates, which were incubated in the dark, at 23°C, for 72h, to recreate the storage conditions used for saline solutions in pharmaceutical settings.

Considering the results obtained, all of the isolates tested seem to be intrinsically resistant to the action of BZK, requiring high concentrations of the biocide to inhibit bacterial growth. From the three isolates in study, IST612 appears to be the most resistant, followed by the clinical isolate IST4152. IST701 is apparently the most susceptible of the group (**Table 7**). These results are apparently not consistent with what was observed in the long-term viability assay (**section 4.3.1**), where IST701 attained the highest CFU counts during long-term exposure to 0.05% BZK (**Figure 10C**), indicating that it is more tolerant to BZK. Nonetheless, the MIC results concern only to short-term exposure to the chemical (3 days), while the viability assay evaluates the effects of long-term exposure, which might explain the verified discrepancies. Moreover, in this experiment, cells are grown in nutrient rich medium, which eliminates the problem of nutrient scarcity and lack of energy sources, verified in the viability assay.

Table 7 – MIC values obtained for three original *B. cepacia* isolates in study (IST612, IST701 and IST4152), as an indicator of their intrinsic resistance towards BZK. All values are means of at least two replicates and three biologically independent experiments.

Original Isolate	MIC Value for BZK (µg/mL)
IST612	256/384
IST701	192
IST4152	192/256

4.5. Monitorization of *B. cepacia* Bacterial Populations' Viability During the First 24h of Incubation in Saline Solutions Supplemented or Not With BZK

To have a better perception about the population viability dynamics during the first 24 hours of exposure to a nutrient depleted environment and to stress induced by the presence of BZK, a viability assay was conducted. Saline solutions' isolates IST612 and IST701, from *B. cepacia*, previously grown to exponential phase in LB medium, were introduced in glass flasks containing only saline solution (NaCl 0.9%) or saline solution supplemented with 0.0053% or 0.05% BZK. Cellular viability was evaluated by plating samples of each isolate on solid TSA media, followed by CFU counting.

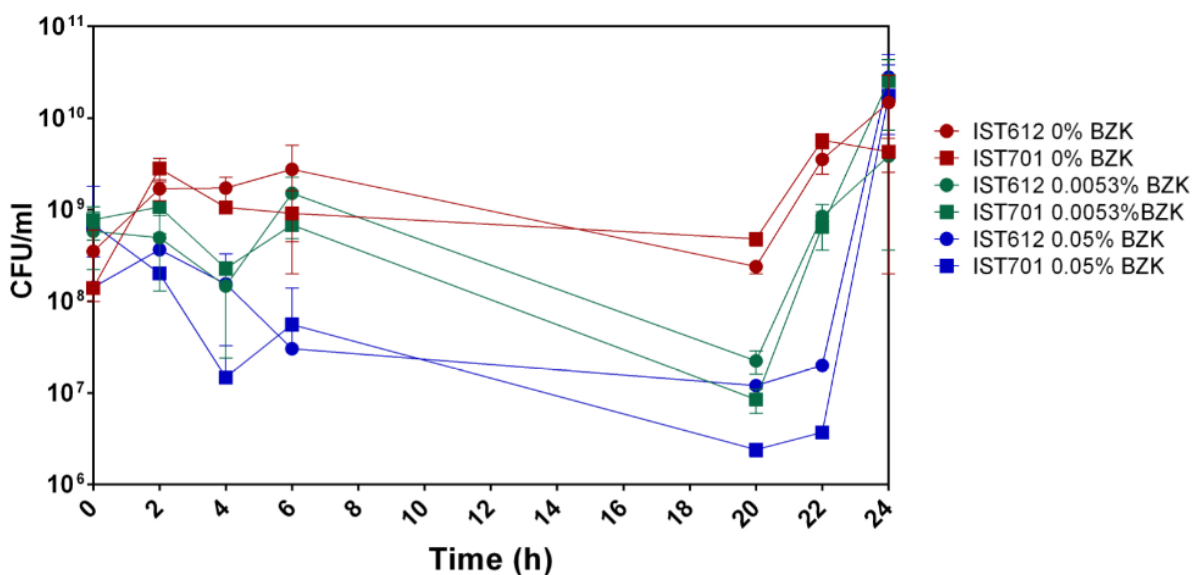


Figure 16 – Evolution of cellular viability during the first 24h of incubation of the *B. cepacia* IST612 (circles) and IST701 (squares) bacterial populations in saline solutions (red) and saline solutions supplemented with 0.0053% (green) or 0.05% BZK (blue). Cell viability was assessed in terms of CFU's/mL, obtained through colony counts from three separate plates, correspondent to a range of three different serial dilutions.

Considering that the formation of cellular aggregates might influence the conclusions taken from assays that use CFU counts as a way of estimating cellular viability, as already mentioned in **section 4.3.1**, the results obtained during the first 24 hours of incubation in the presence of BZK might not reflect the real status of the cellular populations. For that reason, the fluctuations registered throughout the experiment might be the result of an under/overestimation of the real CFU values, especially during the last 4 hours, where an apparent and unexpected increase in CFU/mL was verified (**Figure 16**). Overall, given the results and the expected experimental errors associated with the technique used to assess viability, it is not possible, at this point, to establish a correlation between the presence of increasing BZK concentrations and its short-term effects on cellular viability. Moreover, it is likely that cell division is not occurring at this stage and that the number of viable cells in the bacterial populations are in a relatively stable state, during a 24h incubation period.

4.6. Cellular Aggregates/Biofilm-Like Structures Formed by Bcc Isolates in Response to Long-Term Incubation in Nutrient Limited Conditions and BZK Induced Stress

Throughout the course of the experiment, apart from the differences observed at the level of colony size and morphology, alterations in the general aspect of the bacterial suspensions inoculated in the glass flasks were also detected. Namely, while the flasks containing only saline solution or saline solution supplemented with 0.0053% BZK remained clear or presented just slight turbidity after homogenization, respectively (**Figure 17**), it was possible to observe the formation of a white material that deposited on the bottom of the flasks containing 0.05% BZK (**Annex IV 1A**). Upon homogenization, those deposits were partially resuspended in the volume contained inside the flasks, originating a turbid suspension, in some cases with flocks that could be visualized with the naked eye (**Figure 17; Annex IV 1C**).

(A) *B. cepacia* IST612

(B) *B. contaminans* IST601

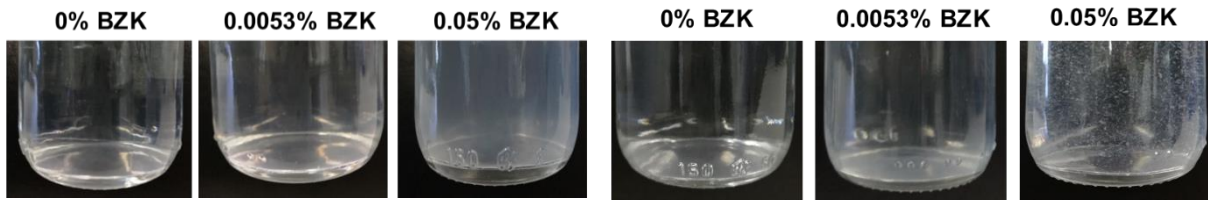


Figure 17 - General aspect of bacterial suspensions correspondent to *B. cepacia* IST612 (A) and *B. contaminans* IST601 (B) after 16 months of incubation in saline solutions and in saline solutions containing 0.0053% or 0.05% BZK.

In general, the *B. cepacia* isolates incubated in 0.05% BZK exhibited a homogeneously turbid appearance (**Figure 17A**), while the *B. contaminans* isolates formed visible floccular structures (**Figure 17B**). These observations are suggestive of cell growth and biofilm/aggregates formation induced by high concentrations of the biocide. Microscopic observation of samples from cell suspensions belonging to IST612 (*B. cepacia*) and IST601 (*B. contaminans*) was performed using a confocal microscope, after 16 months of incubation in the three stress conditions described. Cellular viability was assessed by co-staining of bacterial samples with SYTO™ 9 green-fluorescent probe and TO-PRO™-3 Iodide red-fluorescent probe.

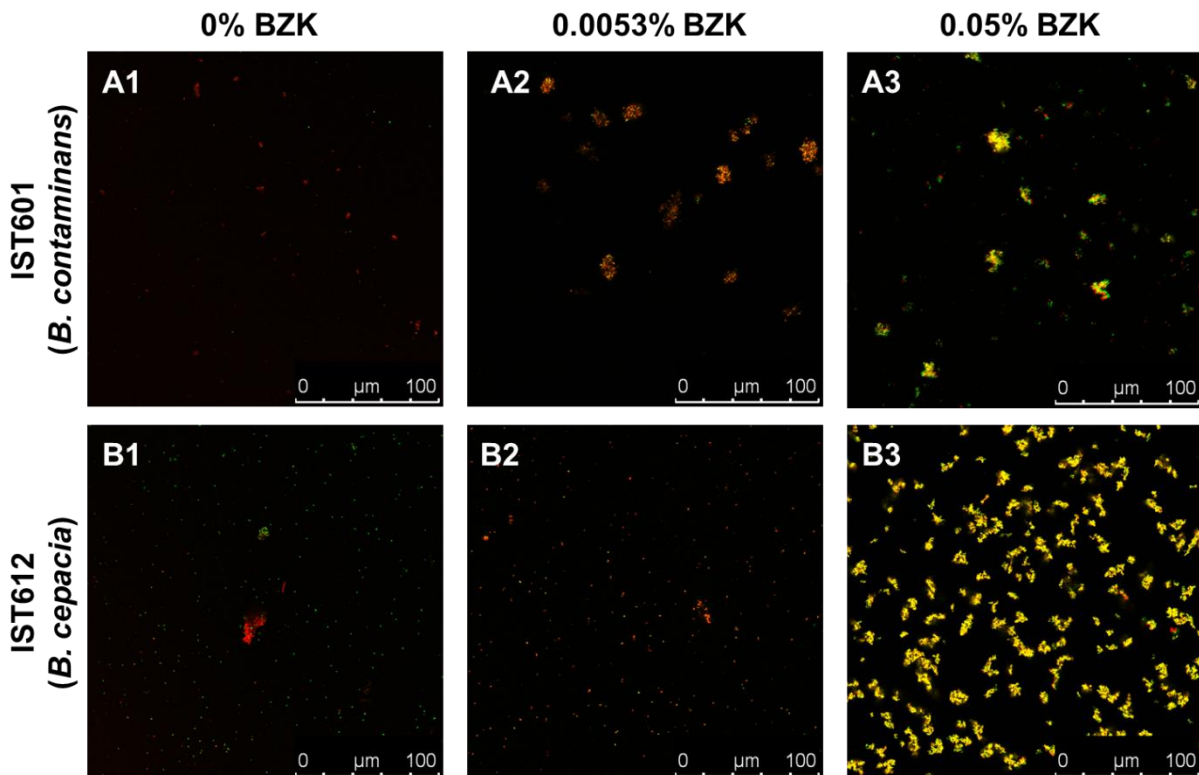


Figure 18 - Microscopic observation of the structures formed by *B. cepacia* IST612 and *B. contaminans* IST601, after 16 months of exposure to saline solutions supplemented with increasing concentrations of BZK. (A1; B1) Control, with only saline solution (NaCl 0.9% (w/v)); (A2; B2) Cells exposed to 0.0053% (w/v) of BZK; (A3; B3) Cells exposed to 0.05% (w/v) of BZK. Cellular viability was assessed through co-staining of cells with SYTO 9 (green) and TO-PRO-3 iodide (red). Images were acquired using a confocal microscope (the same settings were applied for each image) and are equally scaled to allow direct comparison.

Incubation in saline solutions without BZK led to the development of a dispersed cellular population, essentially composed of single cells. The *B. contaminans* IST601 cellular population displayed some small groups of 2/3 cells, which were mainly dead (**Figure 18A1**). The *B. cepacia* isolate IST612, incubated in the same conditions, produced a population mainly constituted by live single cells, although a cellular aggregate of considerable size was also spotted (**Figure 18B1**). Cells displaying a yellow fluorescence are either dead or at least have a compromised membrane, i.e. possess small pores through which the TO-PRO-3 iodide probe might access the cell interior. *B. contaminans* bacterial populations, incubated in the presence of 0.0053% BZK, were generally composed by cellular aggregates of intermediate size, with mostly dead or membrane compromised cells. Nevertheless, some live cells were spotted residing within those aggregates (**Figure 18A2**). The *B. cepacia* cellular population, incubated in the same conditions, did not display any aggregates of considerable size, but the majority of the cells were also dead/membrane compromised (**Figure 18B2**). For the highest BZK concentration (0.05%), the bacterial populations showed a clear tendency to form denser and bigger aggregate structures (**Figure 18A3; Figure 18B3**). This is particularly notorious for *B. cepacia* IST612, which did not develop cellular aggregates in the presence of 0.0053% BZK (**Figure 18B3**). Within those structures, it was also possible to visualize live, dead and membrane compromised cells.

According to the results, BZK seems to trigger aggregate formation and possibly induces the development of a higher cellular concentration, since those structures were rarely to not observed at all in its absence. The aggregate structure might help to protect the cells residing on its inside to remain viable under such stressful conditions. The observation of a significant number of live cells within the biofilm structure contrasts with the lower CFU counts registered for isolates incubated in the presence of 0.05% BZK. These results confirm that aggregate formation might lead to an underestimation of the actual viability by traditional cultivation methods. Interestingly, it was also observed that after 16 months of incubation in stressful conditions, cells from both species did not display the typical Gram-negative bacilli shape, but a morphology closer to coccus/coccobacilli (**Figure 19**).

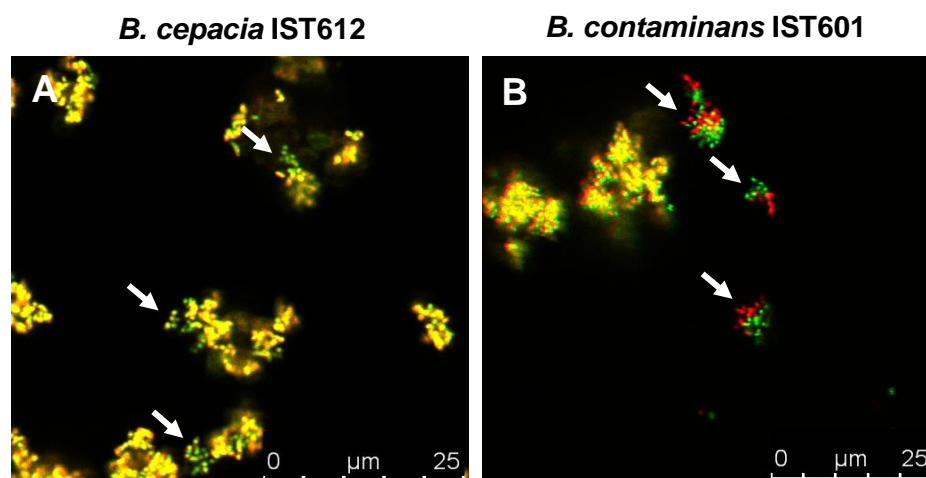


Figure 19 - Detailed microscopic observation of the biofilm structures formed by *B. cepacia* IST612 (**A**) and *B. contaminans* IST601 (**B**), after 16 months of exposure to saline solutions supplemented with 0.05% BZK, where the coccus/coccobacilli-like shape of bacterial cells is observable (indicated by solid arrows). Images were acquired using a confocal microscope (the same settings were applied for each image) and are equally scaled to allow direct comparison.

4.7. Characterization of the Cellular Aggregates Produced by *B. cepacia* and *B. contaminans* Bacterial Populations

4.7.1. Comparison of the polysaccharide/protein ratio of the cellular aggregates

To assess the composition of the aggregates/biofilm-like structures produced by the Bcc isolates in study, in response to the presence of BZK, the ratio between polysaccharides and protein concentration was determined. This assay was intended to quantify only the polysaccharide and protein content of the cellular aggregates; therefore, after centrifugation, the cell free supernatants were discarded. To measure the total sugar content of the aggregate matrix, the phenol-sulphuric acid method was applied to the pellets. In parallel, the Biuret method was employed to assess the protein concentration within the aggregates. The standard curves used to estimate the polysaccharide and protein concentrations can be consulted in **Annex V**.

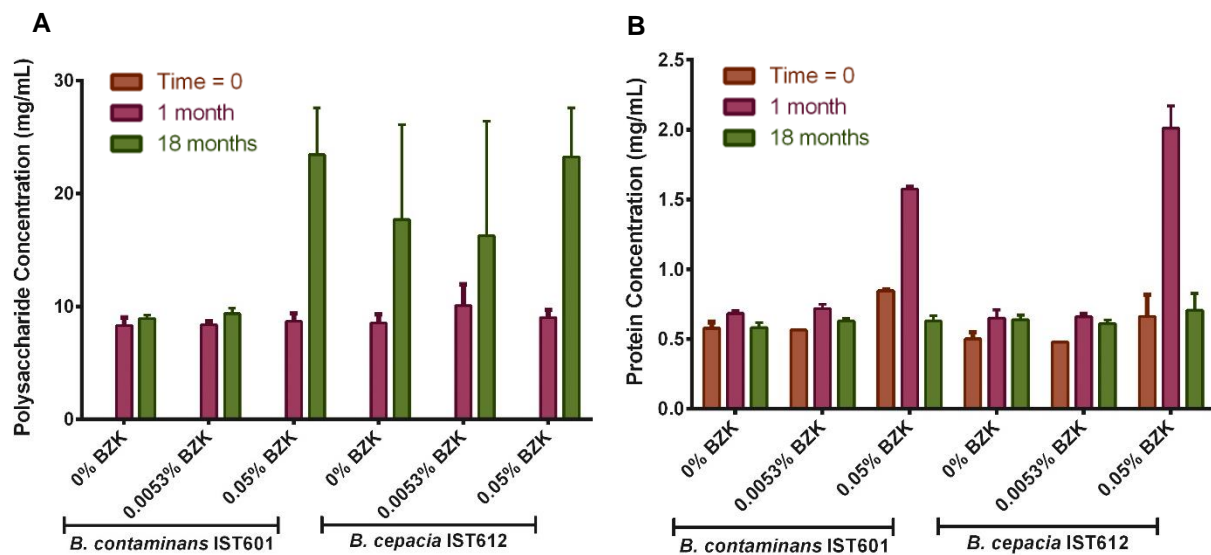


Figure 20 - Levels of polysaccharide (A) and protein (B) produced by the *B. cepacia* isolate IST612 and the *B. contaminans* isolate IST601, assessed by the phenol-sulphuric method and expressed in mg per mL of bacterial sample, at initial incubation (“Time = 0”) and after 1 and 18 months of incubation in saline solutions and saline solutions supplemented with 0.0053% or 0.05% BZK,. The results are means of two independent experiments with three replicates each. At initial inoculation (“Time = 0”) no polysaccharides were detected.

After 18 months of incubation in saline solutions and saline solutions containing two different BZK concentrations, the polysaccharide content of the cellular aggregates was higher, in comparison with the values obtained after one month, for both *B. cepacia* and *B. contaminans* populations (**Figure 20A**; **Figure 21**). At initial inoculation (“time zero”), polysaccharides were not detected within the bacterial samples analysed. The results indicate that the composition of the cellular aggregate’s matrix changes over time, becoming richer in polysaccharides during long-term incubation. This increase was particularly notorious for the highest 0.05% BZK, for which the polysaccharide content increased the most between the three time-points analysed (**Figure 20A**; **Figure 21**). These observations suggest that cellular populations adapt to the presence of higher BZK concentrations by producing aggregates rich in polysaccharides, which is also corroborated by the macroscopic observation of these structures.

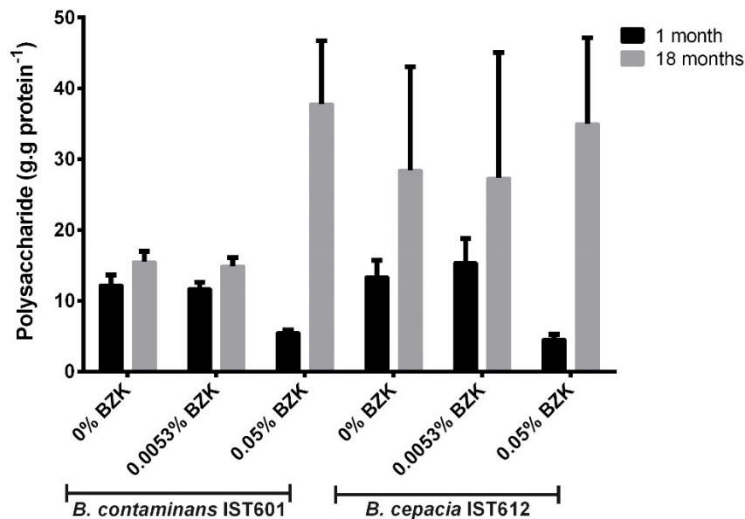


Figure 21 - Ratio of polysaccharides/proteins present within the aggregate structures produced by *B. cepacia* IST612 and the *B. contaminans* IST601, assessed by the phenol-sulphuric acid method and expressed in grams of total sugars per grams of protein (g.g protein⁻¹), after 1 and 18 months of incubation in saline solutions and saline solutions supplemented with 0.0053% or 0.05% BZK. The results are means of two independent experiments with three replicates each. The ratios of polysaccharide/protein at initial inoculation ("Time = 0") are not represented, due to the lack of polysaccharides registered at that time.

The protein concentration remained relatively constant throughout the incubation time, for both cellular populations incubated either without BZK or with 0.0053% of the biocide (**Figure 20B**). Nevertheless, for the highest BZK concentration (0.05%), there was an apparent increase of the protein content during the first month of incubation. However, from the first to the 18th month, there was a significant decrease in the protein concentration (**Figure 20B**), which might have been due to membrane permeabilization induced by the biocide, leading to protein leakage, or even to its degradation during the incubation period, resulting in the formation of amino acids or small oligopeptides, for which the Biuret method does not provide enough detection sensitivity. The increase in the polysaccharide content verified in the case of *B. cepacia* IST612, after 18 months of incubation without BZK was unexpected, since no considerable aggregate structures were observed both macro and microscopically. In this case, cells might be producing polysaccharides by using the intracellular components of dead cells, which might constitute an energy saving strategy under nutrient starvation. In the presence of 0.0053% BZK, the increase in the polysaccharide concentration was less significant, but since the maximum specific death rate was lower in comparison with the value registered in the absence of BZK, the biocide is probably used for cellular maintenance.

4.7.2. Polysaccharide staining with Alcian blue

To further characterize the composition of the aggregate structures formed during incubation in saline solutions containing 0.05% BZK, bright field microscopic observation of cell suspensions stained with Alcian blue was performed. Alcian blue is a polyvalent basic dye, which is typically used to stain mucopolysaccharides and bacterial capsules (165).

For the highest BZK concentration tested (0.05%), the bacterial populations of both *B. cepacia* and *B. contaminans* produced materials that were stainable by Alcian blue, confirming that the cellular

aggregates are at least partially composed by polysaccharides. For both of the Bcc species analysed, Alcian blue staining revealed that these polysaccharides were concentrated in the aggregates and also dispersed within the cellular populations (**Figure 22**).

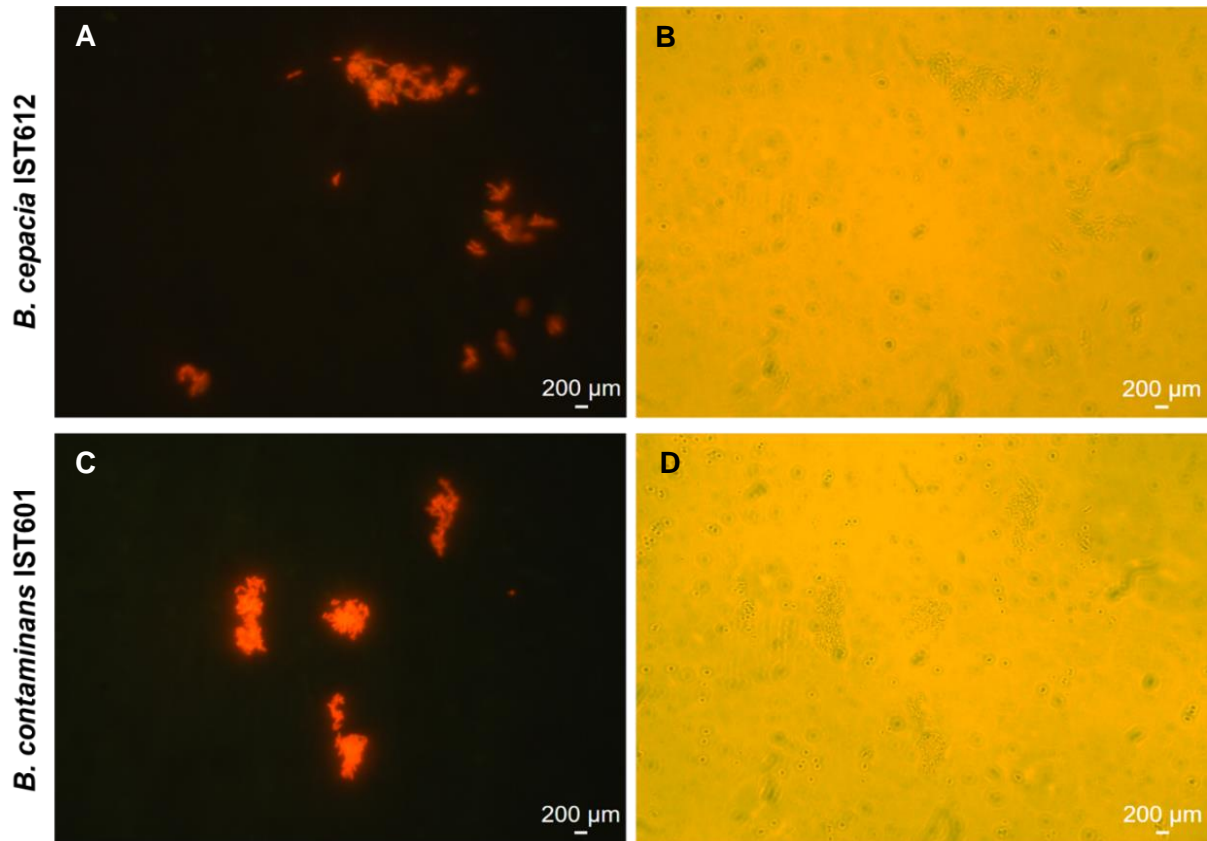


Figure 22 - Microscopic observation of the bacterial population corresponding to *B. cepacia* IST612 and *B. contaminans* IST601, after exposure to saline solutions supplemented with 0.05% BZK. Cell populations were visualized using fluorescence microscopy (**A, C**). Polysaccharides stained with Alcian blue were visualized using bright field microscopy (**B, D**). Cellular viability was assessed through co-staining of cells with SYTO 9 (green) and propidium iodide (red). Images **A/B** and **C/D** correspond to the exact same field. The same scaling was applied, to allow direct comparison.

4.8. Genomic Analysis of the *B. cepacia* Saline Solutions' Isolates IST612 and IST701: Focus on Benzalkonium and Nutrient Starvation Tolerance Genes

4.8.1. Whole genome alignment – identification of genomic rearrangements

The two *B. cepacia* saline solutions isolates examined in the phenotypic analysis (IST612 and IST701, recovered from contaminated saline solutions in 2003 and 2006, by INFARMED), which are phylogenetically very close, were selected for further genomic analysis. Whole genome alignment was performed for both isolates, using the Mauve software (The Darling Lab), in order to compare each genome's architecture, identify regions of homology, and possible genomic rearrangements.

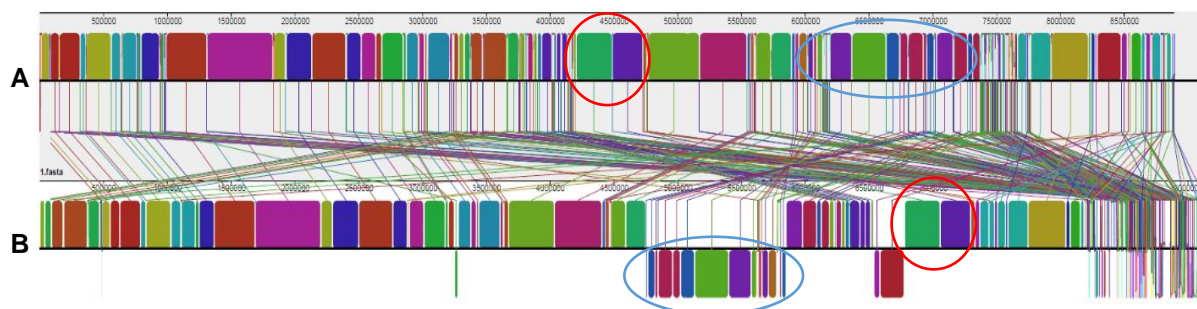


Figure 23 – Multiple genome alignment of the *B. cepacia* isolates IST612 **(A)** and IST701 **(B)**, performed with Mauve (The Darling Lab). Boxes sharing the same color correspond to local colinear blocks (LCB) and denote shared homologous regions, without sequence rearrangements. Blocks displayed below the central black line indicate regions that align in the reverse complement (inverse) orientation. Red circles – genomic translocation; Blue circles – genomic inversion.

Comparison of the two genomes using the Mauve software showed a tendency for a greater conservation level within the first third of the genomes (~ 3500000 bp), in which larger homologous local colinear blocks (LCB) were identified (**Figure 23**). Along the rest of the genome sequences, there is a lower conservation level, with multiple complex genomic rearrangements taking place. In comparison to IST612, IST701 displayed a major genomic inversion (highlighted in **Figure 23** with a blue circle). One example of a translocation is highlighted with a red circle.

4.8.2. Identification of genes related with tolerance to nutrient starvation and BZK catabolism in the genomes of *B. cepacia* IST612 and IST701

To try to identify the presence of genes that could explain the apparent inherent resistance of the original *B. cepacia* isolates IST612 and IST701 (which were object of phenotypic studies and whose genome sequences were available) to both nutrient starvation and the presence of BZK, the genome sequences of those isolates were compared against 178 gene sequences reported in the literature to be involved in these phenomena, using the BLASTN tool.

The best described Bcc species in terms of BZK resistance is *B. cenocepacia* AU1054, the strain used by Ahn *et al.* (2016) to perform transcriptomic studies that allowed the identification of two main mechanisms responsible for BZK resistance (efflux activity and metabolic inactivation through biodegradation) as well as the putative metabolic pathway responsible for its degradation (10). For this analysis, the 117 *B. cenocepacia* AU1054 genes encoding transporters of various categories and the 15 genes encoding BZK degradation enzymes described by Ahn *et al.* (2016) were searched for in the *Burkholderia* Genome Database (155) and the respective sequences were retrieved for the comparative analysis. The mechanisms underlying Bcc tolerance to nutrient starvation have still not been broadly assessed and there are currently no published reports identifying specific *Burkholderia* genes involved in that process. However, Lewenza *et al.* (2018) have explored the ability of *P. aeruginosa* PAO1 to survive during long-term exposure to a nutrient depleted environment. The 46 genes reported in that study were searched in the *Pseudomonas* Genome Database (156) and their sequences were equally retrieved for the comparative analysis.

The BLASTN analysis indicated that 127 of the *B. cenocepacia* AU1054 genes, including all of those encoding BZK degradative enzymes and 112 transporter-encoding genes, had corresponding homologues in the *B. cepacia* IST612 and IST701 genomes. Interestingly, only 7 of the 46 genes related to nutrient starvation were also identified in the genomes of IST612 and IST701. A complete list of the 178 genes screened in this analysis and their respective functions is provided in **Table 8**.

Table 8 - List of the 178 genes reported in the literature to be involved in BZK resistance and survival under nutrient starvation. The genes are divided in three main categories (genes encoding transporters, genes encoding degradative enzymes and genes related to nutrient starvation tolerance). The locus tag is indicated for each gene, as well as the main function. The genes that were absent from the genomes of *B. cepacia* IST612 and IST701 are highlighted in grey.

TRANSPORTER ENCODING GENES		
Locus Tag	Transporter Family	Substrate
Bcen_0139	The ATP-binding Cassette (ABC) Superfamily	sugar (ribose?)
Bcen_0489	The ATP-binding Cassette (ABC) Superfamily	sugar
Bcen_0491	The ATP-binding Cassette (ABC) Superfamily	sugar
Bcen_0492	The ATP-binding Cassette (ABC) Superfamily	polyamine
Bcen_0582	The ATP-binding Cassette (ABC) Superfamily	methionine
Bcen_0612	The Multidrug/Oligosaccharidyl-lipid/Polysaccharide (MOP) Flippase Superfamily	multidrug efflux
Bcen_0733	The Aromatic Acid Exporter (ArAE) Family	fusaric acid efflux?
Bcen_0977	The Major Facilitator Superfamily (MFS)	multidrug efflux
Bcen_1073	The ATP-binding Cassette (ABC) Superfamily	amino acid (glutamine/glutamate/aspartate?)
Bcen_1121	The ATP-binding Cassette (ABC) Superfamily	sulfate/thiosulfate
Bcen_1124	The ATP-binding Cassette (ABC) Superfamily	sulfate
Bcen_1792	The ATP-binding Cassette (ABC) Superfamily	amino acid (glutamine/glutamate/aspartate?)
Bcen_2220	The ATP-binding Cassette (ABC) Superfamily	methionine
Bcen_2356	The Unknown BART Superfamily-1 (UBS1) Family	sodium ion/?
Bcen_2527	The ATP-binding Cassette (ABC) Superfamily	amino acid (glutamine/glutamate/aspartate?)
Bcen_2686	The ATP-binding Cassette (ABC) Superfamily	polysaccharide export
Bcen_2931	The P-type ATPase (P-ATPase) Superfamily	zinc/cadmium/cobalt ion
Bcen_3803	The P-type ATPase (P-ATPase) Superfamily	magnesium ion
Bcen_4122	The ATP-binding Cassette (ABC) Superfamily	iron(III)
Bcen_4504	The ATP-binding Cassette (ABC) Superfamily	mobydenate
Bcen_4566	The ATP-binding Cassette (ABC) Superfamily	lipid A
Bcen_5366	The P-type ATPase (P-ATPase) Superfamily	zinc/cadmium/cobalt ion
Bcen_5602	The ATP-binding Cassette (ABC) Superfamily	amino acid (glutamine/glutamate/aspartate?)
Bcen_5813	The Aromatic Acid Exporter (ArAE) Family	fusaric acid efflux?
Bcen_5834	The ATP-binding Cassette (ABC) Superfamily	nitrate/sulfonate/taurine
Bcen_0138	The ATP-binding Cassette (ABC) Superfamily	ribose
Bcen_0186	The ATP-binding Cassette (ABC) Superfamily	amino acid (glutamine/glutamate/aspartate?)
Bcen_0490	The ATP-binding Cassette (ABC) Superfamily	sugar
Bcen_0697	The ATP-binding Cassette (ABC) Superfamily	amino acid (lysine/arginine/ornithine/histidine/octopine)
Bcen_0730	The ATP-binding Cassette (ABC) Superfamily	2-aminoethylphosphonate
Bcen_1061	The ATP-binding Cassette (ABC) Superfamily	rhamnose
Bcen_1062	The ATP-binding Cassette (ABC) Superfamily	ribose
Bcen_1136	The Major Facilitator Superfamily (MFS)	multidrug efflux
Bcen_1159	The ATP-binding Cassette (ABC) Superfamily	pyoverdin (siderophore) exporter PvdE
Bcen_1643	The ATP-binding Cassette (ABC) Superfamily	urea
Bcen_1695	The ATP-binding Cassette (ABC) Superfamily	lipid A
Bcen_1786	The ATP-binding Cassette (ABC) Superfamily	nitrate/sulfonate/taurine
Bcen_1981	The ATP-binding Cassette (ABC) Superfamily	polyamine
Bcen_1985	The ATP-binding Cassette (ABC) Superfamily	sugar
Bcen_2207	Sugar Specific PTS	glucose/maltose/N-acetylglucosamine
Bcen_2331	The ATP-binding Cassette (ABC) Superfamily	sulfate/thiosulfate
Bcen_2397	The Chromate Ion Transporter (CHR) Family	chromate ion
Bcen_2399	The Nucleobase:Cation Symporter-2 (NCS2) Family	xanthine/uracil
Bcen_2429	The ATP-binding Cassette (ABC) Superfamily	dipeptide/oligopeptide
Bcen_2430	The ATP-binding Cassette (ABC) Superfamily	dipeptide/oligopeptide

Bcen_2431	The ATP-binding Cassette (ABC) Superfamily	dipeptide/oligopeptide
Bcen_2601	The Amino Acid-Polyamine-Organocation (APC) Family	amino acid
Bcen_2649	The ATP-binding Cassette (ABC) Superfamily	amino acid (glutamine/glutamate/aspartate?)
Bcen_2698	The ATP-binding Cassette (ABC) Superfamily	multidrug
Bcen_2709	The ATP-binding Cassette (ABC) Superfamily	polyamine
Bcen_2829	The ATP-binding Cassette (ABC) Superfamily	leucine/valine
Bcen_2966	The ATP-binding Cassette (ABC) Superfamily	leucine/valine
Bcen_3226	The ATP-binding Cassette (ABC) Superfamily	glycine betaine
Bcen_3348	The ATP-binding Cassette (ABC) Superfamily	leucine/valine
Bcen_3350	The ATP-binding Cassette (ABC) Superfamily	branched-chain amino acid
Bcen_3377	The Major Facilitator Superfamily (MFS)	Acetyl-CoA:CoA antiporter
Bcen_3392	The Nucleobase:Cation Symporter-2 (NCS2) Family	xanthine/uracil
Bcen_4579	The Monovalent Cation:Proton Antiporter-1 (CPA1) Family	sodium ion:proton antiporter
Bcen_4881	The ATP-binding Cassette (ABC) Superfamily	polyamine
Bcen_5321	The ATP-binding Cassette (ABC) Superfamily	lipoprotein
Bcen_5429	The ATP-binding Cassette (ABC) Superfamily	iron-hydroxamate
Bcen_5438	The ATP-binding Cassette (ABC) Superfamily	amino acid (glutamine/glutamate/aspartate?)
Bcen_5578	The Dicarboxylate/Amino Acid:Cation (Na+ or H+) Symporter (DAACS) Family	proton/sodium ion:glutamate/aspartate symporter
Bcen_5748	The ATP-binding Cassette (ABC) Superfamily	phosphate
Bcen_5751	The ATP-binding Cassette (ABC) Superfamily	amino acid (glutamine/glutamate/aspartate?)
Bcen_5783	The ATP-binding Cassette (ABC) Superfamily	leucine/valine
Bcen_6280	The K+ Uptake Permease (KUP) Family	potassium ion uptake
Bcen_0729	The ATP-binding Cassette (ABC) Superfamily	iron(III)
Bcen_1063	The ATP-binding Cassette (ABC) Superfamily	sugar (ribose?)
Bcen_1126	The ATP-binding Cassette (ABC) Superfamily	rhamnose
Bcen_1420	The Anion Channel-forming Bestrophin (Bestrophin) Family	Bestrophin anion channel
Bcen_2044	The Major Facilitator Superfamily (MFS)	multidrug efflux
Bcen_2382	The ATP-binding Cassette (ABC) Superfamily	spermidine/putrescine
Bcen_2712	The ATP-binding Cassette (ABC) Superfamily	sugar
Bcen_2970	The ATP-binding Cassette (ABC) Superfamily	urea
Bcen_3198	The ATP-binding Cassette (ABC) Superfamily	choline
Bcen_3372	The ATP-binding Cassette (ABC) Superfamily	lipid A
Bcen_3373	The ATP-binding Cassette (ABC) Superfamily	lipid A
Bcen_3806	The ATP-binding Cassette (ABC) Superfamily	amino acid (glutamine/glutamate/aspartate?)
Bcen_4008	The ATP-binding Cassette (ABC) Superfamily	leucine/valine
Bcen_4140	The Monovalent Cation:Proton Antiporter-2 (CPA2) Family	potassium/sodium ion:proton antiporter
Bcen_4203	The ATP-binding Cassette (ABC) Superfamily	dipeptide/oligopeptide
Bcen_4447	The ATP-binding Cassette (ABC) Superfamily	spermidine/putrescine
Bcen_5318	The ATP-binding Cassette (ABC) Superfamily	oligopeptide
Bcen_0292	The ATP-binding Cassette (ABC) Superfamily	daunorubicin
Bcen_2166	The Autoinducer-2 Exporter (AI-2E) Family (Formerly the PerM Family, TC #9.B.22)	Autoinducer-2 export
Bcen_2839	The Type III (Virulence-related) Secretory Pathway (IIISP) Family	
Bcen_2853	The OmpA-OmpF Porin (OOP) Family	
Bcen_2854	The H+- or Na+-translocating Bacterial Flagellar Motor 1ExbBD Outer Membrane Transport Energizer	
Bcen_4124	The ATP-binding Cassette (ABC) Superfamily	polyamine
Bcen_4629	The OmpA-OmpF Porin (OOP) Family	
Bcen_5184	The ATP-binding Cassette (ABC) Superfamily	toluene tolerance
Bcen_5964	The ATP-binding Cassette (ABC) Superfamily	lipoprotein
Bcen_6306	The ATP-binding Cassette (ABC) Superfamily	phosphate
Bcen_6358	The CorA Metal Ion Transporter (MIT) Family	magnesium/cobalt ion
Bcen_0469	The YggT or Fanciful K+ Uptake-B (FkuB; YggT) Family	
Bcen_2284	The ATP-binding Cassette (ABC) Superfamily	toluene tolerance
Bcen_2687	The ATP-binding Cassette (ABC) Superfamily	daunorubicin
Bcen_2691	The ATP-binding Cassette (ABC) Superfamily	toluene tolerance
Bcen_2950	The H+- or Na+-translocating F-type, V-type and A-type ATPase (F-ATPase) Superfamily	protons
Bcen_1749	The ATP-binding Cassette (ABC) Superfamily	heme
Bcen_1785	The ATP-binding Cassette (ABC) Superfamily	glycine betaine
Bcen_2450	The Type III (Virulence-related) Secretory Pathway (IIISP) Family	
Bcen_0548	The Major Facilitator Superfamily (MFS)	multidrug efflux
Bcen_1843	The ATP-binding Cassette (ABC) Superfamily	phosphonate
Bcen_2693	The ATP-binding Cassette (ABC) Superfamily	glycine betaine
Bcen_2972	The ATP-binding Cassette (ABC) Superfamily	daunorubicin

Bcen_3015	The Resistance-Nodulation-Cell Division (RND) Superfamily	multidrug/solvent efflux (HAE1 subfamily)
Bcen_3195	The ATP-binding Cassette (ABC) Superfamily	glycine betaine
Bcen_3330	The ATP-binding Cassette (ABC) Superfamily	rhamnose
Bcen_3547	The ATP-binding Cassette (ABC) Superfamily	xylose
Bcen_3773	The ATP-binding Cassette (ABC) Superfamily	sulphate
Bcen_3832	The Tripartite ATP-independent Periplasmic Transporter (TRAP-T) Family	C4-dicarboxylate
Bcen_4318	The Major Facilitator Superfamily (MFS)	multidrug efflux
Bcen_4471	The Resistance-Nodulation-Cell Division (RND) Superfamily	multidrug/solvent efflux (HAE1 subfamily)
Bcen_5427	The ATP-binding Cassette (ABC) Superfamily	phosphonate
Bcen_5703	The ATP-binding Cassette (ABC) Superfamily	amino acid (glutamine/glutamate/aspartate?)

GENES ENCODING BZK DEGRADATIVE ENZYMES

Locus tag	Protein Type
Bcen_5179	Amine oxidase
Bcen_4588	Rieske-type oxygenase
Bcen_1307	catechol 1,2-dioxygenase
Bcen_5677	coniferyl aldehyde dehydrogenase
Bcen_1311	benzaldehyde dehydrogenase
Bcen_1304	NADH oxidase
Bcen_1306	benzoate 1,2-dioxygenase subunit alpha
Bcen_1303	1,6-dihydroxycyclohexa-2,4-diene-1-carboxylate dehydrogenase
Bcen_4594	catechol 1,2-dioxygenase
Bcen_4593	muconate cycloisomerase
Bcen_4595	muconolactone delta-isomerase
Bcen_5110	3-oxoadipate enol-lactonase
Bcen_5112	3-oxoadipate CoA-transferase subunit B
Bcen_5113	3-oxoadipate CoA-transferase subunit A
Bcen_2107	acetyl-CoA acetyltransferase

GENES INVOLVED IN NUTRIENT STARVATION TOLERANCE

Locus Tag	Gene Function
PA2961	DNA polymerase III, delta prime subunit
PA5280	site-specific recombinase Sss
PA3344	ATP-dependent DNA helicase RecQ
PA0966	Holliday junction DNA helicase RuvA
PA4316	exodeoxyribonuclease I
PA4281	exonuclease SbcD
PA0382	DNA mismatch repair protein MicA
PA5493	DNA polymerase I
PA4704	cAMP-binding protein A
PA2738	integration host factor, alpha subunit
PA3092	2,4-dienoyl-CoA reductase FadH1
PA4814	2,4-dienoyl-CoA reductase FadH2
PA4911	probable permease of ABC branched-chain amino acid transporter
PA4072	probable amino acid permease
PA0958	Basic amino acid, basic peptide and imipenem outer membrane porin OprD precursor
PA3831	leucine aminopeptidase
PA0899	N2-Succinylarginine dihydrolase
PA0870	aromatic amino acid aminotransferase
PA1027	delta1-Piperideine-6-carboxylate dehydrogenase
PA0447	glutaryl-CoA dehydrogenase
PA0353	dihydroxy-acid dehydratase
PA1483	cytochrome c-type biogenesis protein
PA1318	cytochrome o ubiquinol oxidase subunit I
PA1319	cytochrome o ubiquinol oxidase subunit III
PA4587	cytochrome c551 peroxidase precursor
PA0958	Basic amino acid, basic peptide and imipenem outer membrane porin OprD precursor
PA0302	polyamine transport protein PotG
PA4598	Resistance-Nodulation-Cell Division (RND) multidrug efflux transporter MexD
PA0397	probable cation efflux system protein
PA0450	probable phosphate transporter
PA4126	probable major facilitator superfamily (MFS) transporter
PA3840	conserved hypothetical protein
PA0163	probable transcriptional regulator
PA3782	probable transcriptional regulator
PA5179	probable transcriptional regulator
PA0272	probable transcriptional regulator
PA0527	transcriptional regulator Dnr
PA4856	RetS (Regulator of Exopolysaccharide and Type III Secretion)

PA5360	two-component response regulator PhoB
PA4546	two-component sensor PilS
PA4293	two-component sensor PprA
PA1085	flagellar protein FlgJ
PA1443	flagellar motor switch protein FlhM
PA1086	flagellar hook-associated protein 1 FlgK
PA1452	flagellar biosynthesis protein FlhA
PA1092	flagellin type B

Considering that 134 of the 178 putative interesting genes, based on the available literature, were present in the genomes of the *B. cepacia* isolates IST612 and IST701, including all of the reported BZK degradation enzymes and the majority of transporters, it is possible to validate the existence of a degradation pathway for BZK and that it might be used as a carbon and energy source. All in all, the number and the type of genes present in the *B. cepacia* isolates' genomes seem to indicate a global response and metabolism rewiring, not only to the presence of BZK, but also to the lack of nutrients, which is another of the stress conditions that can be imposed during storage in pharmaceutical settings.

4.8.3. Identification of BZK catabolism genes in *B. cepacia* IST612 and IST701

After confirming the existence of a catabolic pathway for BZK degradation in *B. cepacia* IST612 and IST701, the 15 genes encoding BZK degradation enzymes, previously reported in the literature for *B. cenocepacia* AU1054 (described in **Table 8**), were compared against the genome sequences of IST612 and IST701, using the ACT Artemis software (157). Putative gene position, genomic inversions and gene order (synteny) were the parameters considered for this analysis. **Table 9** summarizes the putative coordinates of each gene (in bp) within the draft genomes of the *B. cepacia* isolates and their respective identity percentages, relative to the *B. cenocepacia* AU1054 reference strain.

Table 9 - Putative coordinates (in base pairs) of the genes from the BZK degradation pathway within the draft genomes (after assembly) of *B. cepacia* IST612 and IST701, originally recovered from contaminated saline solutions in 2003 and 2006, respectively. The percentage of identity obtained after comparison against the *B. cenocepacia* AU1054 reference genome are also indicated. These results were obtained using the ACT Artemis.

Locus Tag	Putative Gene Coordinates (in bp)			
	IST612	% of Identity	IST701	% of Identity
Bcen_5179	2638312-2639565	92%	2536-3789	92%
Bcen_4588	1713442-1714714	95%	3703-4975	95%
Bcen_1307	761201-762145	90%	7812-8756	90%
Bcen_5677	226747-228187	89%	9-1403	89%
Bcen_1311	768531-770003	91%	1-1426	91%
Bcen_1304	758178-759200	92%	10757-11779	92%
Bcen_1306	759725-761083	94%	8874-10232	94%
Bcen_1303	757405-758181	91%	11776-12552	91%
Bcen_4594	1718336-1719238	93%	8639-9541	93%
Bcen_4593	1717171-1718304	95%	7474-8607	95%
Bcen_4595	1719282-1719572	94%	9585-9875	94%
Bcen_5110	2522844-2523629	93%	5194-5979	93%
Bcen_5112	2525092-2525749	96%	3074-3731	96%
Bcen_5113	2525763-2526479	96%	2344-3060	96%
Bcen_2107	1624141-1625341	96%	19563-20763	96%

The same set of 15 BZK catabolism genes was further analysed, to compare their organization within the genomes of IST612 and IST701, using the same software (ACT Artemis). For this analysis, the *B. cenocepacia* AU1054 genome was considered as the reference, and gene orientation was assigned in relation to that strain's genome. The information extracted from ACT Artemis' outputs was analysed and used to infer the organization of the 15 homologues of the *B. cenocepacia* AU1054 BZK catabolism genes, identified within the genomes of IST612 and IST701 (**Figure 24**).

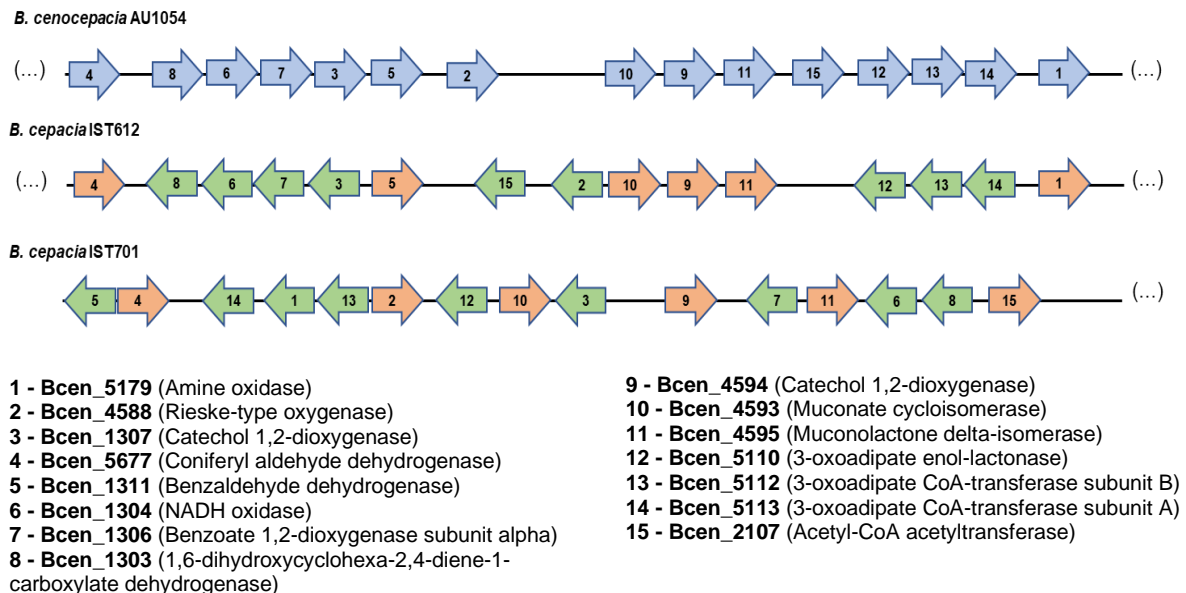


Figure 24 – Schematic diagram of the genomic organization of the 15 homologues of the *B. cenocepacia* AU1054 BZK catabolism genes, identified within the genomes of *B. cepacia* IST612 and IST701. *B. cenocepacia* AU1054 was used as a reference genome. Genes are represented by labelled arrows and their respective locus-tag and products are listed below the diagram. Blue arrows – reference genes; Green arrows – genes inverted with respect to the reference genome; Orange arrows – genes that are in the same orientation with respect to the reference genome. The real distances between the genes were modified to assist visual interpretation. Image not to scale.

In terms of genomic organization, considering only the genes involved in BZK catabolism, *B. cepacia* IST612 (isolated in 2003) is the most similar to the reference genome, sharing the same pattern of gene distribution (synteny) for 13 of the 15 genes analysed. Nevertheless, more than half of the genes were inverted with respect to the reference strain, indicating the occurrence of genomic rearrangements. IST701, originally isolated in 2006, displayed major differences in comparison to the reference genome and to IST612, with several genomic inversions and lower synteny (the only gene whose position is shared among the three strains is Bcen_4594, encoding a catechol 1,2-dioxygenase). These observations suggest that, in this particular region, the isolates recovered in 2006 have evolved differently in comparison with those recovered in 2003, despite the fact that these isolates were phylogenetically related (as described in **section 4.2**). The differences registered at the genome level, might explain the different behaviours exhibited by the two isolates in study, when subjected to extended incubation in saline solutions containing high BZK concentrations, since IST701 (isolated in 2006) appears to be more tolerant to the presence of BZK, in comparison to IST612 (isolated in 2003), which registered a faster and more significant viability loss. According to the information obtained from INFARMED, the BZK concentration present in the saline solutions detected in 2006 was higher than the concentration applied in 2003, as an attempt to control the growth of Bcc contaminants.

5. DISCUSSION

Bacteria of the *Burkholderia cepacia* complex (Bcc) are still a major public health concern, due to their easy propagation and potential to cause contamination, especially of water supplies, raising an alarming concern in pharmaceutical settings. Moreover, these bacteria can proliferate and consequently be transmitted to humans through the use of contaminated products. This group of bacteria is well known for presenting an intrinsic resistance to multiple antibiotics and antiseptics as well as the capacity to grow in nutritionally limited environments. These features can be attributed to a highly plastic genome, which enables genetic adaptation, translating into an enhanced capacity to withstand the multiple selective pressures acting upon a constantly changing environment. The present work provides insights into the adaptation mechanisms developed by different clonal isolates of *B. cepacia* and *B. contaminans*, obtained from batches of contaminated saline solutions for nasal application, detected during a market surveillance performed by INFARMED in 2003 and in March 2006, or from the sputum of two CF patients under surveillance at Hospital de Santa Maria (HSM), when subjected to long-term incubation in saline solutions and in saline solutions supplemented with different concentrations of benzalkonium chloride (BZK), mimicking the effects of nutrient starvation and the presence of this preservative in pharmaceutical products' formulations.

RAPD analysis revealed an identical fingerprinting profile for all of the 22 *B. cepacia* isolates obtained from intrinsically contaminated saline solutions in 2003 and 2006, indicating that, apparently, isolates obtained on different isolation dates are clonal variants of the same *B. cepacia* strain. However, by *in silico* MLST analysis, isolate IST708 presented an allelic profile corresponding to *B. fungorum*, which is not a member of the Bcc. The discrepancies registered between the two methods might mean that RAPD does not provide enough discriminatory power to detect certain differences among the bacterial isolates. It might also be the case that the original sample collected from saline solutions could have contained a mixed population of *B. cepacia* and *B. fungorum* and that each species was detected by a different technique. Nevertheless, the fact that clonal variants of the isolates recovered in 2003 were detected again in 2006 indicates that any preventive measures eventually applied by the manufacturers to control *B. cepacia*-related contamination were not effective.

Phylogenetic analysis of the same 22 *B. cepacia* isolates, based on their genome sequences, identified two main groups (clades): one was homogeneous, composed by isolates that were phylogenetically indistinguishable and very closely related to the reference genome (from isolate IST612, sequenced by PacBio technology); the other clade was considerably heterogeneous and phylogenetically distant from the reference genome. Since both clades harbour isolates recovered in 2003 and 2006, it is not possible to distinguish the *B. cepacia* isolates based on their respective isolation dates. The identities of the manufacturers that produced contaminated saline solutions are not known and cannot be disclosed due to confidentiality constraints. However, it is known that the products in question were produced by two different manufacturers – manufacturer A, which produced only one brand of contaminated saline solutions (K), detected in 2003, and manufacturer B, which produced 3 brands of contaminated saline solutions (brand X, where *B. cepacia* was detected in 2003 and 2006, as well as brands Y and Z,

identified to be contaminated in 2006) (16). Given that, isolates from clade B, which were phylogenetically very close, probably correspond to the same manufacturer and brand (B[X], since it is the only one that contains isolates recovered in both years). Due to its heterogeneity, clade A most probably contains isolates from both manufacturers (A and B) and different brands within the same manufacturer.

Long-term incubation in different stress conditions (nutrient starvation and the presence of two distinct BZK concentrations) seems to affect the general behaviour of the bacterial populations under study. Upon incubation in saline solutions without BZK (mimicking a nutrient depleted environment), the bacterial populations of both *B. cepacia* and *B. contaminans* remained viable, with stable colony forming units (CFU) counts for ~8 and ~10 months, in the case of clinical and saline solutions' isolates, respectively. However, in the last six months of incubation in the absence of BZK, there was a tendency towards a faster decline in the bacterial populations' cellular viability, reaching even higher specific death rates in comparison with cells incubated in the presence of 0.0053% BZK, indicating that after long-term incubation in the absence of nutrients, part of the cell population entered a death phase, while cells incubated with the lower BZK concentration have apparently adapted to the incubation conditions. Upon incubation in saline solutions supplemented with 0.0053% BZK, the initial phase observed in the absence of the biocide was replaced by a continuous decline of cellular viability, characterized by steady death rates throughout the entire incubation period. The additional stress imposed by the presence of BZK might explain why the bacterial populations start to lose viability earlier on, when compared to the isolates incubated without BZK. Long-term incubation in saline solutions supplemented with 0.05% BZK had more pronounced effects in terms of viability loss, also evidenced by the lack of an initial stable phase, as already observed for 0.0053% BZK. However, for the higher biocide concentration, a period of exponential death (with a duration of approximately one month), characterized by high death rates, was observed after cells were suddenly exposed to saline solutions containing this high biocide concentration. Contrarily to what was observed for the lower BZK concentration, during the rest of the incubation period, a stabilization of the bacterial populations incubated with 0.05% BZK was verified, reaching very low specific death rates, which might coincide with the development of bacterial persistence. In fact, this kind of pattern corresponds to a biphasic killing curve, characteristic of persister cells, where initially the majority of the cells die in an exponential manner, followed by a period of slower killing rate (the killing curve reaches a plateau), correspondent to the enrichment of the population with persister cells (66, 68, 166).

Cellular viability analysis revealed that both of the Bcc species tested were able to survive for at least 16 months in nutrient depleted saline solutions and also in the presence of 0.0053% and 0.05% BZK. Despite the significant viability decrease registered in all situations, viable cells persist and were still observed for the bacterial populations of both saline solutions and clinical isolates, during the course of the experiment, upon plating on TSA solid medium. From the bacterial populations incubated in saline solutions without BZK, the *B. cepacia* isolate IST701 appears to be the most resistant to nutrient starvation, registering a viability decrease of ~34%, while the remaining *B. cepacia* and *B. contaminans* isolates suffered a decline of viable population in the range of 91 to 99%. The highest decrease in the

viable population was verified in the presence of BZK (~99.9% for both of the concentrations tested). However, for 0.05% BZK, this decrease occurred within the first month of incubation, after which the percentage of viable population remained broadly unchanged, corresponding to approximately 0.1% of the initial population, which is situated within the typically reported range of bacterial persisters present in a bacterial population (66). Contrastingly, the viability loss verified for the bacterial populations incubated with 0.0053% BZK was continuous throughout the incubation period and, even after 16 months, the cellular populations had not yet stabilized. These results suggest that even in the absence of any external carbon and energy sources, the *B. cepacia* and *B. contaminans* bacterial populations were able to survive, implying that, at some point, a strategy for nutrient obtention must have been developed. This could be achieved through a “sacrifice-for-survival” mechanism, in which intracellular components released by dead cells might be used to maintain a smaller viable population. Despite of BZK’s deleterious effects, after the bacterial populations are adapted to its presence, the biocide might also be used as carbon and energy source to maintain cellular viability. Early studies have shown that a *B. cepacia* strain incubated in ammonium acetate solutions supplemented with 0.05% BZK was able to use both compounds as substrates for growth, allowing bacterial survival for 14 years in such conditions (7).

Under the sole influence of nutrient starvation, bacterial populations corresponding to the isolates of *B. cepacia* obtained from saline solutions remained viable, with relatively consistent CFU counts, for a longer period of time in comparison with those corresponding to clinical isolates. This observation might be due to the fact that isolates from saline solutions are more adapted to nutrient scarcity, resulting from the conditions in which they were previously stored, while the clinical isolates might be better adapted to the CF lung environment, where nutrients are available, starting to lose viability earlier on, when switched to nutrient depleted conditions. In fact, the accumulation of mucous secretions in the respiratory tract of CF patients constitutes an abundant nutrient source, providing sugars, fatty acids, phospholipids and amino acids (168), (169). Moreover, mucins, the major constituents of mucus, can also serve as carbon and nitrogen sources (169). The patient infected with *B. cepacia* (patient AL) is still being followed at the major Portuguese CF Center in HSM, but the Bcc infection was already eradicated. The forced expiration (FEV) values were 87.1% after the first isolation, 91.2% and 105.5%, one and three years after the first measurement, respectively (unpublished data). These values are considered normal, indicating that the patient’s status remained stable. Therefore, punctual differences among the sequential clinical isolates cannot be attributed to a deterioration of the patient’s health.

Antimicrobial preservatives, such as biocides, are commonly included in pharmaceutical products’ formulations, as a means of avoiding intrinsic contamination during storage processes. However, the results of this study indicate that this preventive measure might not be effective to eradicate Bcc bacteria, mainly due to intrinsic and/or acquired resistance phenomena and to the capacity of specific microorganisms, as it is the case of Bcc bacteria, to degrade biocides, in particular BZK, and using them as carbon and energy source for metabolism and to fuel stress responses. Traditional MIC assays, in which cells were exposed to increasing concentrations of BZK during a short period of time, revealed that the *B. cepacia* isolates examined were intrinsically resistant to high BZK concentrations, with

susceptible concentrations ranging from 192 to 384 $\mu\text{g/mL}$. However, the fact that viable cells could be recovered from flasks containing 0.05% (w/v) BZK, even after 16 months of incubation, indicates that the bacterial populations became even more resistant after exposure to the biocide, suggesting that this higher concentration would also be ineffective in preventing contamination with Bcc microorganisms. According to the MIC value, isolate IST612, which was recovered in 2003, seems to be more resistant to BZK than isolate IST701, collected in 2006. However, during long-term incubation, IST701 exhibited higher resistance, suggesting that this isolate might have developed more effective mechanisms that conferred adaptive advantage during long-term incubation. After detection of the presence of Bcc bacteria in batches of saline solutions for nasal application by INFARMED in 2003, manufacturers increased the concentration of BZK in subsequent manufacturing processes. In that sense, being previously exposed to higher concentrations of the biocide could have contributed for IST701 increased long-term resistance. The ability of Bcc bacteria to thrive in the presence of this biocide has already been reported (7, 8) and the resistance mechanisms have also been studied in several Gram-negative bacteria. In *E. coli*, the upregulation of genes encoding efflux pumps, outer membrane porins and proteins involved in protecting the cell from oxidative and osmotic stress are examples of adaptive responses detected in the presence of BZK (167). In Bcc bacteria, the mechanisms may involve extrusion of the chemical by chromosomally encoded efflux pumps and the inherent production of metabolic enzymes capable of degrading the biocide (10). It was also reported that Bcc bacteria have the ability to generate acetyl-CoA from BZK, which can be used in the central carbon metabolism, helping cells to remain viable, besides being an effective way of degrading BZK without accumulation of intermediates or toxic metabolites (10). The typical concentrations of BZK used in a variety of commercial products range from 0.02% (200 $\mu\text{g/mL}$) to 5% (50,000 $\mu\text{g/mL}$) (9). The present study confirms that product formulations supplemented with the lowest commercially used BZK concentrations would not have been sufficient to kill the bacterial populations examined in this experiment.

A clear tendency for a gradual and consistent decrease in colony size during long-term incubation in saline solutions was observed. This pattern was observed to be further enhanced in the presence of BZK, especially for higher concentrations, suggesting that it might be implicated in inducing a faster decline in the overall colony size, exerting a selective pressure towards the formation of smaller colonies, also in a dose dependent manner. Moreover, long-term incubation resulted in the alteration of cell shape, from typical Gram-negative bacilli to a coccoid/coccobacilli-like shape. One of the most commonly observed manifestations of colony size reduction was the development of small colony variants (SCVs), which are slow-growing bacterial subpopulations characterized by being one-tenth the size of the wild-type bacteria (59, 60). This particular phenotype was observed to arise in all of the conditions tested, but much more significantly for higher BZK concentrations (0.05%), constituting 100% of the bacterial population corresponding to the *B. cepacia* isolates IST612, IST701 and the *B. contaminans* isolate IST4241, after 16 months of incubation. SCVs usually have deficiencies in the electron transport chain, which translate into lower ATP production and reduced metabolic state (59, 60). Since ATP production is essential for cell wall and membrane biosynthesis and production of pigments, the “dormancy” state that characterizes SCVs might explain their reduced size and general lack of pigmentation (59, 60). The capacity of conversion into a state of low metabolic activity (dormancy) has been reported to contribute

for bacterial persistence and tolerance to the presence of antimicrobial agents (67, 68), leading to recurrent and often fatal infections (62, 64). The formation of SCVs is also a pathogenesis factor and it seems to be the strategy employed, for example, by *S. aureus* to persist within the vascular endothelium, where they are able to evade the host's immune system (63). Alteration of cellular shape has also been reported to occur in response to nutrient starvation, in *P. aeruginosa*, *P. putida* and *B. pseudomallei* (54, 55, 58). The selection of smaller colonies induced by the presence of BZK might constitute an adaptive strategy for energy conservation, contributing to bacterial survival under nutrient depleted conditions or in the context of CF infections.

Long-term incubation in different stress conditions resulted in the appearance of distinct colony morphologies. On one hand, cells exposed only to nutrient starvation presented an overall rough morphology, with essentially nonmucoid colonies. In the presence of BZK, cells transitioned to a smooth and mucoid phenotype. For the lowest BZK concentration tested (0.0053%), both rough and smooth colonies were present, however, for the highest concentration of the biocide, only smooth mucoid colonies were observed, suggesting that BZK might induce the switch from nonmucoid to mucoid morphotype. For Bcc bacteria, the transition from a mucoid to a nonmucoid phenotype is more common in the context of CF infections, where the nonmucoid phenotype is associated with increased virulence, leading to a faster lung function decline (80, 81). Contrastingly, the mucoid phenotype is associated with persistence and decreased virulence, which might be more favourable in stressful environmental conditions, such as nutrient starvation and/or the presence of BZK.

One of the most striking observations was the formation of macroscopically visible cellular aggregates/biofilm-like structures, in the presence of 0.05% BZK. The flasks containing *B. cepacia* populations presented turbidity and those containing *B. contaminans* populations additionally displayed floccular structures. Microscopic observation of bacterial samples also confirmed the development of cellular aggregates, suggesting that BZK might have induced this trait. Characterization of the aggregates' matrix revealed that these structures were mainly composed by polysaccharides. Moreover, the polysaccharide content significantly increased during long-term incubation, a tendency that was accompanied by the development of denser cellular aggregates, especially for higher biocide concentrations. This biomass production suggests that BZK might be catabolized within the cells and further used as carbon and energy source, possibly even providing carbon backbones for polysaccharide production, as well as the ATP required for detoxification. Considering the results of the viability assessment and the fact that the protein concentration remained broadly unchanged for the bacterial populations incubated without BZK or in the presence of 0.0053% of the biocide, cell growth (division) is likely not occurring. The increase in the protein concentration after one month of incubation with 0.05% BZK is probably not a result of cell division, since the majority of the cellular population had already died at that stage. Proteins might have leaked out from the cells, becoming trapped within the aggregates' matrix. During long-term incubation, the protein existent within the matrix was probably degraded, explaining the decrease of protein concentration from the first to the 18th month of incubation. Since polysaccharide and biofilm production implies a significant carbon and energy expense, the lower concentration displayed by the bacterial populations incubated in the absence of BZK is consistent with

the carbon and energy starvation expected in a nutrient depleted environment. However, these bacterial populations still retained a certain level of polysaccharide production, especially for the *B. cepacia* isolate IST612, implying the existence of an alternative carbon and energy source that could be used to sustain metabolic activity, which might come from the intracellular components released by dead cells. Overall, polysaccharide production might constitute a long-term adaptation trait, allowing the consolidation of the aggregates' structure, and increasing even more the chances of bacterial survival in the presence of BZK. During long-term incubation the aggregate structures can be seen macroscopically as flocks located in the bottom of the incubation flasks.

Whole genome alignment of the saline solutions' isolates IST612 (isolated in 2003) and IST701 (isolated in 2006), which were also studied in terms of phenotypic adaptation to nutrient starvation and the presence of BZK, revealed several differences between the genomes of the two *B. cepacia* isolates, despite their close phylogenetic relatedness. Although a certain degree of conservation was verified within the first ~3500000 bp, various translocations and two considerable inversions were also registered. The presence of genes involved in the BZK degradation pathway, as well as genes encoding several efflux pumps, described in the literature for *B. cenocepacia* AU1054 (10), was also verified for the *B. cepacia* isolates IST612 and IST701, confirming that BZK can be catabolized by the *B. cepacia* strains examined, as already suspected. Moreover, BZK degradation and its expulsion from the cell might work synergistically to increase bacterial resistance, contributing as well to reduce the biocide's toxic effects and, upon degradation, allowing its reuse as a source of carbon, energy and even nitrogen. However, the great majority of genes related with tolerance to nutrient scarcity were absent from the genome of the two *B. cepacia* isolates analysed. Since studies pertaining to the mechanisms responsible for Bcc survival in nutrient depleted water-based environments are scarce and, to our knowledge, specific genes involved in that phenomenon have not yet been identified, the use of a *Pseudomonas* dataset might not exactly reflect Bcc's situation. Further analysis of the putative BZK catabolism genes validated the presence of all of the 15 genes described in the literature (for *B. cenocepacia* AU1054) within the genomes of *B. cepacia* IST612 and IST701, attaining high identity percentages, ranging from 89 to 96%. In terms of genomic organization, isolate IST612 presented a high degree of synteny with respect to the reference genome (*B. cenocepacia* AU1054), while isolate IST701 (isolated in 2006) differed significantly from both the reference genome and IST612 (isolated in 2003), suggesting the occurrence of evolutionary events between the two isolation dates, which might explain why the bacterial population corresponding to isolate IST701 appears to have a higher tolerance to the presence of BZK.

This study constitutes a practical demonstration of the great phenotypic plasticity and metabolic diversity that characterizes Bcc bacteria. Even in the absence of nutrients and energy, the bacterial populations corresponding to the *B. cepacia* and *B. contaminans* strains examined were still able to maintain a residual viable population, tolerating the presence of BZK, possibly through its degradation and use as carbon and energy source. These observations highlight the potential hazards imposed by the presence of Bcc in pharmaceutical manufacturing and the inefficacy of using specific biocides as a preventive measure to avoid Bcc-related contaminations.

6. CONCLUSIONS AND FUTURE PERSPECTIVES

The bacterial populations of *B. cepacia* and *B. contaminans* examined in the present study were able to endure and survive during long-term exposure to stressful environmental conditions, namely nutrient starvation and the presence of BZK. Different incubation conditions resulted in the emergence of sub-populations with distinct morphotypes, typically associated with persistence and chronicity of lung infections, including the progressive decrease of colony size, associated with the development of SCVs, and a morphology switch towards smooth and mucoid colonies. Formation of SCVs raises a serious problem for clinical microbiologists, since their reduced size and growth rate hamper detection by conventional diagnostic tests, more than often leading to false-negative results. The undetected presence of Bcc bacteria during quality control of pharmaceutical products constitutes a serious healthcare problem, especially if these contaminated products are used by infected patients, negatively affecting their treatment options and general prognosis. Bcc resistance to BZK appears to be a multifactorial phenomenon, involving the emergence of different phenotypes and induction of the genetic machinery required for the use of the biocide as a carbon and energy source.

It would be of great interest to sequence the genomes of representative clonal variants of each original bacterial population obtained after long-term incubation under nutrient starvation, whether in the presence or absence of BZK (in particular SCVs and normal sized colonies, but also rough and smooth morphotypes) and compare them against the original isolates, in order to identify possible alterations induced by such stressful conditions in a chronologic manner. In addition to studying the genomic alterations suffered by the saline solutions' isolates, the clinical isolates should also be included in that analysis. Transcriptomic analysis by RNA-seq and quantitative proteomic analysis for both the original and the adapted isolates (including the different aforementioned clonal variants) would also be pertinent, to evaluate the gene expression patterns before and after exposure to BZK and nutrient starvation and identify key genes that could be responsible for Bcc bacteria's tolerance under those conditions. The monitoring of BZK concentration throughout the incubation period would also be important to understand the process underlying its hypothesized degradation inside the cells.

The present study constitutes further evidence for the role of Bcc bacteria as emergent opportunistic pathogens and the implications of Bcc related contaminations in the pharmaceutical industry, reinforcing the urgent need to re-evaluate the application of biocides in pharmaceutical products' formulations and the concentrations in which they are used, in order to prevent contamination and subsequent infection outbreaks. Although this work provides new insights on the adaptation mechanisms developed by Bcc bacteria when exposed to stressful environments for long periods of time, more studies are required in order to fully understand Bcc's capacity to adapt to hostile conditions, mainly in what concerns phenotypic variation, interaction with biocides and the biological reasons leading to their designation as one of the major contaminant agents of non-sterile water-based pharmaceutical products.

7. REFERENCES

1. Depoorter E, Bull MJ, Peeters C, Coenye T, Vandamme P, Mahenthiralingam E. 2016. *Burkholderia*: an update on taxonomy and biotechnological potential as antibiotic producers. *Appl Microbiol Biotechnol* 100:5215–5229.
2. Lessie TG, Hendrickson W, Manning BD, Devereux R. 1996. Genomic complexity and plasticity of *Burkholderia cepacia*. *FEMS Microbiol Lett* 144:117–128.
3. Sutton S, Jimenez L. 2012. A Review of Reported Recalls Involving Microbiological Control 2004-2011 with Emphasis on FDA Considerations of “Objectionable Organisms.” *Am Pharm Rev* 15:42–57.
4. Sousa SA, Ramos CG, Leitao JH. 2010. *Burkholderia cepacia* complex: emerging multihost pathogens equipped with a wide range of virulence factors and determinants. *Int J Microbiol* 2011:607575.
5. Jimenez L, Kulko E, Barron E, Flannery T. 2015. *Burkholderia cepacia*: a problem that does not go away! *EC Microbiol* 2:205–210.
6. Weber DJ, Rutala WA, Sickbert-Bennett EE. 2007. Outbreaks associated with contaminated antiseptics and disinfectants. *Antimicrob Agents Chemother* 51:4217–4224.
7. Geftic SG, Heymann H, Adair FW. 1979. Fourteen-year survival of *Pseudomonas cepacia* in a salts solution preserved with benzalkonium chloride. *Appl Environ Microbiol* 37:505–510.
8. Ahn Y, Kim JM, Lee Y-J, LiPuma J, Hussong D, Marasa B, Cerniglia C. 2017. Effects of extended storage of chlorhexidine gluconate and benzalkonium chloride solutions on the viability of *Burkholderia cenocepacia*. *J Microbiol Biotechnol* 27:2211–2220.
9. Kim JM, Ahn Y, LiPuma JJ, Hussong D, Cerniglia CE. 2015. Survival and susceptibility of *Burkholderia cepacia* complex in chlorhexidine gluconate and benzalkonium chloride. *J Ind Microbiol Biotechnol* 42:905–913.
10. Ahn Y, Kim JM, Kweon O, Kim S-J, Jones RC, Woodling K, Da Costa GG, LiPuma JJ, Hussong D, Marasa BS, Cerniglia CE. 2016. Intrinsic resistance of *Burkholderia cepacia* complex to benzalkonium chloride. *MBio* 7:e01716-16.
11. Kampf G. 2018. Adaptive microbial response to low level benzalkonium chloride exposure. *J Hosp Infect* 100:e1–e22.
12. Knapp L, Rushton L, Stapleton H, Sass A, Stewart S, Amezquita A, McClure P, Mahenthiralingam E, Maillard J. 2013. The effect of cationic microbicide exposure against *Burkholderia cepacia* complex (Bcc); the use of *Burkholderia lata* strain 383 as a model bacterium. *J Appl Microbiol* 115:1117–1126.

13. Gugliera P, Pasca MR, De Rossi E, Buroni S, Arrigo P, Manina G, Riccardi G. 2006. Efflux pump genes of the resistance-nodulation-division family in *Burkholderia cenocepacia* genome. BMC Microbiol 6:66.
14. Ahn Y, Kim JM, Ahn H, Lee Y-J, LiPuma JJ, Hussong D, Cerniglia CE. 2014. Evaluation of liquid and solid culture media for the recovery and enrichment of *Burkholderia cenocepacia* from distilled water. J Ind Microbiol Biotechnol 41:1109–1118.
15. Cunha M V, Leitao JH, Mahenthiralingam E, Vandamme P, Lito L, Barreto C, Salgado MJ, Sá-Correia I. 2003. Molecular analysis of *Burkholderia cepacia* complex isolates from a Portuguese cystic fibrosis center: a 7-year study. J Clin Microbiol 41:4113–4120.
16. Cunha M V, Pinto-de-Oliveira A, Meirinhos-Soares L, Salgado MJ, Melo-Cristino J, Correia S, Barreto C, Sá-Correia I. 2007. Exceptionally high representation of *Burkholderia cepacia* among *B. cepacia* complex isolates recovered from the major Portuguese cystic fibrosis center. J Clin Microbiol 45:1628–1633.
17. Coutinho CP, Barreto C, Pereira L, Lito L, Cristino JM, Sá-Correia I. 2015. Incidence of *Burkholderia contaminans* at a cystic fibrosis centre with an unusually high representation of *Burkholderia cepacia* during 15 years of epidemiological surveillance. J Med Microbiol 64:927–935.
18. Drevinek P, Mahenthiralingam E. 2010. *Burkholderia cenocepacia* in cystic fibrosis: epidemiology and molecular mechanisms of virulence. Clin Microbiol Infect 16:821–830.
19. Medina-Pascual MJ, Valdezate S, Carrasco G, Villalón P, Garrido N, Saéz-Nieto JA. 2015. Increase in isolation of *Burkholderia contaminans* from Spanish patients with cystic fibrosis. Clin Microbiol Infect 21:150–156.
20. Martina P, Bettiol M, Vescina C, Montanaro P, Mannino MC, Prieto CI, Vay C, Naumann D, Schmitt J, Yantorno O. 2013. Genetic diversity of *Burkholderia contaminans* isolates from cystic fibrosis patients in Argentina. J Clin Microbiol 51:339–344.
21. Moehring RW, Lewis SS, Isaacs PJ, Schell WA, Thomann WR, Althaus MM, Hazen KC, Dicks K V, LiPuma JJ, Chen LF, Sexton D. 2014. Outbreak of bacteremia due to *Burkholderia contaminans* linked to intravenous fentanyl from an institutional compounding pharmacy. JAMA Intern Med 174:606–612.
22. Nannini EC, Ponessa A, Muratori R, Marchiaro P, Ballerini V, Flynn L, Limansky AS. 2015. Polyclonal outbreak of bacteremia caused by *Burkholderia cepacia* complex and the presumptive role of ultrasound gel. Brazilian J Infect Dis 19:543–545.
23. Savi D, Quattrucci S, Trancassini M, Dalmastrì C, De Biase R V, Maggisano M, Palange P, Bevivino A. 2019. Impact of clonally-related *Burkholderia contaminans* strains in two patients attending an Italian cystic fibrosis centre: a case report. BMC Pulm Med 19:164.

24. De Smet B, Mayo M, Peeters C, Zlosnik JEA, Spilker T, Hird TJ, LiPuma JJ, Kidd TJ, Kaestli M, Ginther JL, Wagner DM, Keim P, Bell SC, Jacobs JA, Currie BJ, Vandamme P. 2015. *Burkholderia stagnalis* sp. nov. and *Burkholderia territorii* sp. nov., two novel *Burkholderia cepacia* complex species from environmental and human sources. *Int J Syst Evol Microbiol* 65:2265–2271.
25. Martina P, Leguizamon M, Prieto CI, Sousa SA, Montanaro P, Draghi WO, Stämmli M, Bettiol M, de Carvalho CCCR, Palau J, Figoli C, Alvarez F, Benetti S, Lejona S, Vescina C, Ferreras J, Lasch P, Lagares A, Zorreguieta A, Leitão JH, Yantorno OM, Bosch A. 2018. *Burkholderia puraquae* sp. nov., a novel species of the *Burkholderia cepacia* complex isolated from hospital settings and agricultural soils. *Int J Syst Evol Microbiol* 68:14–20.
26. Ong KS, Aw YK, Lee LH, Yule CM, Cheow YL, Lee SM. 2016. *Burkholderia paludis* sp. nov., an antibiotic-siderophore producing novel *Burkholderia cepacia* complex species, isolated from Malaysian tropical peat swamp soil. *Front Microbiol* 7:2046.
27. Bach E, Sant'Anna FH, Magrich dos Passos JF, Balsanelli E, de Baura VA, Pedrosa FO, de Souza EM, Passaglia LMP. 2017. Detection of misidentifications of species from the *Burkholderia cepacia* complex and description of a new member, the soil bacterium *Burkholderia catarinensis* sp. nov. *Pathog Dis* 75:ftx076.
28. Weber CF, King GM. 2017. Volcanic soils as sources of novel CO-oxidizing *Paraburkholderia* and *Burkholderia*: *Paraburkholderia hiiakae* sp. nov., *Paraburkholderia metrosideri* sp. nov., *Paraburkholderia paradisi* sp. nov., *Paraburkholderia peleae*. *Front Microbiol* 8:207.
29. Burkholder WH. 1950. Sour skin, a bacterial rot. *Phytopathology* 40:115–117.
30. Yabuuchi E, Kosako Y, Oyaizu H, Yano I, Hotta H, Hashimoto Y, Ezaki T, Arakawa M. 1992. Proposal of *Burkholderia* gen. nov. and transfer of seven species of the genus *Pseudomonas* homology group II to the new genus, with the type species *Burkholderia cepacia* (Palleroni and Holmes 1981) comb. nov. *Microbiol Immunol* 36:1251–1275.
31. Vandamme P, Holmes B, Vancanneyt M, Coenye T, Hoste B, Coopman R, Revets H, Lauwers S, Gillis M, Kersters K. 1997. Occurrence of multiple genomovars of *Burkholderia cepacia* in cystic fibrosis patients and proposal of *Burkholderia multivorans* sp. nov. *Int J Syst Evol Microbiol* 47:1188–1200.
32. Coenye T, Vandamme P, Govan JRW, LiPuma JJ. 2001. Taxonomy and identification of the *Burkholderia cepacia* complex. *J Clin Microbiol* 39:3427–3436.
33. Vanlaere E, Baldwin A, Gevers D, Henry D, De Brandt E, LiPuma JJ, Mahenthiralingam E, Speert DP, Dowson C, Vandamme P. 2009. Taxon K, a complex within the *Burkholderia cepacia* complex, comprises at least two novel species, *Burkholderia contaminans* sp. nov. and *Burkholderia lata* sp. nov. *Int J Syst Evol Microbiol* 59:102–111.

34. Mahenthiralingam E, Urban TA, Goldberg JB. 2005. The multifarious, multireplicon *Burkholderia cepacia* complex. *Nat Rev Microbiol* 3:144–156.
35. Vandamme P, Dawyndt P. 2011. Classification and identification of the *Burkholderia cepacia* complex: past, present and future. *Syst Appl Microbiol* 34:87–95.
36. Parke JL, Gurian-Sherman D. 2001. Diversity of the *Burkholderia cepacia* complex and implications for risk assessment of biological control strains. *Annu Rev Phytopathol* 39:225–258.
37. Holden MTG, Seth-Smith HMB, Crossman LC, Sebahia M, Bentley SD, Cerdeño-Tárraga AM, Thomson NR, Bason N, Quail MA, Sharp S. 2009. The genome of *Burkholderia cenocepacia* J2315, an epidemic pathogen of cystic fibrosis patients. *J Bacteriol* 191:261–277.
38. Mahenthiralingam E, Baldwin A, Dowson CG. 2008. *Burkholderia cepacia* complex bacteria: opportunistic pathogens with important natural biology. *J Appl Microbiol* 104:1539–1551.
39. Eberl L, Vandamme P. 2016. Members of the genus *Burkholderia*: good and bad guys. *F1000Research* 5:1007.
40. Compant S, Nowak J, Coenye T, Clément C, Ait Barka E. 2008. Diversity and occurrence of *Burkholderia* spp. in the natural environment. *FEMS Microbiol Rev* 32:607–626.
41. Chiarini L, Bevivino A, Dalmastrì C, Tabacchioni S, Visca P. 2006. *Burkholderia cepacia* complex species: health hazards and biotechnological potential. *Trends Microbiol* 14:277–286.
42. Zanetti F, De Luca G, Stampi S. 2000. Recovery of *Burkholderia pseudomallei* and *B. cepacia* from drinking water. *Int J Food Microbiol* 59:67–72.
43. Vermis K, Brachkova M, Vandamme P, Nelis H. 2003. Isolation of *Burkholderia cepacia* complex genomovars from waters. *Syst Appl Microbiol* 26:595–600.
44. Fang Y, Xie G, Lou M, Li B, Muhammad I. 2011. Diversity analysis of *Burkholderia cepacia* complex in the water bodies of West Lake, Hangzhou, China. *J Microbiol* 49:309–314.
45. LiPuma JJ, Spilker T, Coenye T, Gonzalez CF. 2002. An epidemic *Burkholderia cepacia* complex strain identified in soil. *Lancet* 359:2002–2003.
46. Coutinho CP, de Carvalho CCCR, Madeira A, Pinto-de-Oliveira A, Sá-Correia I. 2011. *Burkholderia cenocepacia* phenotypic clonal variation during a 3.5-year colonization in the lungs of a cystic fibrosis patient. *Infect Immun* 79:2950–2960.
47. Coutinho CP, Dos Santos SC, Madeira A, Mira NP, Moreira AS, Sá-Correia I. 2011. Long-term colonization of the cystic fibrosis lung by *Burkholderia cepacia* complex bacteria: epidemiology, clonal variation, and genome-wide expression alterations. *Front Cell Infect Microbiol* 1:12.
48. McClean S, Callaghan M. 2009. *Burkholderia cepacia* complex: epithelial cell–pathogen confrontations and potential for therapeutic intervention. *J Med Microbiol* 58:1–12.

49. Reik R, Spilker T, LiPuma JJ. 2005. Distribution of *Burkholderia cepacia* complex species among isolates recovered from persons with or without cystic fibrosis. *J Clin Microbiol* 43:2926–2928.
50. Kalish LA, Waltz DA, Dovey M, Potter-Bynoe G, McAdam AJ, LiPuma JJ, Gerard C, Goldmann D. 2006. Impact of *Burkholderia dolosa* on lung function and survival in cystic fibrosis. *Am J Respir Crit Care Med* 173:421–425.
51. LiPuma JJ. 2010. The changing microbial epidemiology in cystic fibrosis. *Clin Microbiol Rev* 23:299–323.
52. Carson LA, Favero MS, Bond WW, Petersen NJ. 1973. Morphological, biochemical, and growth characteristics of *Pseudomonas cepacia* from distilled water. *Appl Microbiol* 25:476–483.
53. Moore RA, Tuanyok A, Woods DE. 2008. Survival of *Burkholderia pseudomallei* in water. *BMC Res Notes* 1:11.
54. Pumpuang A, Chantratita N, Wikraiphat C, Saiprom N, Day NPJ, Peacock SJ, Wuthiekanun V. 2011. Survival of *Burkholderia pseudomallei* in distilled water for 16 years. *Trans R Soc Trop Med Hyg* 105:598–600.
55. Lewenza S, Abboud J, Poon K, Kobryn M, Humplik I, Bell JR, Mardan L, Reckseidler-Zenteno S. 2018. *Pseudomonas aeruginosa* displays a dormancy phenotype during long-term survival in water. *PLoS One* 13:e0198384.
56. Gilbert SE, Rose LJ. 2012. Survival and persistence of nonspore-forming biothreat agents in water. *Letts Appl Microbiol* 55:189–194.
57. Bergkessel M, Basta DW, Newman DK. 2016. The physiology of growth arrest: uniting molecular and environmental microbiology. *Nat Rev Microbiol* 14:549–562.
58. Givskov M, Eberl L, Møller S, Poulsen LK, Molin S. 1994. Responses to nutrient starvation in *Pseudomonas putida* KT2442: analysis of general cross-protection, cell shape, and macromolecular content. *J Bacteriol* 176:7–14.
59. Johns BE, Purdy KJ, Tucker NP, Maddocks SE. 2015. Phenotypic and genotypic characteristics of small colony variants and their role in chronic infection. *Microbiol insights* 8:15–23.
60. Proctor RA, Von Eiff C, Kahl BC, Becker K, McNamara P, Herrmann M, Peters G. 2006. Small colony variants: a pathogenic form of bacteria that facilitates persistent and recurrent infections. *Nat Rev Microbiol* 4:295–305.
61. Häußler S, Ziegler I, Löttel A, Götz F v, Rohde M, Wehmhöhner D, Saravanamuthu S, Tümmler B, Steinmetz I. 2003. Highly adherent small-colony variants of *Pseudomonas aeruginosa* in cystic fibrosis lung infection. *J Med Microbiol* 52:295–301.
62. Malone JG. 2015. Role of small colony variants in persistence of *Pseudomonas aeruginosa* infections in cystic fibrosis lungs. *Infect Drug Resist* 8:237–247.

63. Schröder A, Kland R, Peschel A, von Eiff C, Aepfelbacher M. 2006. Live cell imaging of phagosome maturation in *Staphylococcus aureus* infected human endothelial cells: small colony variants are able to survive in lysosomes. *Med Microbiol Immunol* 195:185–194.
64. Häussler S, Lehmann C, Breselge C, Rohde M, Classen M, Tümmler B, Vandamme P, Steinmetz I. 2003. Fatal outcome of lung transplantation in cystic fibrosis patients due to small-colony variants of the *Burkholderia cepacia* complex. *Eur J Clin Microbiol Infect Dis* 22:249–253.
65. Irvine S, Bunk B, Bayes H, Spröer C, Connolly JPR, Six A, Evans TJ, Roe AJ, Overmann J, Walker D. 2018. Genomic inversion drives small colony variant formation and increased virulence in *P. aeruginosa*. *bioRxiv* 356386.
66. Van den Bergh B, Fauvart M, Michiels J. 2017. Formation, physiology, ecology, evolution and clinical importance of bacterial persisters. *FEMS Microbiol Rev* 41:219–251.
67. Fisher RA, Gollan B, Helaine S. 2017. Persistent bacterial infections and persister cells. *Nat Rev Microbiol* 15:453–464.
68. Maisonneuve E, Gerdes K. 2014. Molecular mechanisms underlying bacterial persisters. *Cell* 157:539–548.
69. Prax M, Bertram R. 2014. Metabolic aspects of bacterial persisters. *Front Cell Infect Microbiol* 4:148.
70. Lewis ERG, Torres AG. 2016. The art of persistence—the secrets to *Burkholderia* chronic infections. *Pathog Dis* 74:ftw070.
71. Van Acker H, Sass A, Dhondt I, Nelis HJ, Coenye T. 2014. Involvement of toxin–antitoxin modules in *Burkholderia cenocepacia* biofilm persistence. *Pathog Dis* 71:326–335.
72. Costerton JW, Stewart PS, Greenberg EP. 1999. Bacterial biofilms: a common cause of persistent infections. *Science* 284:1318–1322.
73. Cunha M V, Sousa SA, Leitao JH, Moreira LM, Videira PA, Sá-Correia I. 2004. Studies on the involvement of the exopolysaccharide produced by cystic fibrosis-associated isolates of the *Burkholderia cepacia* complex in biofilm formation and in persistence of respiratory infections. *J Clin Microbiol* 42:3052–3058.
74. Traverse CC, Mayo-Smith LM, Poltak SR, Cooper VS. 2013. Tangled bank of experimentally evolved *Burkholderia* biofilms reflects selection during chronic infections. *Proc Natl Acad Sci U S A* 110:E250–E259.
75. Lewis K. 2010. Persister cells. *Annu Rev Microbiol* 64:357–372.
76. Van Acker H, Sass A, Bazzini S, De Roy K, Udine C, Messiaen T, Riccardi G, Boon N, Nelis HJ, Mahenthiralingam E. 2013. Biofilm-grown *Burkholderia cepacia* complex cells survive antibiotic treatment by avoiding production of reactive oxygen species. *PLoS One* 8:e58943.

77. Ferreira AS, Silva IN, Oliveira VH, Cunha R, Moreira LM. 2011. Insights into the role of extracellular polysaccharides in *Burkholderia* adaptation to different environments. *Front Cell Infect Microbiol* 1:16.
78. Ferreira AS, Silva IN, Moreira LM. 2011. Mechanisms controlling the expression of the exopolysaccharide of *Burkholderia* and role in niche adaptation, p. 147–164. *In* IntechOpen (ed.), *Biotechnology of Biopolymers*. BoD–Books on Demand.
79. Ferreira AS, Leitão JH, Silva IN, Pinheiro PF, Sousa SA, Ramos CG, Moreira LM. 2010. Distribution of cepacian biosynthesis genes among environmental and clinical *Burkholderia* strains and role of cepacian exopolysaccharide in resistance to stress conditions. *Appl Environ Microbiol* 76:441–450.
80. Zlosnik JEA, Hird TJ, Fraenkel MC, Moreira LM, Henry DA, Speert DP. 2008. Differential mucoid exopolysaccharide production by members of the *Burkholderia cepacia* complex. *J Clin Microbiol* 46:1470–1473.
81. Zlosnik JEA, Costa PS, Brant R, Mori PYB, Hird TJ, Fraenkel MC, Wilcox PG, Davidson AGF, Speert DP. 2011. Mucoïd and nonmucoïd *Burkholderia cepacia* complex bacteria in cystic fibrosis infections. *Am J Respir Crit Care Med* 183:67–72.
82. Potts M. 1994. Desiccation tolerance of prokaryotes. *Microbiol Mol Biol Rev* 58:755–805.
83. Herasimenka Y, Benincasa M, Mattiuzzo M, Cescutti P, Gennaro R, Rizzo R. 2005. Interaction of antimicrobial peptides with bacterial polysaccharides from lung pathogens. *Peptides* 26:1127–1132.
84. Ali M. 2016. *Burkholderia Cepacia* in Pharmaceutical Industries. *Int J Vaccines Vaccin* 3:00064.
85. United States Food and Drug Administration. 2019. Recalls, Market Withdrawals, & Safety Alerts. <https://www.fda.gov/safety/recalls-market-withdrawals-safety-alerts>. Accessed 25 May 2019.
86. United States Food and Drug Administration. 2017. FDA Updates on Multistate Outbreak of *Burkholderia cepacia* Infections. <https://www.fda.gov/drugs/drug-safety-and-availability/fda-updates-multistate-outbreak-burkholderia-cepacia-infections>. Accessed 25 May 2019.
87. United States Food and Drug Administration. 2017. FDA updates on 2017 *Burkholderia cepacia* contamination. <https://www.fda.gov/drugs/drug-safety-and-availability/fda-updates-2017-burkholderia-cepacia-contamination>. Accessed 25 May 2019.
88. United States Food and Drug Administration. 2018. FDA alerts consumers, pet owners not to use products manufactured by King Bio, including Dr. King’s label, homeopathic drug and pet products. <https://www.fda.gov/news-events/press-announcements/fda-alerts-consumers-pet-owners-not-use-products-manufactured-king-bio-including-dr-kings-label>. Accessed 25 May 2019.

89. Torbeck L, Raccasi D, Guilfoyle DE, Friedman RL, Hussong D. 2011. *Burkholderia cepacia*: this decision is overdue. *PDA J Pharm Sci Technol* 65:535–543.
90. Jimenez L. 2007. Microbial diversity in pharmaceutical product recalls and environments. *PDA J Pharm Sci Technol* 61:383–399.
91. Palleroni NJ. 2015. *Burkholderia*, p. 1–50. In Whitman W. B. (ed.): *Bergey's Manual of Systematics of Archaea and Bacteria*. Wiley & Sons, in association with Bergey's Manual Trust.
92. Kang JW, Doty SL. 2014. Cometabolic degradation of trichloroethylene by *Burkholderia cepacia* G4 with poplar leaf homogenate. *Can J Microbiol* 60:487–490.
93. Ju K-S, Parales RE. 2010. Nitroaromatic compounds, from synthesis to biodegradation. *Microbiol Mol Biol Rev* 74:250–272.
94. Ratajczak M, Kubicka MM, Kamińska D, Sawicka P, Długaszewska J. 2015. Microbiological quality of non-sterile pharmaceutical products. *Saudi Pharm J* 23:303–307.
95. Jimenez L. 2004. *Microbial contamination control in the pharmaceutical industry*, 1st ed. Marcel Dekker Publishers, New York, N.Y.
96. Parenteral Drug Association. 2014. PDA Exclusion of Objectionable Microorganisms from Nonsterile Pharmaceuticals, Medical Devices, and Cosmetics Technical Report Team. Technical Report No . 67 Exclusion of Objectionable Microorganisms from Nonsterile Pharmaceuticals, Medical Devices, and Cosmetics. https://store.pda.org/TableOfContents/TR67_TOC.pdf
97. Sutton S. 2012. What is an objectionable organism. *Am Pharm Rev* 15:36–48.
98. Rose H, Baldwin A, Dowson CG, Mahenthiralingam E. 2009. Biocide susceptibility of the *Burkholderia cepacia* complex. *J Antimicrob Chemother* 63:502–510.
99. United States Pharmacopeia. 2008. United States Pharmacopeial Convention. USP <61> Microbiological Examination of Non-Sterile Products: Microbial Enumeration Tests <https://hmc.usp.org/sites/default/files/documents/HMC/GCs-Pdfs/c61.pdf>. Accessed 24 September 2019.
100. United States Pharmacopeia. 2008. United States Pharmacopeial Convention. USP <62> Microbiological Examination of Non-Sterile Products: Tests for Specified Microorganisms. <https://hmc.usp.org/sites/default/files/documents/HMC/GCs-Pdfs/c62.pdf>. Accessed 24 September 2019.
101. United States Food and Drug Administration. 2017. FDA advises drug manufacturers that *Burkholderia cepacia* complex poses a contamination risk in non-sterile, water-based drug products. <https://www.fda.gov/drugs/drug-safety-and-availability/fda-advises-drug-manufacturers-burkholderia-cepacia-complex-poses-contamination-risk-non-sterile>. Accessed 25 May 2019.

102. Cundell T. 2019. Excluding *Burkholderia cepacia* complex from Aqueous, Non-Sterile Drug Products. Am Pharm Rev. <https://www.americanpharmaceuticalreview.com/Featured-Articles/358427-Excluding-i-Burkholderia-cepacia-i-complex-from-Aqueous-Non-Sterile-Drug-Products/>. Accessed 25 May 2019.
103. United States Food and Drug Administration. 2014. Water for Pharmaceutical Use. <https://www.fda.gov/inspections-compliance-enforcement-and-criminal-investigations/inspection-technical-guides/water-pharmaceutical-use>. Accessed 24 September 2019.
104. United States Pharmacopeia. 2012. United States Pharmacopeial Convention. USP <1112> Application of Water Activity Determination To Nonsterile Pharmaceutical Products <http://www.triphasepharmasolutions.com/Private/USP%201112%20APPLICATION%20OF%20WATER%20ACTIVITY%20DETERMINATION%20TO%20NONSTERILE%20PHARMACEUTICAL%20PRODUCTS.pdf>. Accessed 24 September 2019.
105. McDonnell G, Russell AD. 1999. Antiseptics and disinfectants: activity, action, and resistance. Clin Microbiol Rev 12:147–179.
106. Gnanadhas DP, Marathe SA, Chakravorty D. 2013. Biocides—resistance, cross-resistance mechanisms and assessment. Expert Opin Investig Drugs 22:191–206.
107. Wiggins P. 2004. Efflux pumps: an answer to Gram-negative bacterial resistance? Expert Opin Investig Drugs 13:899–902.
108. Mira NP, Madeira A, Moreira AS, Coutinho CP, Sá-Correia I. 2011. Genomic expression analysis reveals strategies of *Burkholderia cenocepacia* to adapt to cystic fibrosis patients' airways and antimicrobial therapy. PLoS One 6:e28831.
109. Nagai K, Murata T, Ohta S, Zenda H, Ohnishi M, Hayashi T. 2003. Two different mechanisms are involved in the extremely high-level benzalkonium chloride resistance of a *Pseudomonas fluorescens* strain. Microbiol Immunol 47:709–715.
110. European Medicines Agency (EMA). 2017. Committee for Human Medicinal Products (CHMP). Benzalkonium chloride used as an excipient. https://www.ema.europa.eu/en/documents/report/benzalkonium-chloride-used-excipient-report-published-support-questions-answers-benzalkonium_en.pdf
111. Fazlara A, Ekhtelat M. 2012. The disinfectant effects of benzalkonium chloride on some important foodborne pathogens. Am J Agric Environ Sci 12:23–29.
112. Patrauchan MA, Oriel PJ. 2003. Degradation of benzyldimethylalkylammonium chloride by *Aeromonas hydrophila* sp. K. J Appl Microbiol 94:266–272.

113. Abdallah M, Abdallah HA, Memish ZA. 2018. *Burkholderia cepacia* complex outbreaks among non-cystic fibrosis patients in the intensive care units: A review of adult and pediatric literature. *La Infez Med* 26:299–307.
114. Lalitha P, Das M, Purva PS, Karpagam R, Geetha M, Priya JL, Babu KN. 2014. Postoperative endophthalmitis due to *Burkholderia cepacia* complex from contaminated anaesthetic eye drops. *Br J Ophthalmol* 98:1498–1502.
115. Zurita J, Mejia L, Zapata S, Trueba G, Vargas AC, Aguirre S, Falconi G. 2014. Healthcare-associated respiratory tract infection and colonization in an intensive care unit caused by *Burkholderia cepacia* isolated in mouthwash. *Int J Infect Dis* 29:96–99.
116. Singhal T, Shah S, Naik R. 2015. Outbreak of *Burkholderia cepacia* complex bacteremia in a chemotherapy day care unit due to intrinsic contamination of an antiemetic drug. *Indian J Med Microbiol* 33:117–119.
117. Ko S, An H-S, Bang JH, Park S-W. 2015. An outbreak of *Burkholderia cepacia* complex pseudobacteremia associated with intrinsically contaminated commercial 0.5% chlorhexidine solution. *Am J Infect Control* 43:266–268.
118. Song JE, Kwak YG, Um TH, Cho CR, Kim S, Park IS, Hwang JH, Kim N, Oh GB. 2018. Outbreak of *Burkholderia cepacia* pseudobacteraemia caused by intrinsically contaminated commercial 0.5% chlorhexidine solution in neonatal intensive care units. *J Hosp Infect* 98:295–299.
119. Gleeson S, Mulroy E, Bryce E, Fox S, Taylor SL, Talreja H. 2019. *Burkholderia cepacia*: An Outbreak in the Peritoneal Dialysis Unit. *Perit Dial Int* 39:92–95.
120. Süer K, Güvenir M, Otlu B, Tunç E. 2016. Outbreak of *Burkholderia cepacia* complex associated with contaminated liquid soap for hospital use: a case study. *African J Microbiol Res* 10:791–795.
121. Shrivastava B, Sriram A, Shetty S, Doshi R, Varior R. 2016. An unusual source of *Burkholderia cepacia* outbreak in a neonatal intensive care unit. *J Hosp Infect* 94:358–360.
122. Antony B, Cherian EV, Bolor R, Shenoy KV. 2016. A sporadic outbreak of *Burkholderia cepacia* complex bacteremia in pediatric intensive care unit of a tertiary care hospital in coastal Karnataka, South India. *Indian J Pathol Microbiol* 59:197–199.
123. Paul LM, Hegde A, Pai T, Shetty S, Baliga S, Shenoy S. 2016. An outbreak of *Burkholderia cepacia* bacteremia in a neonatal intensive care unit. *Indian J Pediatr* 83:285–288.
124. El Chakhtoura NG, Saade E, Wilson BM, Perez F, Papp-Wallace KM, Bonomo RA. 2017. A 17-Year Nationwide Study of *Burkholderia cepacia* Complex Bloodstream Infections Among Patients in the United States Veterans Health Administration. *Clin Infect Dis* 65:1253–1259.

125. Marquez L, Jones KN, Whaley EM, Koy TH, Revell PA, Taylor RS, Bernhardt MB, Wagner JL, Dunn JJ, LiPuma JJ, Campbell JR. 2017. An outbreak of *Burkholderia cepacia* complex infections associated with contaminated liquid docusate. *Infect Control Hosp Epidemiol* 38:567–573.
126. Akinboyo IC, Sick-Samuels AC, Singeltary E, Fackler J, Ascenzi J, Carroll KC, Maldonado Y, Brooks RB, Benowitz I, Wilson LE, LiPuma JJ, Milstone AM. 2018. Multistate outbreak of an emerging *Burkholderia cepacia* complex strain associated with contaminated oral liquid docusate sodium. *Infect Control Hosp Epidemiol* 39:237–239.
127. Ortiz AR, Rios-González CM. 2017. Outbreak of *Burkholderia cepacia* in a hemodialysis unit of Paraguay, 2014. *J Infect Public Health* 10:688–689.
128. Sommerstein R, Führer U, Lo Priore E, Casanova C, Meinel DM, Seth-Smith HMB, Kronenberg A, Koch D, Senn L, Widmer AF, Egli A, Marschall J. 2017. *Burkholderia stabilis* outbreak associated with contaminated commercially-available washing gloves, Switzerland, May 2015 to August 2016. *Eurosurveillance* 22.
129. Guo L, Li G, Wang J, Zhao X, Wang S, Zhai L, Jia H, Cao B. 2017. Suspicious outbreak of ventilator-associated pneumonia caused by *Burkholderia cepacia* in a surgical intensive care unit. *Am J Infect Control* 45:660–666.
130. Brooks RB, Mitchell PK, Miller JR, Vasquez AM, Havlicek J, Lee H, Quinn M, Adams E, Baker D, Greeley R, Ross K, Daskalaki I, Walrath J, Moulton-Meissner H, Crist MB. 2018. Multistate Outbreak of *Burkholderia cepacia* Complex Bloodstream Infections After Exposure to Contaminated Saline Flush Syringes: United States, 2016–2017. *Clin Infect Dis* 69:445–449.
131. Wang M, Zhang L, Xia S, Wu H, Zhang R, Fan M, Wang T. 2014. An investigation on surgical-site infection among post cesarean section patients with *Burkholderia cepacia* contaminated ultrasonic couplant. *Zhonghua liu xing bing xue za zhi* 35:566–568.
132. Wang L, Wang M, Zhang J, Wu W, Lu Y, Fan Y. 2015. An outbreak of *Burkholderia stabilis* colonization in a nasal ward. *Int J Infect Dis* 33:71–74.
133. Montano-Remacha C, Márquez-Cruz MD, Hidalgo-Guzman P, Sanchez-Porto A, Téllez-Pérez PF. 2015. An outbreak of *Burkholderia cepacia* bacteremia in a hemodialysis unit, Cadiz, 2014. *Enferm Infecc Microbiol Clin* 33:646–650.
134. Marquez L, Jones K, Koy T, Whaley E, Dunn J, Lipuma J, Campbell J. 2016. An Outbreak of *Burkholderia cepacia* Complex Infections in Pediatric, Non-Cystic Fibrosis Patients, p. 1413. *In Open Forum Infectious Diseases*. Oxford University Press.
135. Nimri L, Sulaiman M, Hani OB. 2017. Community-acquired urinary tract infections caused by *Burkholderia cepacia* complex in patients with no underlying risk factor. *JMM case reports* 4:e005081.

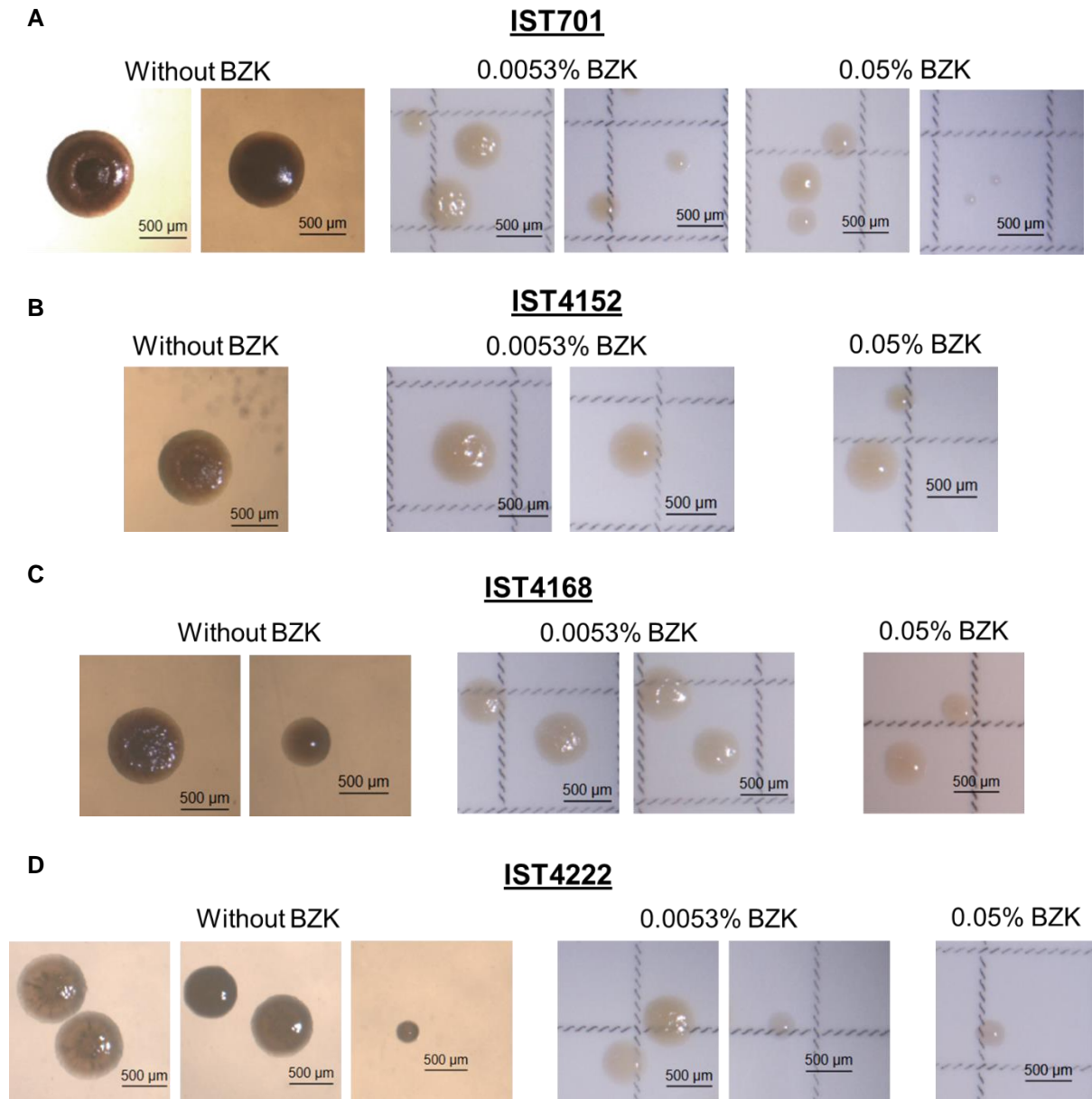
136. Shaban RZ, Maloney S, Gerrard J, Collignon P, Macbeth D, Cruickshank M, Hume A, Jennison A V, Graham RMA, Bergh H, Wilson HL, Derrington P. 2017. Outbreak of health care-associated *Burkholderia cenocepacia* bacteremia and infection attributed to contaminated sterile gel used for central line insertion under ultrasound guidance and other procedures. *Am J Infect Control* 45:954–958.
137. Mali S, Dash L, Gautam V, Shastri J, Kumar S. 2017. An outbreak of *Burkholderia cepacia* complex in the paediatric unit of a tertiary care hospital. *Indian J Med Microbiol* 35:216–220.
138. Abdelfattah R, Al-Jumaah S, Al-Qahtani A, Al-Thawadi S, Barron I, Al-Mofada S. 2018. Outbreak of *Burkholderia cepacia* bacteraemia in a tertiary care centre due to contaminated ultrasound probe gel. *J Hosp Infect* 98:289–294.
139. Becker SL, Berger FK, Feldner SK, Karliova I, Haber M, Mellmann A, Schäfers H-J, Gärtner B. 2018. Outbreak of *Burkholderia cepacia* complex infections associated with contaminated octenidine mouthwash solution, Germany, August to September 2018. *Eurosurveillance* 23.
140. Leong LEX, Lagana D, Carter GP, Wang Q, Smith K, Stinear TP, Shaw D, Sintchenko V, Wesselingh SL, Bastian I, Rogers GB. 2018. *Burkholderia lata* Infections from Intrinsically Contaminated Chlorhexidine Mouthwash, Australia, 2016. *Emerg Infect Dis* 24:2109–2111.
141. Glowicz J, Crist M, Gould C, Moulton-Meissner H, Noble-Wang J, de Man TJB, Perry KA, Miller Z, Yang WC, Langille S, Ross J, Garcia B, Kim J, Epton E, Black S, Pacilli M, LiPuma JJ, Fagan R. 2018. A multistate investigation of health care-associated *Burkholderia cepacia* complex infections related to liquid docusate sodium contamination, January-October 2016. *Am J Infect Control* 46:649–655.
142. Nazik S, Topal B, Şahin AR, Ateş S. 2018. Nosocomial *Burkholderia cepacia* infection in a tertiary hospital; Five-year surveillance: A retrospective cross-sectional study. *Urology* 6:10–13.
143. Rastogi N, Khurana S, Veeraraghavan B, Inbanathan FY, Sekar SKR, Gupta D, Goyal K, Bindra A, Sokhal N, Panda A, Malhotra R, Mathur P. 2019. Epidemiological investigation and successful management of a *Burkholderia cepacia* outbreak in a neurotrauma intensive care unit. *Int J Infect Dis* 79:4–11.
144. Kozak M. 2018. Long-term survival and phenotypic variation of *Burkholderia cepacia* complex bacteria in saline solutions with or without benzalkonium and direct molecular detection of these bacteria. Instituto Superior Técnico.
145. Mahenthalingam E, Campbell ME, Henry DA, Speert DP. 1996. Epidemiology of *Burkholderia cepacia* infection in patients with cystic fibrosis: analysis by randomly amplified polymorphic DNA fingerprinting. *J Clin Microbiol* 34:2914–2920.
146. Mahenthalingam E, Campbell ME, Foster J, Lam JS, Speert DP. 1996. Random amplified polymorphic DNA typing of *Pseudomonas aeruginosa* isolates recovered from patients with cystic fibrosis. *J Clin Microbiol* 34:1129–1135.

147. Dubois M, Gilles KA, Hamilton JK, Rebers PA t, Smith F. 1956. Colorimetric method for determination of sugars and related substances. *Anal Chem* 28:350–356.
148. Herbert D, Phipps PJ, Strange RE. 1971. Chapter III chemical analysis of microbial cells. *Methods Microbiol* 5:209–344.
149. Bolger AM, Lohse M, Usadel B. 2014. Trimmomatic: a flexible trimmer for Illumina sequence data. *Bioinformatics* 30:2114–2120.
150. Bankevich A, Nurk S, Antipov D, Gurevich AA, Dvorkin M, Kulikov AS, Lesin VM, Nikolenko SI, Pham S, Prjibelski AD. 2012. SPAdes: a new genome assembly algorithm and its applications to single-cell sequencing. *J Comput Biol* 19:455–477.
151. Zerbino DR. 2010. Using the velvet de novo assembler for short-read sequencing technologies. *Curr Protoc Bioinforma* 31:11–15.
152. Zerbino DR, Birney E. 2008. Velvet: algorithms for de novo short read assembly using de Bruijn graphs. *Genome Res* 18:821–829.
153. Gurevich A, Saveliev V, Vyahhi N, Tesler G. 2013. QUAST: quality assessment tool for genome assemblies. *Bioinformatics* 29:1072–1075.
154. Walker BJ, Abeel T, Shea T, Priest M, Abouelliel A, Sakthikumar S, Cuomo CA, Zeng Q, Wortman J, Young SK. 2014. Pilon: an integrated tool for comprehensive microbial variant detection and genome assembly improvement. *PLoS One* 9:e112963.
155. Winsor GL, Khaira B, Van Rossum T, Lo R, Whiteside MD, Brinkman FSL. 2008. The Burkholderia Genome Database: Facilitating flexible queries and comparative analyses. *Bioinformatics* 24:2803–2804.
156. Winsor GL, Griffiths EJ, Lo R, Dhillon BK, Shay JA, Brinkman FSL. 2015. Enhanced annotations and features for comparing thousands of *Pseudomonas* genomes in the *Pseudomonas* genome database. *Nucleic Acids Res* 44:D646–D653.
157. Carver TJ, Rutherford KM, Berriman M, Rajandream M-A, Barrell BG, Parkhill J. 2005. ACT: the Artemis comparison tool. *Bioinformatics* 21:3422–3423.
158. Spilker T, Baldwin A, Bumford A, Dowson CG, Mahenthiralingam E, Lipuma JJ. 2009. Expanded Multilocus Sequence Typing for *Burkholderia* Species. *J Clin Microbiol* 47:2607–2610.
159. Urwin R, Maiden MCJ. 2003. Multi-locus sequence typing: a tool for global epidemiology. *Trends Microbiol* 11:479–487.
160. Furlan JPR, Pitondo-Silva A, Braz VS, Gallo IFL, Stehling EG. 2019. Evaluation of different molecular and phenotypic methods for identification of environmental *Burkholderia cepacia* complex. *World J Microbiol Biotechnol* 35:39.

161. Public databases for molecular typing and microbial genome diversity (PubMLST). 2019. *Burkholderia cepacia* complex MLST Databases. <https://pubmlst.org/bcc/>. Accessed 16 August 2019.
162. Coenye T, Laevens S, Willems A, Ohlén M, Hannant W, Govan JR, Gillis M, Falsen E, Vandamme P. 2001. *Burkholderia fungorum* sp. nov. and *Burkholderia caledonica* sp. nov., two new species isolated from the environment, animals and human clinical samples. *Int J Syst Evol Microbiol* 51:1099–1107.
163. Gerrits GP, Klaassen C, Coenye T, Vandamme P, Meis JF. 2005. *Burkholderia fungorum* septicemia. *Emerg Infect Dis* 11:1115–1117.
164. Balola A. 2018. *Burkholderia cepacia* complex bacteria as contaminants of saline solutions containing benzalkonium: phenotypic characterization of emerging clonal variants. Instituto Superior Técnico.
165. McKinney RE. 1953. Staining bacterial polysaccharides. *J Bacteriol* 66:453–454.
166. Fauvart M, De Groote VN, Michiels J. 2011. Role of persister cells in chronic infections: clinical relevance and perspectives on anti-persister therapies. *J Med Microbiol* 60:699–709.
167. Moen B, Rudi K, Bore E, Langsrud S. 2012. Subminimal inhibitory concentrations of the disinfectant benzalkonium chloride select for a tolerant subpopulation of *Escherichia coli* with inheritable characteristics. *Int J Mol Sci* 13:4101–4123.
168. Barth AL, Pitt TL. 1996. The high amino-acid content of sputum from cystic fibrosis patients promotes growth of auxotrophic *Pseudomonas aeruginosa*. *J Med Microbiol* 45:110–119.
169. Flynn JM, Niccum D, Dunitz JM, Hunter RC. 2016. Evidence and role for bacterial mucin degradation in cystic fibrosis airway disease. *PLoS Pathog* 12:e1005846.

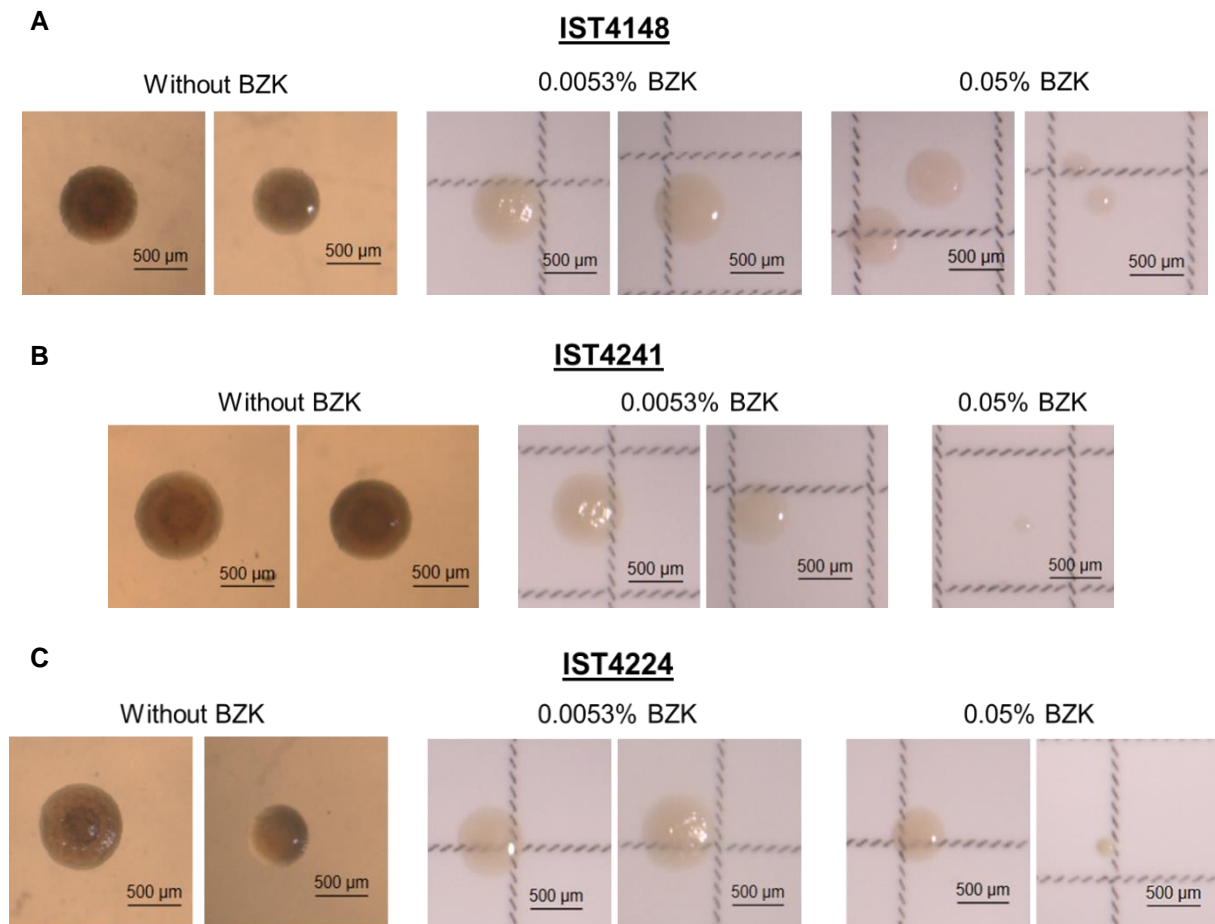
ANNEXES

Annex I



Annex I 1 - Different colony morphologies exhibited by cellular populations of *B. cepacia* IST701 (**A**), IST4152 (**B**), IST4168 (**C**) and IST4222 (**D**) incubated in saline solutions without BZK and in saline solutions supplemented with 0.0053% and 0.05% BZK, after 16 months of incubation.

Annex II



Annex II 1 - Representation of the different morphologies exhibited by the cellular populations of *B. contaminans* IST4148 (**A**), IST4241 (**B**) and IST4224 (**C**), incubated for 16 months in saline solutions without BZK and in saline solutions supplemented with 0.0053% and 0.05% BZK.

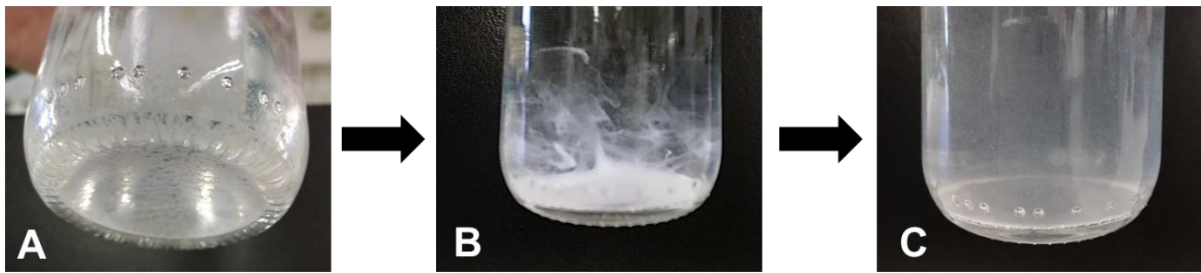
Annex III

Annex III 1 – Mean colony diameters, respective standard deviation (in mm) and colony morphologies displayed by *B. cepacia* and *B. contaminans* cellular populations incubated for 16 months in saline solutions without BZK and in saline solutions supplemented with 0.0053% and 0.05% BZK. Approximately 100 colonies were selected for measurement, and the values displayed in the present table were obtained by calculating the average colony diameter of that population sample.

Isolate	BZK Concentration (%)	Mean Colony Diameter ± SD (mm)		Colony Morphology	
		Non-SCV	SCV		
<i>B. cepacia</i>	IST612	0	1.11 ± 0.14	-	Rough/Smooth
		0.0053	0.76 ± 0.06	0.34 ± 0.00	Rough/Smooth
		0.05	-	0.29 ± 0.03	Smooth
	IST701	0	1.26 ± 0.11	-	Rough/Smooth
		0.0053	0.82 ± 0.14	0.39 ± 0.08	Rough/Smooth
		0.05	-	0.21 ± 0.02	Smooth
	IST4152	0	1.26 ± 0.07	-	Rough
		0.0053	0.86 ± 0.07	-	Rough/Smooth
		0.05	0.79 ± 0.06	0.42 ± 0.05	Smooth
IST4168	0	1.16 ± 0.14	-	Rough/Smooth	
	0.0053	0.87 ± 0.07	-	Rough/Smooth	
	0.05	0.71 ± 0.12	0.40 ± 0.07	Smooth	
IST4222	0	1.12 ± 0.11	0.43 ± 0.02	Rough/Smooth	
	0.0053	0.87 ± 0.09	0.48 ± 0.00	Rough/Smooth	
	0.05	0.54 ± 0.04	0.44 ± 0.06	Smooth	
<i>B. contaminans</i>	IST601	0	1.29 ± 0.12	-	Rough
		0.0053	0.88 ± 0.09	0.42 ± 0.03	Rough/Smooth
		0.05	0.85 ± 0.09	-	Smooth
	IST4148	0	1.11 ± 0.09	-	Rough/Smooth
		0.0053	0.96 ± 0.08	-	Rough/Smooth
		0.05	0.86 ± 0.05	0.42 ± 0.04	Smooth
	IST4241	0	1.16 ± 0.10	-	Rough/Smooth
		0.0053	1.02 ± 0.09	-	Rough/Smooth
		0.05	0.74 ± 0.11	0.43 ± 0.09	Smooth
IST4224	0	1.19 ± 0.08	-	Rough/Smooth	
	0.0053	1.01 ± 0.08	0.87 ± 0.09	Rough/Smooth	
	0.05	-	0.22 ± 0.05	Smooth	

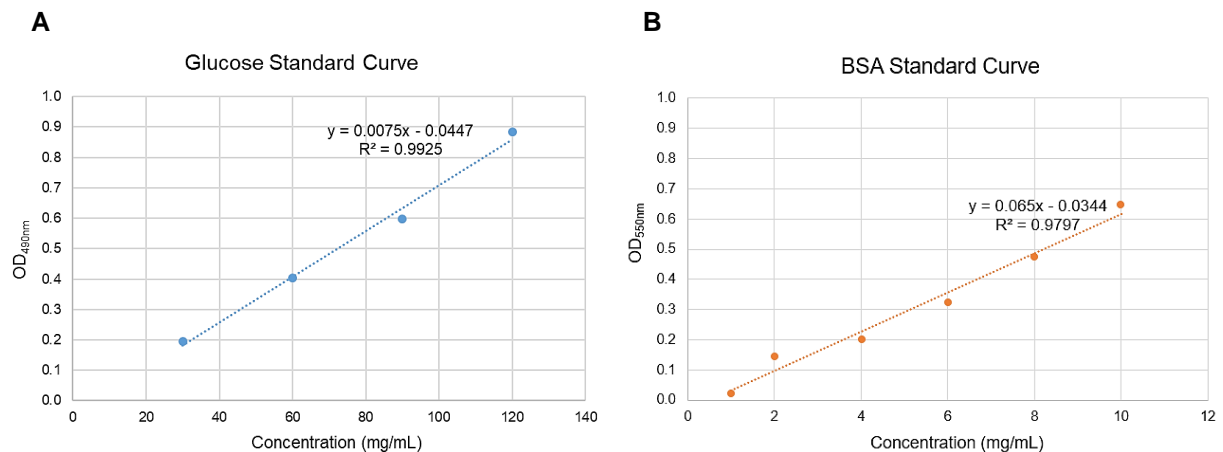
Annex IV

B. cepacia IST4152



Annex IV 1 – Global aspect of the bacterial suspension corresponding to the *B. cepacia* clinical isolate IST4152 after 16 months of incubation in saline solutions supplemented with 0.05% BZK. **(A)** Bacterial suspension prior to homogenization, where the accumulation of white deposits is observable; **(B)** Bacterial suspension after slight homogenization; **(C)** Bacterial suspension after thorough homogenization. The three pictures correspond to the same glass flask.

Annex V



Annex V 1 – Standard curves used for polysaccharide **(A)** and protein **(B)** quantification.